ADDIS ABABA UNIVERSITY

ADDIS ABABA INSTITUTE OF TECHNOLOGY

SCHOOL OF MECHANICAL AND INDUSTRIAL ENGINEERING

Analytical and Numerical Analysis of Adhesive Joints for Vehicle Application

A Thesis Submitted for the Partial Fulfillment of Degree of Masters of Science in Mechanical Engineering (Design)

BY;

Sura Keneni

Advisor

Dr Ermias G.Koricho (Assistant professor)

Co Advisor

Araya Abera (PHD candidate)

Dec, 2018

Addis Ababa, Ethiopia

ADDIS ABABA UNIVERSITY

ADDIS ABABA INSTITUTE OF TECHNOLOGY

SCHOOL OF MECHANICAL AND INDUSTRIAL ENGINEERING

Analytical and numerical analysis of adhesive joint for vehicle application

By

Sura keneni

Approved by board of examiner

Yilma Tadesse (PhD)	----------	----------
Chair man of Department	signature	date
Dr Ermias G. Koricho (assistant professor)	----------	----------
Advisor	signature	date
Araya Abera (PhD candidate)	----------	----------
Co advisor	signature	date
Behailu .M (PhD candidate)	----------	----------
External examiner	signature	date
Haileleoul .S (PhD candidate)	----------	----------
Internal examiner	signature	date

Declaration

I, the under signed, declare that this thesis work is my original work and has not been presented for degree in any other university, and that all resources of material are duly acknowledge

Name: Sura Keneni

Place: Addis Ababa, Ethiopia

Date of submission: ----------

Signature: ----------

Title of the thesis:

Analytical and numerical analysis of adhesive joint for vehicle application

This thesis has been presented for examination with my approval of a university advisor

Dr Ermias G. Koricho (assistant professor)	----------	----------
Advisor	signature	Date
Araya Abera (PhD candidate)	----------	----------
Co-Advisor	signature	Date

ACKNOWLEDGMENT

First of all I would like to thank a God for everything he has done in my life including this thesis work. Next to that, my heartfelt appreciation and gratitude goes to my advisor Dr.Ermias G. koricho for his continual encouragement and patient guidance throughout the course of this work. His deep insight into the field of adhesive joint and its many applications, his infectious enthusiasm, his patience in helping me learn the basics, and his inexhaustible supply of interesting ideas, have all greatly enriched my experience as a graduate student. To be honest this thesis work will be more complex and tedious if it wasn't for him. Many thanks are also extended to my co advisor Areya Abera and all my colleagues and friends who are working as a group member of the vehicle research centre group. Their helpful comments during the research and writing of this thesis are appreciated. At last, but not least, I would like to take this opportunity to thank my Family and my friends for all their help and understanding. Without their encouragement, love and support, this work would never have been accomplished.

ABSTRACT

Adhesively joining technique becomes very important due to capability like joining dissimilar material, lighter vehicle design, and composite material assembly than mechanical fastening. During combining dissimilar or similar materials together there must be adequate understanding of the behavior of multi-material adhesively bonded joints to ensure efficiency, safety and reliability of such joints. This may include adhesive thickness, bond length, amount of load to be applied, type material to be joined, type adhesive to be used and other factors used in analysis parameters. Using Elastomeric adhesives such as polyurethanes Sikaflex 265 as adhesive and steel, aluminum, glass and composite as adherend, analytical and numerical analysis has been done on single lap joint for elastic limit. In analytical, derivation of analytical equation that describe peel and shear stress profiles along adhesive length which is to be validated by comparing to numerical analysis done by Finite Element commercial package ABAQUS for metals. By varying the parameters used in stress equation derivation the effect they have on strength of joint also shown on failure load determination for steel, glass and aluminum. For all metals the analysis done is valid for elastic Range only. Effect of fiber orientation of glass fiber reinforced polymer (GFRP) composite on the joint also analyzed. Selecting suitable failure criteria then failure load for each combination of joint parameters are done.

Key word: Adhesive joint, single lap joint, GFRP, elastomeric adhesive, peel stress, shear stress, parametric study.

Table of Contents

List of figures

List of Tables

List of abbreviation

SLJ –Single Lap Joint

DLJ- Double Lap Joint

MPa- Mega Pascal

2D- Two Dimensions

3D – Three Dimension

GFRP- Glass Fiber Reinforced Polymer

ASTM- American Society for Testing and Materials

NDE - Near Death Experience

FE- Finite Element

CHAPTER ONE

1. INTRODUCTION

1.1. History and background

An adhesive, also known as glue, cement, mucilage, or paste, [1] is any non metallic substance applied to one surface, or both surfaces, of two separate items that binds them together and resists their separation. [2] The earliest human use of adhesive-like substances was approximately 200,000 years ago, [3] when Neanderthals produced tar from the dry distillation of birch bark for use in binding stone tools to wooden handles. [4]

The first references to adhesives in literature first appeared in approximately 2000 BC. The Greeks and Romans made great contributions to the development of adhesives. In Europe, glue was not widely used until the period AD 1500– 1700. From then until the 1900s increases in adhesive use and discovery were relatively gradual. Only since the last century has the development of synthetic adhesives accelerated rapidly, and innovation in the field continues to the present.

The earliest use of adhesives was discovered in central Italy when two stone flakes partially covered with birch-bark tar and a third uncovered stone from the Middle Pleistocene era (circa 200,000 years ago) were found. This is thought to be the oldest discovered human use of tar-hafted stones. [3] The birch-bark-tar adhesive is a simple, one-component adhesive. Although sticky enough, plant-based adhesives are brittle and vulnerable to environmental conditions. The first use of compound adhesives was discovered in Sibudu, South Africa. Here, 70,000-year-old stone segments that were once inserted in axe hafts were discovered covered with an adhesive composed of plant gum and red ochre (natural iron oxide) as adding ochre to plant gum produces a stronger product and protects the gum from disintegrating under wet conditions. [5] The ability to produce stronger adhesives allowed middle Stone Age humans to attach stone segments to sticks in greater variations, which led to the development of new tools. [6] More recent examples of adhesive use by prehistoric humans have been found at the burial sites of ancient tribes. Archaeologists studying the sites found that approximately 6,000 years ago the tribesmen had buried their dead together with food found in broken clay pots repaired with tree resins. [7]

Another investigation by archaeologists uncovered the use of bituminous cements to fasten ivory eyeballs to statues in Babylonian temples dating to approximately 4000 BC. [8] In 2000, a paper revealed the discovery of a 5,200-year-old man nicknamed the "Tyrolean Iceman" or "Ötzi", who was preserved in a glacier near the Austria-Italy border.

The first references to adhesives in literature first appeared in approximately 2000 BC. Further historical records of adhesive use are found from the period spanning 1500– 1000 BC. Artifacts from this period include paintings depicting wood gluing operations and a casket made of wood and glue in King Tutan khamun's tomb. [7] Other ancient Egyptian artifacts employ animal glue for bonding or lamination. Such lamination of wood for bows and furniture is thought to have extended their life and was accomplished using casein (milk protein)-based glues.

The ancient Egyptians also developed starch-based pastes for the bonding of papyrus to clothing and a plaster of Paris- like material made of calcined gypsum. [8] From AD 1 to 500 the Greeks and Romans made great contributions to the development of adhesives. Wood veneering and marquetry were developed, the production of animal and fish glues refined, and other materials utilized. Egg-based pastes were used to bond gold leaves incorporated various natural ingredients such as blood, bone, hide, milk, cheese, vegetables, and grains.[7] The Greeks began the use of slaked lime as mortar while the Romans furthered mortar development by mixing lime with volcanic ash and sand. This material, known as pozzolanic cement, was used in the construction of the Roman Coliseum and Pantheon. [8] The Romans were also the first people known to have used tar and beeswax as caulk and sealant between the wooden planks of their boats and ships. [7] Beeswax Modern slaked lime factory in Ukraine in Central Asia, the rise of the Mongols in approximately AD 1000 can be partially attributed to the good range and power of the bows of Genghis Khan's hordes. These bows were constructed with laminated lemonwood and bullhorn bonded by an unknown adhesive. [10]

In Europe, glue fell into disuse until the period AD 1500– 1700. At this time, world-renowned cabinet and furniture makers such as Thomas Chippendale and Duncan Phyfe began to use adhesives to hold their products together. [7] The development of modern adhesives began in 1690 with the founding of the first commercial glue plant in Holland. This plant produced glues from animal hides. [8] Liquid animal glue in 1750, the first British glue patent was issued for fish glue. The following decades of the next century witnessed the manufacture of casein glues in

German and Swiss factories. In 1876, the first US patent (number 183,024) was issued to the Ross brothers for the production of casein glue.[11] Casein glue preparation the first US postage stamps used starch-based adhesives when issued in 1840.

The first US patent (number 61,991) on dextrin (a starch derivative) adhesive was issued in 1867.Natural rubber was first used as material for adhesives starting in 1830.[12] In 1862, a British patent (number 3288) was issued for the plating of metal with brass by electrode position to obtain a stronger bond to rubber. [8] The development of the automobile and the need for rubber shock mounts required stronger and more durable bonds of rubber and metal. This spurred the development of cyclized rubber treated in strong acids. By 1927, this process was used to produce solvent-based thermoplastic rubber cements for metal to rubber bonding. [8] Natural rubber-based sticky adhesives were first used on a backing by Henry Day (US Patent 3,965) in 1845. [18] Later these kinds of adhesives were used in cloth backed surgical and electric tapes. By 1925, the pressure-sensitive tape industry was born. [2] Today, sticky notes, Scotch tape, and other tapes are examples of PSA (pressure-sensitive adhesives). [13] A key step in the development of synthetic plastics was the introduction of a thermo set plastic known as Bakelite phenolic in 1910. Within two years, phenolic resin was applied to plywood as a coating varnish.

In the early 1930s, phenolic gained importance as adhesive resins. The 1920s, 1930s, and 1940s witnessed great advances in the development and production of new plastics and resins due to the First and Second World Wars. These advances greatly improved the development of adhesives by allowing the use of newly developed materials that exhibited a variety of properties. With changing needs and ever evolving technology, the development of new synthetic adhesives continues to the present. However, due to their low cost, natural adhesives are still more commonly used. Economic importance In the course of time and during their development, adhesives have gained a stable position in an increasing number of production processes. There is hardly any product in our surroundings that does not contain at least one adhesive—be it the label on a beverage bottle, protective coatings on automobiles, or profiles on window frames. Market researchers forecast a turnover of almost US$50 billion for the global adhesives market in 2019. In particular, the economic development of emerging countries such as China, India, Russia, and Brazil will cause a rising demand for adhesives in the future. [14]

In our country also use of this adhesive have been increasing rapidly especially in wood and furniture works, metal works and glass works. But still they way they interact with this type of technology are nothing more than purchasing it from market and simply applying it by traditional way without doing any analysis.

1.1.1. Types of adhesives

Adhesives touch our lives every day. They are never more than an arm's length away, even though we may not be aware of their presence. A description of some of the more common types of adhesives and their uses should make you more aware of how adhesives touch your life' [15].

Animal Glues are made from the protein extracted from the bones, hide, hoofs, and horns of animals by boiling. The extract is cooked to form a gelatin material. The gelatin can then be re-liquefied with heat, which gives it quick setting properties. Its major use has been in the wood and furniture industry. If you have seen a heated glue pot with a brush in it, it was probably animal glue. Animal byproducts from meat processing have been the source of supply for this type of glue as well as the sources of jokes about old Dobbin being past his prime and only good for the "glue pot."

Fish Glue — is similar protein-based glue made from the skins and bones of fish. An exceptionally clear adhesive can be made from fish and was the first adhesive used for photographic emulsions for photo film and photo resist coatings for photoengraving processes.

Casein Glue — is made from a protein isolated from milk. The extraction process creates an adhesive that is waterproof. Its first use was in bonding the seam of cigarette paper. It provides a fast-setting bond that requires very little adhesive; one gram of adhesive can bond 2,000 cigarettes.

Starch — is a carbohydrate extracted from vegetable plants such as corn, rice, wheat, potatoes, and is probably better known as paste. Major use area is in bonding paper and paper products such as bookbinding, corrugated boxes, paper bags, and wallpaper paste (non removable); it is

also used as a sizing in textiles. The laundry uses starch on your shirt collars to stiffen and give shape to your shirt.

Cellulose Adhesive — is made from a natural polymer found in trees and woody plants. It is the adhesive used on the cellophane wrapper on cigarette packs; it is the adhesive on decals we put on windows; and, interestingly enough, the adhesive used on the strippable wallpaper we have in our homes that allows us to remove the paper easily.

Rubber-Based Solvent Cements — are adhesives made by combining one or more rubbers or elastomers in a solvent. These solutions are further modified with additives to improve the tack or stickiness, the degree of peel strength, flexibility, viscosity, or body. Rubber-based adhesives are used in a wide variety of applications, such as contact adhesive for plastic laminates like counter tops, cabinets, desks, and tables. It is the adhesive on pressure-sensitive tapes used as floor tile adhesive and carpeting adhesive. Self sealing envelopes and shipping containers use rubber cements. Solvent-based rubber adhesives have been the mainstay of the shoe and leather industry.

Epoxies — are adhesive systems made by a complex chemical reaction. Various resins are made synthetically by reacting two or more chemicals. The resultant resin can then be reacted or cured by the addition of another chemical called a hardener, or catalyst. The basic epoxy resin systems are further modified to change their physical properties by the addition of such things as: flexibilizers for impact resistance and flexibility; dilutents or solvents to reduce the viscosity fillers; and reinforcements like glass fiber, alumina, silica sand, clay, metal powders and flakes to change properties such as heat and electrical resistance, fire retardance, strength and adhesion to certain substrates or materials. Epoxy adhesives can bond a wide variety of substrates (particularly metals) with high strength. They have been used to replace some traditional metalworking methods of joining like nuts and bolts, rivets, welding, crimping, brazing, and soldering. High strength epoxies are used to construct rotor blades for helicopters and to attach aluminum skins to the struts of aircraft wings and tail sections.

Hot Melt Adhesives — are thermoplastic polymers that are tough and solid at room temperature but are very liquid at elevated temperatures. The origin of hot melts probably started with the use of sealing wax used to seal documents and letters with a signature ring or stamp, but the art of

hot melts was not pursued until the 1960s. The major use of hot melt adhesive is in case and carton sealing. Probably if you purchased products such as frozen food, breakfast cereal, laundry detergent, a case of beer, or anything shipped in a corrugated box, the flaps were bonded with a hot melt adhesive. Hot melts are also used in home workshops for fast repairs around the home.

Other adhesives that you may have heard of that represent higher technology and/or complicated chemical processes include:

RTV Silicone Adhesives — are a rubber-like polymer called polydimethysiloxanes. RTV stands for room temperature vulcanizing, or simply a rubber that cures at room temperature. Silicone rubber adhesives are made from a complicated process that turns elemental silicon metal made from sand (silica) into a rubbery polymer when cured. Silicone rubber adhesives/sealants have excellent resistance to heat (500-600F) and moisture, which makes them exceptionally suited for outdoor weathering applications as sealants and caulking compounds in the construction industry. Because of their exceptional properties, silicone adhesives have been used in some exotic applications, such as the soles of boots worn by the first astronauts to walk on the moon. Silicone adhesive/sealants are used to seal windows, doors, and portholes on the space shuttle and many satellite missiles. A special silicone adhesive is used to bond the heat shield tiles on the space shuttle.

Anaerobic Adhesives — are derived from Methacrylate, a monomer related to acrylics or more commonly known as Plexiglas. The term anaerobic is used to describe this family of adhesives because this type of adhesive "comes to life" or hardens in the absence of air. There are many different types of anaerobic used for specific applications such as thread locking, thread sealing, flange sealing, or retaining.

Cyanoacrylate — are extremely rapid curing adhesives commonly called superglue." These adhesives were actually discovered by accident at Eastman Chemical Company. In trying to characterize certain polymers, they ended up gluing their microscope slides together. Cyanoacrylate are typically used in applications where there is a need for a rapid-curing, single component adhesive that provides high adhesion, high tensile strength, and easy dispensing.

The following list demonstrates a few common, everyday items that use adhesives in some form and that would most likely not be around today if not for the existence of adhesives:

Table 1.1a few common, everyday items adhesives use

Item	Category
Cardboard cartons	Hot melt adhesive
Golf club heads	epoxy adhesives
Cigarette packs	casein glue
Furniture joints	animal glue
Wallpaper	wetting glues and pressure sensitive adhesives
Envelopes	wetting glues and pressure sensitive adhesives
Bookbinding	starch paste
Baby diapers	pressure sensitive adhesives
Floor tiles	pressure sensitive adhesives

1.1.2. Defects and types of failure in adhesive bond

Several types of defects occur in adhesive bonds [16, 17]. These may be considered to fall into three main categories, see Fig.1.1 The first type is an inclusion, which is the physical inclusion of a foreign material in the adhesive joint, as in Fig. 1.1.a. This could occur, for example, if positioning tape is left on the adherend and has adhesive applied over it. The second types are voids, which are the inclusion of air in the joint, see Fig.1.1.b. This could occur between the adhesive and adherend during joint assembly or be found in the adhesive itself if air is introduced during mixing of a two part adhesive. Voids may also be found in the adherend. The final category of defect are kissing defects, see Fig.1.1c. Kissing defects are the result of improper adhesion between the adhesive and the adherend where the adhesive/adherend interface is not as strong as expected for that joint configuration [18]. A decreased level of adhesion leads to reduced joint strength and is a significant threat to structural integrity. As all components of the

joint are present and in contact, kissing defects are the most difficult type of defect to detect using near death experience techniques as very little material property contrast is created.

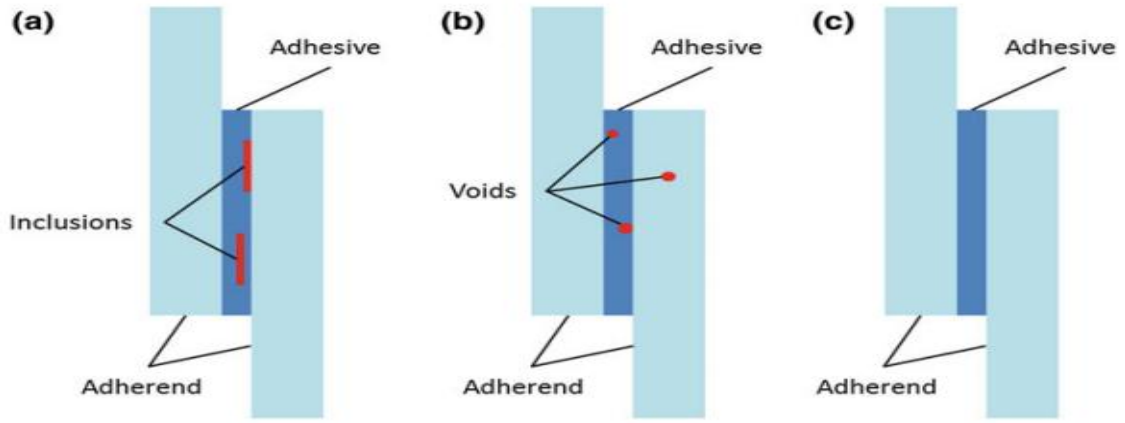

Figure 1-1.Three categories of defects typically found in adhesive joints ;(a) inclusions, (b) voids and (c) kissing defects[50]

Adhesive bonds may fail in three ways as [19]: Adherend failure, cohesive failure and Adhesive failure. If the bond fails via adherend failure the bond has been properly designed and manufactured, as the bond is not the weakest part of the structure and the adherend material has been used to its full potential. This type of failure is not due to problems with the bond. Cohesive failure is failure within the adhesive itself. This may be caused by excessive shear or peel stresses in the bond resulting from a poor joint design and is characterized by the presence of adhesive on both adherend surfaces of a failed joint. Adhesive failure is the failure between the adhesive and adherend, also known as interfacial failure and is caused by the improper preparation or pairing of the adherend and adhesive pairing. Adhesive failure is reported to only occur if there is a problem in the initial joint construction and is not caused through fatigue of the joint [20]. It is noted that for the early failure to be attributed to a kissing defect the failure mode must be adhesive, i.e. at the interface between the adhesive and adherend. As an attempt to quantitatively define a kissing defect a minimum strength reduction of 80 % of the shear strength of a perfect joint found during a lap shear test has been suggested to confirm that joints contained kissing defects [21]. It is acknowledged that this criteria is partly arbitrary, although is based on the observed nature of kissing defects.

1.1.3. Benefit of adhesive joining

The versatility of adhesives to join almost any material combination is one of the largest benefits of this technology [22]. The advantages that adhesives bestow upon a joint are many and include:

- joints with a uniform stress distribution in contrast to the localized approach of mechanical fastening and the inherent thermal stresses from welding processes
- the ability to form an aesthetically pleasing structure with the absence of holes or additional forming of the substrates
- the ability to form a complete seal over the entire joint area
- The ability to join almost any material irrespective of type, shape or form.
- provision of large, stress-bearing area
- excellent fatigue strength
- good shock absorption and reduced galvanic corrosion
- no need to have access to far-side of adherend to make joint
- improved damping which increases structural stiffness
- reduction in distortion and metallurgical changes due to low levels of heat
- good strength to weight ratio
- ability to join heat sensitive materials using room temperature curing materials

Disadvantages:

- surfaces will generally need to be cleaned and degreased
- significant cure-times may be required
- heat and pressure may be needed to cure an adhesive
- jigs and fixtures may be required to locate components whilst the joint cures
- rigid process control is required to obtain consistent results
- conventional non-destructive inspection of bonded joints is difficult
- adhesives will have a shelf-life and may require special storage conditions in relation to their good performance in compression and shear loading, adhesives
- have relatively poor resistance to tensile stresses caused by peel and cleavage forces
- adhesives have an upper temperature limit above which they will degrade

1.1.4. Application area

Nowadays adhesive joints are widely accepted and used by many industries. Some of them are listed below [22]

- Automotive, aerospace
- domestic appliance
- biomedical/dental, general industrial, consumer electronics, construction
- industrial-machine, marine, sports equipment

1.2. PROBLEM STATEMENT

In our country, Companies like airlines, defense and other body building garages used adhesive type of joining to join sheet metals. But some of them(Anbessa body building garage) haven't done any scientifically analysis on this issue and yet the joint they are producing is not standardized and lack quality as well as quantity and leads to malfunctioning and many problems like delaminating, over thickening and bad looking.

In addition to that they use traditional joining mechanism like welding, bolt, and fusion which result in material property and shape distortion due heat, local stress concentration around bolt hole and also far away from a trend of weight reduction technology by using the adhesive joining.

1.3. OBJECTIVE

1.3.1. General objective

The general of objective of this research is to analyze the performance of adhesive joint by using Multimatterial for vehicle application.

1.3.2. Specific objective

The specific object of this thesis work is to

- Analyze the joints under tensile load, bending load and shear load
- Validate the analytical analysis by comparing it to numerical analysis for metals
- Analyze the effect of Multimatterial
- Analyze the effect of geometry

1.4. METHODOLOGY

These research work is done by two method; analytically and numerically. For numerical one the commercial software used is ABAQUS. The first step is Literatures survey from different sources such as journals, books, websites and other sources. For the analytical one the selected reference is a work of two researchers called Bigwood and Crocombe [34] for the reason mentioned in literature. By doing so finally the equation that represents the stress profile through various part of adhesive is derived. Then by putting the mechanical properties of candidate the adhesive and adherend, the effect of adhesive thickness and length has been shown. Again also by applying suitable failure criteria, failure load for each combination of adherend and adhesive is determined.

Similarly to validate the analytical results of steel, aluminum and glass, numerical analysis also done by ABAQUS software. This start by modeling single lap joint, then selecting suitable element type, then meshing, applying suitable boundary conditions, applying loads, submitting the job, interpreting the result then to determine the failure load, changing values of loads until the corresponding stresses falls in safe region of failure envelope. The work flow chart is shown below in fig 1.2.below

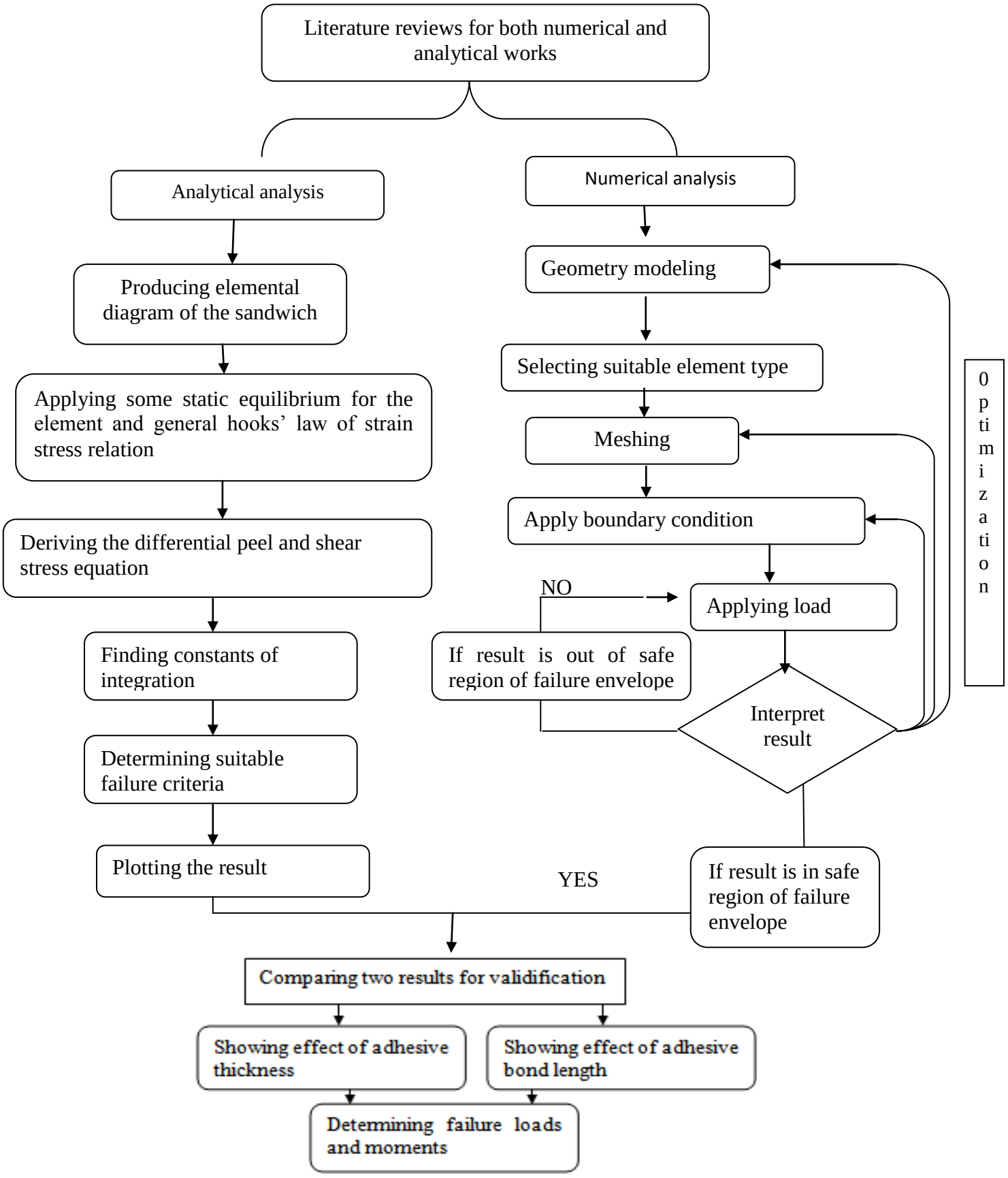

Figure 1-2.Work Flow chart

1.5. SIGNIFICANCE OF THE WORK

Nowadays, concerning joining materials together many advances have been made. From those improvement adhesive joining the major one. Despite the other European countries has already started adopting this joining technique, some of companies in our country started using this adhesive and apply it in traditional way. So that this trend of using this joining technique in traditional way has to be transformed to scientific way and loss and damage due to poor application and use of it should be minimized and this is way this research is important.

1.6. SCOPE AND LIMITATION

This research work include the tasks like driving the formulas and equations for peel and shear stress equation for single lap joints, determining the suitable failure criteria for determining failure loads, showing the effect of stress due to changing some variables. The analysis is valid for only linear analysis or only for elastic range. To validate the analytical work numerical analysis done parallel. The input adherends are steel, aluminum, glass and composite. Adhesive used is called Sikaflex 265 which one component polyurethane adhesive. Validification the works are only for steel, aluminum and glass. Because the analytical equation derived is not applicable for composite material. In addition to that since the analytical equation do not include effect of stress singularity at the end corners of the joint; it can be used only to show the stress profile at middle of the adhesive film. To show how the joint fails (cohesive, adhesive or adherend failure) it is mandatory to model the joint by cohesive zone modeling analysis type. But this job is not included due to lack of many mechanical properties required to analyze for this specific local adhesive and needs lab work that require standard and high quality labs equipment.

1.7. ORGANIZATION OF THE THESIS

The first chapter of the thesis deals with different aspects of the research. It discusses introduction, background/history and gave the necessary background to proceed throughout the thesis. It also includes the objectives and need of the research work. The second chapter deals with the previous research works carried in the field of adhesive joint by comparing their work relatively and put some limitations and their strong sides. In the third chapter, the detail peel stress and shears stress equation derivation is done analytically; Numerical modeling of joint and setting suitable failure is included. The forth chapter include discussion of result of analytical and Numerical results for the single lap joint configuration ,validification of the two analysis method, and also include parametric study for two selected variable. In addition to that effect of fiber orientation of composite lamina on joint strength is analyzed. Chapter five is the last chapter and covers conclusion, recommendation, future works, references' and appendix of the thesis work

CHAPTER TWO

2. LITERATURE REVIEWS

Recent advances in the formulation of adhesives enhanced the use of bonding as structural fastening technique. However the full potential of use of modern adhesive has been restricted because of difficulties encountered in evaluating the strength of proposed joint. These difficulties arise because there is no technique that is readily available to the design engineer for analyzing the wide range of possible joint configuration.

The elastic analysis of adhesive joints effectively began as far back as 1938 with the parallel adherend shear lag analysis of Volkersen [23]. In this analysis Volkersen considered the problem of riveted joint between two metal plates, in which the rivets were replaced in the calculation by an ideal connecting elastic interlayer. The interlayer was subjected to shear loading caused by the differential straining of the adherend, which were subjected to tension loading only. The first significant improvement over this analysis was made by Goland and Reissner [24] in 1944. Their paper deals with the determination of stresses in cemented single lap joint. Expression were derived for tension, shear force and bending moment acting at the end of the overlap region of the joint in terms of a bending moment factor which accounted for joint rotation. The stress in the bond line due to these applied loads were also determined by considering the single lap joint to be represented by two cylindrically bent plates joined by an elastic interlayer. The joint was analyzed using plate bending theory and both bending and stretching of adherends were modeled. expression were obtained for longitudinal shear and transverse direct stress in adhesive layer .Volkersen[25] improved on his original analysis in 1965 with double lap joint analysis which included a normal stress component in adhesive which was variable across the adhesive thickness.

In 1973, Hart-Smith [26] presented an analysis of the adhesive influence of various factors on the strength of adhesive bonded single lap joints. The approach of Goland and Reissner [24] was discussed and Hart-Smith noted that determination of the moment applied to the end of the joint was subject to severe restrictions and was only strictly applicable to light loads and short overlaps.

Hart-Smith takes account a more practical bending stress distribution across the end of overlap to produce a more realistic bending moment factor.

General improvements were also made to the adhesive single lap joint model by including the possible stiffness imbalance between different adherend and considering the influence of laminated filamentary composite adherends. He also produced reports analyzing various different joint configurations, including the symmetric or double lap joint [26] and the scarf-and stepped–lap joints [28]

Renton and Vinson[29,30] produced an analysis with the combined capabilities of the flexible analyses described ,but in addition, by considering the equilibrium of adhesive separately, the analysis was able to model the stress free state at the end of the adhesive in the overlap region. Renton and Vinson results were compared with those Goland and Reissner, the effect of the assumption made in deriving their analysis is to reduce the transverse and shear stress peaks in the adhesive layer with the latter having its peak shifted inboard to accommodate the zero shear stress boundary condition at adhesive terminus. The completed analysis was used to study the influence of various parameters on adhesive and adherend stress distribution of single lap joint.

In 1976 Grant and Taig [31] investigated various analytical techniques for determining the distribution of adhesive stress in bonded joint of different configuration. They showed the shear-lag technique of Volkersen [24] to be adequate for predicting the shear stress in double-lap joint. And also included non linear adhesive material properties in its formulation .they concluded that the presence of transverse joint deformation in single lap joint necessitated the development of a more general analysis technique and produced a general stepped-lap joint analysis. They used finite element formulation to validate analysis.

An improvement in the way the adhesive layer in the single lap joint was modeled came in paper by Allman[32],in which the stress distribution in a joint were expressed in terms of stress free stress function, the form of which were determined by minimizing the strain energy of the joint. The stress function permit the fulfillment of all the equations of joint equilibrium and the stress boundary condition, including the stress free surface condition at the end of the overlap and also

the linear variation in peel stress across the adhesive thickness. The adhesive shear stress is however, assumed to be constant across the adhesive thickness.

As with the analysis of Renton and Vinson [29, 30] the theory of Allman yields an almost identical level of average shear stress along the joint as predicted by Goland and Reissner, except for an exponential decay in the region of the ends of the adhesive layer, where a zero value is correctly predicted. In modeling the zero shear stress at the adhesive terminus the peak stress is shifted inboard and appreciably reduced. This effect is not noted with the finite element analysis, where the length of the overlap over which the stress decays is much localized at terminus.

Ojalvo and Eidinoff [33] extended the approach of Goland and Reissner in their analysis of the single lap joint by considering not only a linear variation in shear stress across the adhesive layer but a linear variation in peel stress as well. This is accomplished by using more complete shear strain displacement equation. A reasonable variation of shear stress across the bond line layer is predicted by this theory, and this fact has been borne out by finite element analysis. The added complication to the differential equations produced by considering this variation across the adhesive layer was not included in the derivation of the general elastic analysis by the authors. Several factors contributed to the decision not to include this facility : the equation produced in elastic analysis were to be ultimately suitable for extension to consider non linear material properties and it was felt that this extension to Goland and Reissner equation would prove difficult to implement in non linear formulation. The second reason was it felt that a linear variation in stress was not realistic enough if any variation was to be considered, it would have to be parabolic to more accurately reflect the stress state in adhesive layer.

This inclusion of this form of stress state would involve considerable work and so it was decided to assume constant shear and transverse stress across the adhesive layer initially. The stress free surface modeled by Renton and Vinson [29, 30] and Allman [32] has not been modeled by Ojalvo and Eidinoff [33].

In 1989 two researcher Bigwood and Crocombe [34] derived an equation that represents the stress profile that induced in the adhesive. They assumed the adherends as cylindrically bent plates that is applicable for various configuration of joint under general loading condition. In

these work the equation is applicable for linear analysis only not include non linear one. Normal stress in x-z plane thickness is assumed negligible and the analysis is for 2D. They equate the loading condition at the boundary and corresponding stress induced in the joint and others stress strain equations. For the above main reasons this research work is selected and detail equation derivation is done in chapter three.

Research gap

Despite many of research work done by researchers here in our country in Ethiopia many industries like car body building garage, glass works, wood works and other company are using this joining mechanism simply by purchasing it from market and apply it without doing any scientifically analysis and produces the joint that are not standardized and lack quality

CHAPTER THREE

3. ANALYTICAL AND NUMERICAL MODELLING

3.1. ANALYTICAL FORMULATION DERIVATION

3.1.1. Deriving Peel Stress and Shear Stress Equation

For this research work the work of Bigwood and Crocombe [34] is selected because this analysis procedure include all types of loading condition and can be applied to various configuration of adhesive joint like L-joint, T-joint, T-peel joint, single lap joint, inclined T-peel joint as shown in fig 3.1.Below. [34] And the analysis is not applicable for composite material due to that composite has different material property in different direction and analysis included here is only valid for elastic range.

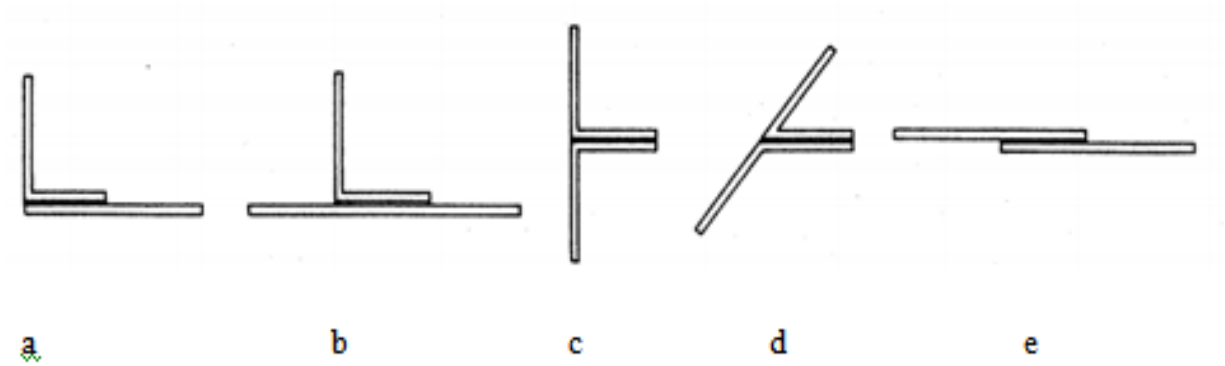

Figure 3-1. .Joint configuration that is suitable for the analysis. (a) L-joint: (b) T-joint: (c) T-peel joint: (d) inclined T-peel joint: (e) single –lap joint [34]

In attempt to rationalize the analysis of adhesive bonded joint Bigwood and Crocombe [34] work to enable a general analysis to be derived which can consider various configuration of adhesive joint under complex loading, overlap region was reduced to simple adherend-adhesive sandwich as shown fig 3.2.below. Using this sandwich it is possible to analyze any joint that can be simplified into this form, and for which the prescribed end loading values can be calculated.

For the purpose of producing general analysis, the sandwich was subjected to general loading at the adherend ends, consisting of tensile and shearing force and bending moment components which are also shown fig.3.3 below

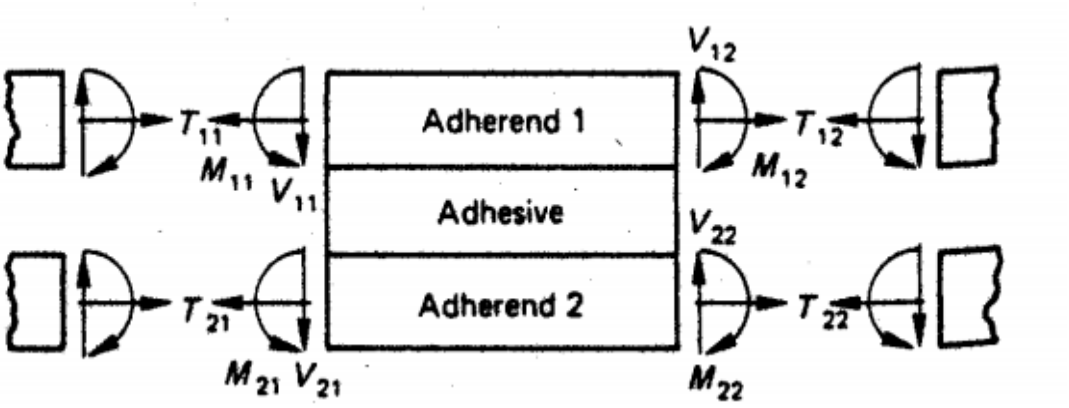

Figure 3-2.The general adherend –adhesive sandwich [21]

The approach taken for the general elastic analysis has been to consider the adherend to act as cylindrically bent plates which are connected along adjacent interfaces by a layer of adhesive which is capable of transmitting both shear and tensile loading. The dissimilar adherends of the general sandwich are analyzed by applying plate bending theory using a relatively simple approach which is essentially an extension of earlier analyses derived by Goland and Reissner [24] and Grant [31].

Justification for the use of this simple approach is two-fold. It allows simplification and the subsequent production of design formulae, and also enables the inclusion of non-linear material characteristics using the same governing differential equations, thus maintaining a consistent approach.

Work of Bigwood and Crocombe [34] has two parts, the general and simplified analysis. In general analysis explicit expression for adhesive stress along the overlap are derived. This analysis has been further simplified to produce two parameter design formulae which enable the peak stress at the ends of the overlap to be easily calculated. These simplified analyses consider the loading applied to the adherend to be transferred through the adhesive in only one of the two directions allowed in the general elastic analysis. Considering the transverse adhesive loading

component separately, an analysis referred to as the simplified peel analysis has been produced and the same thing for simplified shear analysis only by considering shear load.

Consider the following elemental diagram of adherend adhesive sandwich under general loading condition

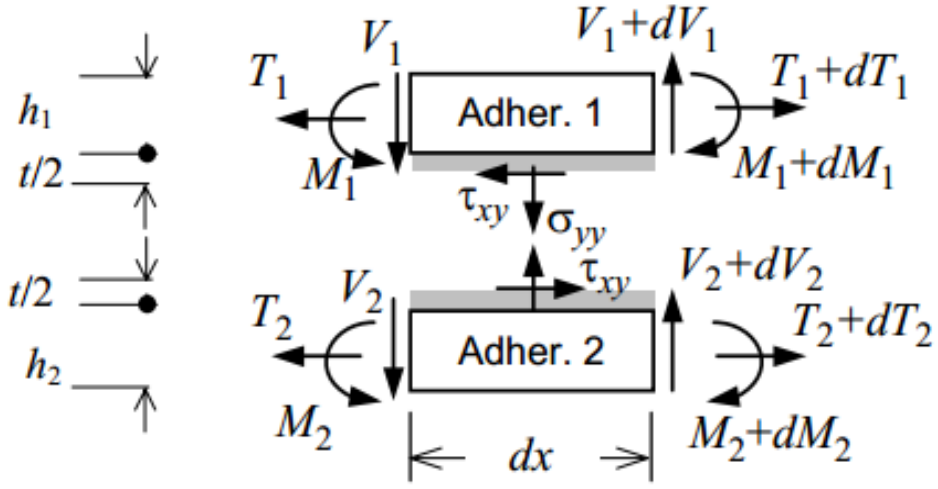

Figure 3-3.Elemental diagram adherend –adhesive sandwich under general loading (loading values per unit width) [34]

As shown in fig 3.3 above the adherends are subjected to general tensile, shearing and bending moment loading, with the adhesive layer transferring the load from the adherends through both transverse tension and shearing. It is possible to produce equilibrium equations which equate loads and corresponding adhesive stress caused by those loads.

In producing these equations it is assumed that the longitudinal direct stress in adhesive is negligible compared with the similar stress in adherends. The adherend are assumed to be isotropic and may have different thickness which are constant for each adherend. The adhesive is also assumed to be isotropic with a constant thickness which is smaller than the thickness of the adherend.

The adherends, which are analyzed as flat plates under bending are assumed to be in state of plane stress in the *x*-*z* plane, such that normal stress through the thickness (σ_y) is neglected.

A further assumption of plane strain in the *x-y* plane has also been made. This is the same assumption made by Goland and Reissner [24] who assume that out-of-plane adherend strains are negligibly small compared to adhesive strains.

The first work of Bigwood and Crocombe [34] assumes that the variation of stress through adhesive thickness is ignored. But later in their modified work [52] they account this variation in their analysis and this research also using the combined work of the two that accounts variation through thickness and specifically at mid of the film.

assuming plane strain in the *x-y* plane and the joint to have a unit thickness in the z- direction, horizontal and vertical force and bending moment equilibrium of equation are establish relating shear and tension loading with shear and transverse stress, τ_{xy} and σ_y respectively

$$\frac{dT_1}{dx} - \tau_{xy} = 0 \quad \text{.....1}$$

$$\frac{dV_1}{dx} - \sigma_y = 0 \quad \text{.....2}$$

$$\frac{dM_1}{dx} - V_1 + \frac{h_1 + t}{2}\tau_{xy} = 0 \quad \text{.....3}$$

Similar expression are produced for adherend 2

Using bending plate theory and considering the adherend to be in a state of plane strain in *x-y* yields

$$\frac{d^2 v_n}{dx^2} = -\frac{M_n}{D_n} \quad \text{.....4}$$

Where $D_n = \frac{E_n {h_n}^3}{12(1-{\mu_n}^2)}$……..…..5

And V_N and M_N are vertical displacement of the adherend and the moment in the adherend at section of interest, and E_N, h_N , μ_N *are* the young's modulus of elasticity, the thickness and poison ratio of adherends respectively.

Further expression relate the adherend strains at adherend adhesive interface, at a given position, x, along the overlap, to tensile and moment loading at that point. Referring fig 3.4 below these expression are found by summing the component stresses due to the tension and bending such that

$$\sigma_{XN} = \frac{T_N}{h_N} + \frac{M_N y}{I_N} \quad \text{……..……..……..6}$$

where I_N is the second moment of area of the adherend. Assuming plane strain in the adherend in both tension and bending, the adherend adhesive interface strains are expressed in terms of adherend loading and the interface displacement in x – direction, denoted by u_N in equation 7

$$\frac{du_N}{dx} = \frac{(1-{\mu_n}^2)}{E_N h_N}\left[T_N + \frac{M_N y_N}{I_N}\right] \quad \text{……..……..…7}$$

And from adhesive stress strain relationship

$$\tau_{xy} = \frac{G_a}{t}(u_1 - u_2) \quad \text{……..……..…8}$$

$$\sigma_y = \frac{E_a}{t}(v_1 - v_2) \quad \text{……..……..…9}$$

Assuming continuity of strain at the adherend adhesive interface and therefore combining the first derivative of equation (8) with expression of (7) for each adherend the following differential equation is produced.

$$\frac{d\tau_{xy}}{dx} = \frac{G_a}{t}\left[\frac{(1-{\mu_1}^2)}{E_1 h_1}\left(T_1 - \frac{6M_1}{h_1}\right) - \frac{(1-{\mu_2}^2)}{E_2 h_2}\left(T_2 - \frac{6M_2}{h_2}\right)\right] \quad \text{……10}$$

Two further differentiations and substitutions for the derivatives of $T_{1,2}$, $M_{1,2,}$ $V_{1,2}$ from equations (1) up to equation (3) and their corresponding lower adherend expressions at the relevant stage yield a third order differential equation in both shear and transverse stresses, given by equation 1

$$\frac{d^3\tau_{xy}}{dx^3} - K_1 \frac{d\tau_{xy}}{dx} = - K_2 \sigma_y \text{.....11}$$

Where $K_1 = \frac{G_a}{t}\left(\frac{(1-\mu_1{}^2)}{E_1 h_1}\left(1 + 3\frac{h_1+t}{h_1}\right) + \frac{(1-\mu_2{}^2)}{E_2 h_2}(1 + 3\frac{h_2+t}{h_2})\right)$ ……12

$$K_2 = \frac{6G_a}{t}\left(\frac{(1-\mu_1{}^2)}{E_1 h_1} + \frac{(1-\mu_2{}^2)}{E_2 h_2}\right)$$ ……13

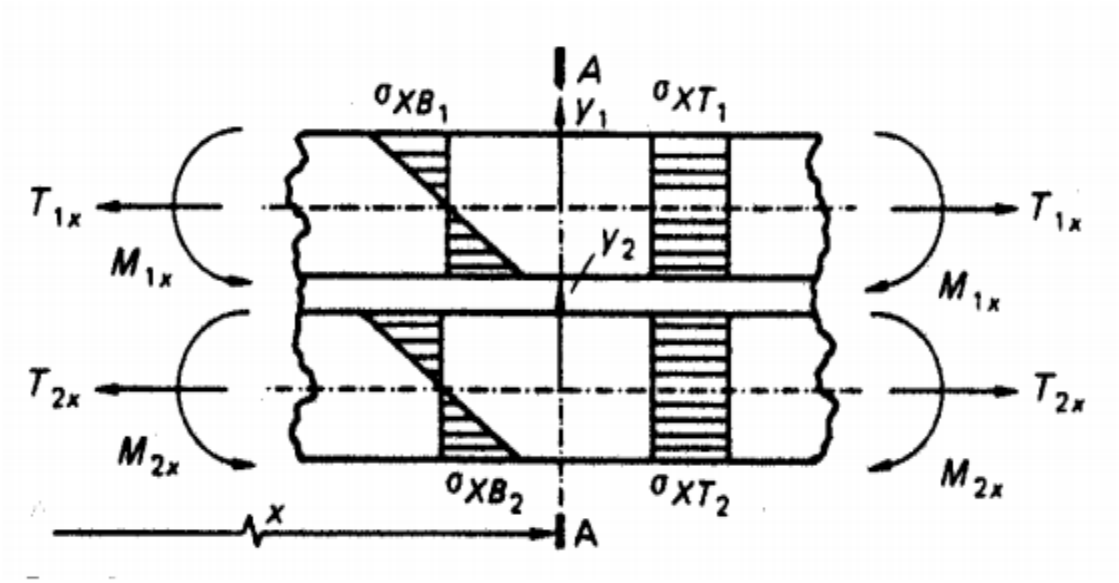

Figure 3-4.Sec A_A across bonded joint subject to general tension and bending moment loading showing tensile and bending stress included[34]

Similarly transverse direct stress can be built up in similar manner by combining the second derivative of equation (9) with equation (4) for both adherend

$$\frac{d^2\sigma_y}{dx^2} = \frac{E_a}{t}\left(\frac{M_2}{D_2} - \frac{M_1}{D_1}\right)\text{……..……..……..…14}$$

Two further differentiation with substitution made for first derivatives of $V_{1,2}$ and $M_{1,2}$ using equations (2) and (3) and their lower adherend equivalents at relevant stage yield a fourth order differential equation in both transverse and shear stresses, given by equation (15) below

$$\frac{d^4\sigma_y}{dx^4} + K_3\,\sigma_y = K_4\frac{d\tau_{xy}}{dx}\text{……..……..……15}$$

Where $K_3 = \frac{E_a}{t}\left(\frac{1}{D_1} + \frac{1}{D_2}\right)$……16

$$K_4 = \frac{E_a}{2t}\left(\frac{h_1+t}{D_1} - \frac{h_2+t}{D_2}\right)\text{……..…..…17}$$

The third and fourth order differential equations in shear given in equation (11) and transverse stresses in equation(15)are further manipulated to separate the variables and produce two uncoupled seventh and six order differential equations as follow

$$\frac{d^7\tau_{xy}}{dx^7} - K_1\frac{d^5\tau_{xy}}{dx^5} + K_3\frac{d^3\tau_{xy}}{dx^3} - K_5\frac{d\tau_{xy}}{dx} = 0\text{……..18}$$

$$\frac{d^6\sigma_y}{dx^6} - K_1\frac{d^4\sigma_y}{dx^4} + K_3\frac{d^2\sigma_y}{dx^2} - K_5\sigma_y = 0\text{……..…19}$$

Where $K_5 = (K_1 K_3 - K_2K_4)$

The differential equations describing the shear and transverse distribution in the adhesive layer are shown to have solutions of the general forms shown in equation 20 and 21 below

$$\tau_{xy} = C_1\cosh(m_1x) + C_2\sinh(m_1x) + C_3\cosh(n_1x)\cosh(n_2x) + C_4\cosh(n_1x)\sin(n_2x)$$

$$+ C_5\sinh(n_1x)\cos(n_2x) + C_6\sinh(n_1x)\sin(n_2x) + C_7\text{……..20}$$

$$\sigma_y = D_1 \cosh(m_1 x) + D_2 \sinh(m_1 x) + D_3 \cosh(n_1 x) \cosh(n_2 x) + D_4 \cosh(n_1 x) \sin(n_2 x)$$

$$+ D_5 \sinh(n_1 x) \cos(n_2 x) + D_6 \sinh(n_1 x) \sin(n_2 x) + \ldots\ldots\ldots\ldots\ldots\ldots\ldots\ldots 21$$

Where the argument multipliers, m_1, n_1, n_2 are calculated from the roots of the auxiliary equation and defined as

$$m_1 = \sqrt{\frac{C^{1/3}}{3*2^{1/3}} + \frac{k_1}{3} - \frac{2^{\frac{1}{3}}(-{k_1}^2+3k_3}{3C^{1/3}}} \ldots\ldots\ldots\ldots\ldots\ldots\ldots\ldots\ldots\ldots\ldots\ldots\ldots\ldots\ldots\ldots\ldots\ldots\ldots 22$$

$$n_1 = \sqrt[4]{(X^2+Y^2)}\ \cos\left(\frac{1}{2}\cos^{-1}\left(\frac{X}{\sqrt{X^2+Y^2}}\right)\right)\ldots\ldots\ldots\ldots\ldots\ldots\ldots\ldots\ldots\ldots\ldots\ldots\ldots 23$$

$$n_2 = \sqrt[4]{(X^2+Y^2)}\sin\left(\frac{1}{2}cos^{-1}\left(\frac{X}{\sqrt{X^2+Y^2}}\right)\right)\ldots\ldots\ldots\ldots\ldots\ldots\ldots\ldots\ldots\ldots\ldots 24$$

Where

$$C = 2{k_1}^3 - 9k_1k_3 + 27k_5 + \sqrt{-4\left({k_1}^2-3k_3\right)^3 + \left(2{k_1}^3 - 9k_1k_3 + 27k_5\right)^2}\ldots\ldots\ldots\ldots 25$$

$$X = \frac{2^{2/3}C^{2/3}+4C^{1/3}k_1-2*2^{1/3}{k_1}^2+6*2^{1/3}k_3}{12C^{1/3}}\ldots\ldots\ldots\ldots\ldots\ldots\ldots\ldots 26$$

$$Y = \frac{2^{1/3}C^{2/3}-2{k_1}^2+6k_3}{2*2^{2/3}\sqrt{3}\,C^{1/3}}\ldots\ldots\ldots\ldots\ldots\ldots\ldots\ldots\ldots\ldots\ldots\ldots\ldots\ldots 27$$

Where X and Y are the real and imaginary coefficients respectively of the complex conjugates which are the second and third roots of the auxiliary equations.

3.1.2. Solution of Constants of Integration in Analysis

Solution of the problem as whole requires the calculation of the 13 equation constants C_1 –C_7 and D_1 –D_6 in equation (20) and (21). This is completed in two parts. Firstly, the shear stress equation, equation (20) is solved with relevant seven boundary conditions.

The first six boundary conditions used in the solution of shear stress deferential equation relate different derivatives of shear stresses at the ends of the overlap with the applied loading at the same points.

Equation (10) is evaluated at either end of the overlap (x = 0 and x= L) producing two boundary conditions

$$\frac{d\tau_{xy}}{dx} = \frac{G_a}{t}\left[\frac{(1-{\mu_1}^2)}{E_1 h_1}\left(T_1 - \frac{6M_1}{h_1}\right) - \frac{(1-{\mu_2}^2)}{E_2 h_2}\left(T_2 - \frac{6M_2}{h_2}\right)\right] \quad \text{.....28}$$

By collecting together multipliers of integration constants we resulting equation is derived in appendix A1 and A2 that is solved at x=0 and x= L

Next to that Equation (11) is differentiated twice and equation (14) is used to substitute for the second derivative of the transverse stress, giving two further boundary condition.

$$\frac{K_1}{K_2}\frac{d^3\tau_{xy}}{dx^3} - \frac{1}{K_2}\frac{d^5\tau_{xy}}{dx^5} = \frac{E_a}{t}\left(\frac{M_2}{D_2} - \frac{M_1}{D_1}\right) \quad \text{.....29}$$

Detail derivation is given in appendix A3 and A4

The fifth and sixth boundary equations are found by differentiating equation (11) three times and using the derivative of equation (14) to substitute for the third derivative of transverse stress giving

$$\frac{K_1}{K_2}\frac{d^4\tau_{xy}}{dx^4} - \frac{1}{K_2}\frac{d^6\tau_{xy}}{dx^6} + \frac{E_a}{2t}\left(\frac{h_{2+t}}{D_2} - \frac{h_{1+t}}{D_1}\right)\tau_{xy} = \frac{E_a}{t}\left(\frac{V_2}{D_2} - \frac{V_1}{D_1}\right) \quad \text{.....30}$$

Detail derivation is given in appendix A5 and A6

A seventh boundary condition relates the net applied tensile load in the upper adherend with the integral of the resulting shear stress in the adhesive layer.

$$\int_0^L \tau_{xy} dx = T_{1(x=L)} - T_{1(x=0)} = T_{12} - T_{11} \quad \text{.....31}$$

Detail derivation is given in appendix A7

Utilizing the fact the equations are coupled at an earlier stage in their derivation, equation (11) and substitution for the relevant derivatives of the solved shear stress equation, a full solution for the shear stress and transverse direct stress in adhesive layer is found.

Again for peel stress the constants of integration are found by the conceptual path that is similar to that followed for the shear stress: three couples of equations are used, based on the derivatives of σ_y evaluated in turn in x=0 and x=L.

Condition 1, 2

$$\frac{d^2\sigma_y}{dx^2} = \frac{E_a}{t}\left(\frac{M_2}{D_2} - \frac{M_1}{D_1}\right) \quad \text{..... 32}$$

Detail derivation is given in appendix A8 and A9

Condtion, 3, 4

$$\frac{d^4\sigma_y}{dx^4} + k_3\sigma_y = k_4 \frac{G_a}{t}\left[\frac{1-{v_1}^2}{E_1}\left(\frac{T_1}{h_1} - \frac{6M_1}{{h_1}^2}\right) - \frac{1-{v_2}^2}{E_1}\left(\frac{T_2}{h_2} - \frac{6M_2}{{h_2}^2}\right)\right] \quad \text{.....33}$$

The corresponding derivative manipulation will be at appendix A10 and A11

Condition 5, 6

$$\frac{d^3\sigma_y}{dx^3} = \frac{E_a}{t}\left[\frac{V_2}{D_2} - \frac{V_1}{D_1} - \frac{1}{2}\left(\frac{h_2+t}{D_2} - \frac{h_1+t}{D_1}\right)\tau_{xy}\right] \quad \text{.....34}$$

Detail derivation at appendix A12 and A13

Using the equation derived in appendix we can easily found constants of integrations and substitute in the peel stress and shear stress equation.

3.2. NUMERICAL MODELING

The analysis of adhesively bonded joints started in 1938 with the closed-form model of Volkersen [23]. The equilibrium equation of a single lap joint led to a simple governing differential equation with a simple algebraic equation. However, if there is yielding of the adhesive and/or the adherends, substantial peeling is present, if composite adherends are used; the adhesive deforms plastically or if there is an adhesive fillet. In those cases, several differential equations of high complexity might be obtained (non-linear and non homogeneous). a more complex model is necessary. The more complete is an analysis, the more complicated it becomes and the more difficult it is to obtain a simple and effective solution. The finite element (FE) method, the boundary element (BE) method and the finite difference (FD) method are the three major numerical methods for solving differential equations in science and engineering.

In order to design structural joints in engineering structures, it is necessary to be able to analyze them. This means to determine stresses and strains under a given loading, and to predict the probable points of failure. There are two basic mathematical approaches for the analyses of adhesively bonded joints: closed-form analyses (analytical methods) and numerical methods (i.e. finite element or FE analyses). Differential equations are derived by applying a physical principle such as conservation of mass, momentum or energy. These equations govern the kinematic and mechanical behavior of general bodies. The analysis of adhesively bonded joints started 70 years ago with the simple closed-from model of Volkersen [23] that considers the adhesive and adherends as elastic, and that the adhesive deforms only in shear. The equilibrium equation of a single lap joint led to a simple governing differential equation with a simple algebraic equation.

The FE method, the boundary element (BE) method and the finite difference (FD) method are the three major numerical methods for solving partial differential equations in science and engineering. The FE is by far the most common technique used in the context of adhesively bonded joints. Adams et al. are among the first to have used the FE method for analyzing adhesive joint stresses (Adams and Peppiatt [35]; Crocombe and Adams [36]; Adams and Harris [37]; Adams and Davies [38]).

One of the first reasons for the use of the FE method was to assess the influence of the spew fillet. The joint rotation and the adherends and adhesive plasticity are other aspects that are easier to treat with a FE analysis. The study of Adams and Harris [37] is one of the first FE analyses taking into account these three aspects. The use of the BE method is still very limited in the analysis of adhesive joints. The FD method is especially used for solving complex governing differential equations in closed-form models.

The FE method is a numerical analysis procedure that provides an approximate solution to problems in various fields of engineering. The FE method is based on the idea of building a complicated object with simple blocks or dividing a complicated object into small and manageable pieces

Basically, FE method involves the discretization of a structure in various sub domains, known as elements, joined at their nodes. Each node has a limited number of degrees of freedom (dof). Hence, the continuum is now represented by a finite number of dof, determined by the number of elements, the number of nodes per element and the number of dof per node. In an element, the field quantity or behavior of the model (for example displacements, d, in stress analyses) is interpolated from the values of the field quantity at the nodes. Connecting the elements by the nodes, the field quantity can be interpolated over the whole structure. The most common formulation method in FE analysis is the variational method. This method involves the solution of a governing partial differential equation (for example the equilibrium equations in elasticity problems), by determining the conditions that make a functional stationary, i.e., maximum or minimum. In elasticity problems, the functional used is the total potential energy of the structure. The optimal values of the field quantity are those that minimize the total energy of the system, satisfying internal compatibility and essential boundary conditions. The process of minimization creates a system of algebraic equations for the field quantity at the nodes.

The matrix symbolism used for that system of equations is

$$K\,d = F \qquad \text{35}$$

Where d is a vector with the values of the field quantity like displacement at the nodes, F is a vector of known loads (for example forces in elasticity problems) And K is a matrix of known constants that represents the property of the elements.

In elasticity problems, K is the stiffness matrix. In stress analyses, to simulate a given loading on the model, boundary conditions and loads or values of d are applied and the output values of d are obtained from Eq.35. However, the stiffness Matrix K in Eq. 35 contains integrals that generally cannot be solved algebraically. Instead, a numerical integration scheme (such as Gauss quadrature) has to be used to determine the stiffness matrix. In general, the integrals can be computed by sampling from a number of points (Gauss points) and multiplying by an appropriate value or weighting factor. As the number of Gauss points increases, more accurate integration results are typically obtained. However, using too many Gauss points would require more computational resources and the results may not improve. The numerical solution of Eq. 35 gives the d values, which in turn allow the calculation of strains and stresses along the whole structure.

The FE method allows studying any type of geometry, i.e., it can take into account variations in the adherends shape and the adhesive fillet, which is very difficult or impossible with the closed-form analyses. Another important advantage of the method is that it enables to calculate all the stress and strain components of a structure for more realistic strength predictions. However, in general parametric FE studies (e.g. study of a geometrical parameter such as the adhesive thickness, t, A) are more difficult than with closed-form models because they generally involve creating a new model for each new configuration.

The commercial FE programs permit to easily include geometric non-linearities such as those occurring in the single lap joint. There are also a variety of material models from linear elastic to visco-plastic. To determine the initial yielding and subsequent plastic deformation in a bonded joint, a yielding model needs to be included for the adhesive and possibly for the adherend. For metallic substrates, the von Mises yield criterion may be applied. For composite adherends, yielding seldom occurs and failure criteria are used instead. In the case of adhesives and polymeric adherends, a yielding model that takes into account the hydrostatic pressure is generally required such as that proposed by Raghava [39]

As seen above, the domain or structure is divided in elements leading to a mesh. Stress concentrations need a fine mesh to capture the stress gradients as show in fig 2.5. In the particular case of stress singularities, mesh refinements may lead to convergence problems since the stress tends to infinity as finer elements are used**.**

3.2.1. Generating the model

The commercial FE package selected to validate this research work is ABAQUS 6.17. In pre-processor tasks like modeling the 3D or 2D model, applying appropriate boundary condition, selecting suitable element type, mesh adjustment, applying loads has to be completed. It is advised to apply the boundary conditions and the loads so that the mesh can be easily modified without altering the boundary conditions, to reduce the meshing effort. The geometry should be modeled with precision using at the same time any symmetry that reduces the size of the model and the number of calculations. The boundary conditions should simulate the reality as closely as possible. The most common boundary conditions for single lap joints are those represented in Fig. 3.5.which simulate gripping and loading in a testing machine and the tabs at the ends of the model is to reduce moment arm created due to non co linearity of fixed end and applied load. The dimensions of adherends and adhesives are done according to ASTM standards [56]

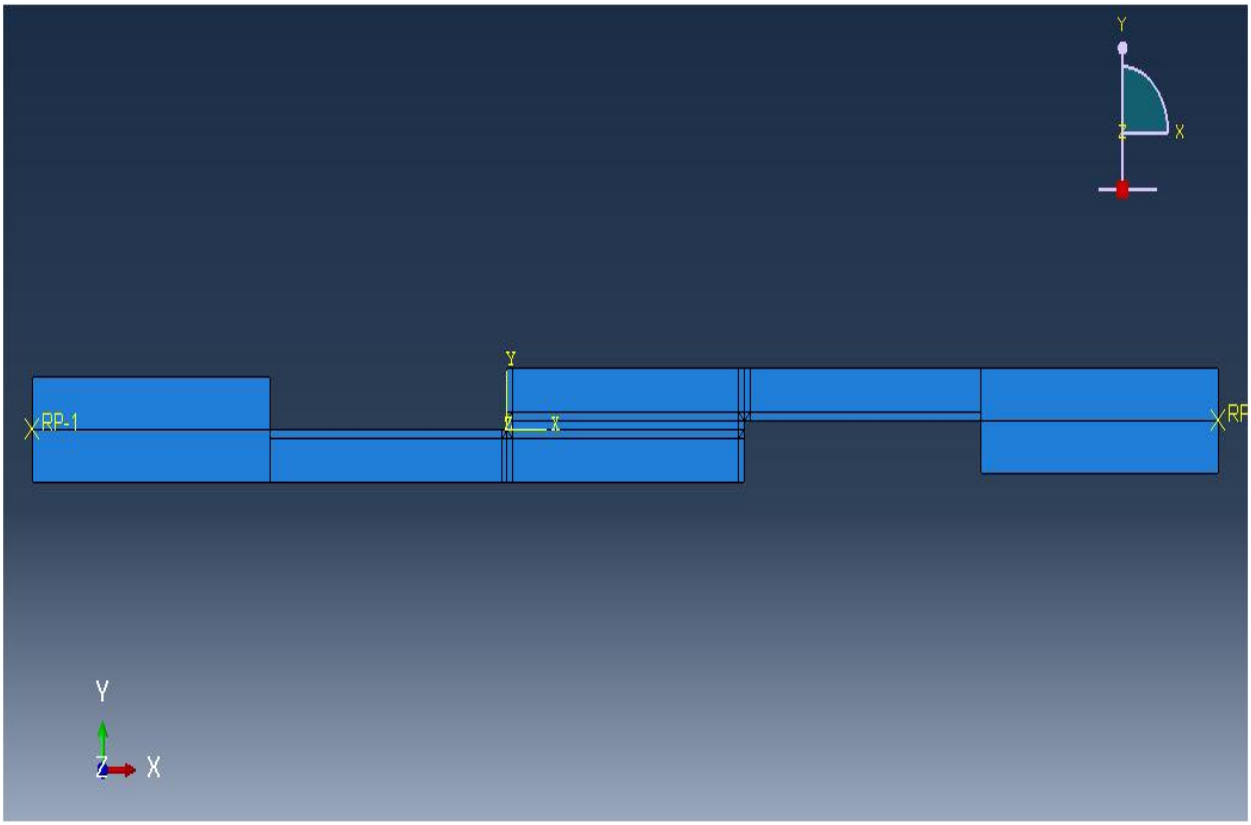

Figure 3-5.Finite element (ABAQUS) model for single lap joint.

3.2.2. Meshing

Various factors should be taken into account when preparing a mesh for a bonded joint, such as the mesh density and the type of element. Generally, a first course mesh is modeled and the mesh is refined progressively (increasing the number of elements by decreasing their size**).** A reduction of the element size increases the stress and strain levels until a point where there is practically no change, in which a converged mesh is attained as shown in fig 3.7 .In the areas where the stress is relatively uniform, a coarser mesh can be used to reduce the computation time. The mesh is usually refined at the ends of the overlap where stress concentrations exist due to the sharp geometry change. The adherends mesh is also refined along the overlap.

Elements Shape should not distorted at area of four corner of adhesive (area of interest) since that area is exhibit high stress magnitude. Distorted element shape will lead to wrong stress values. Therefore to eliminate these difficulties structured type mesh is recommended and shown in fig 3.6 below. The commercial programs have pre-processors which facilitate the mesh generation of complicated shapes.

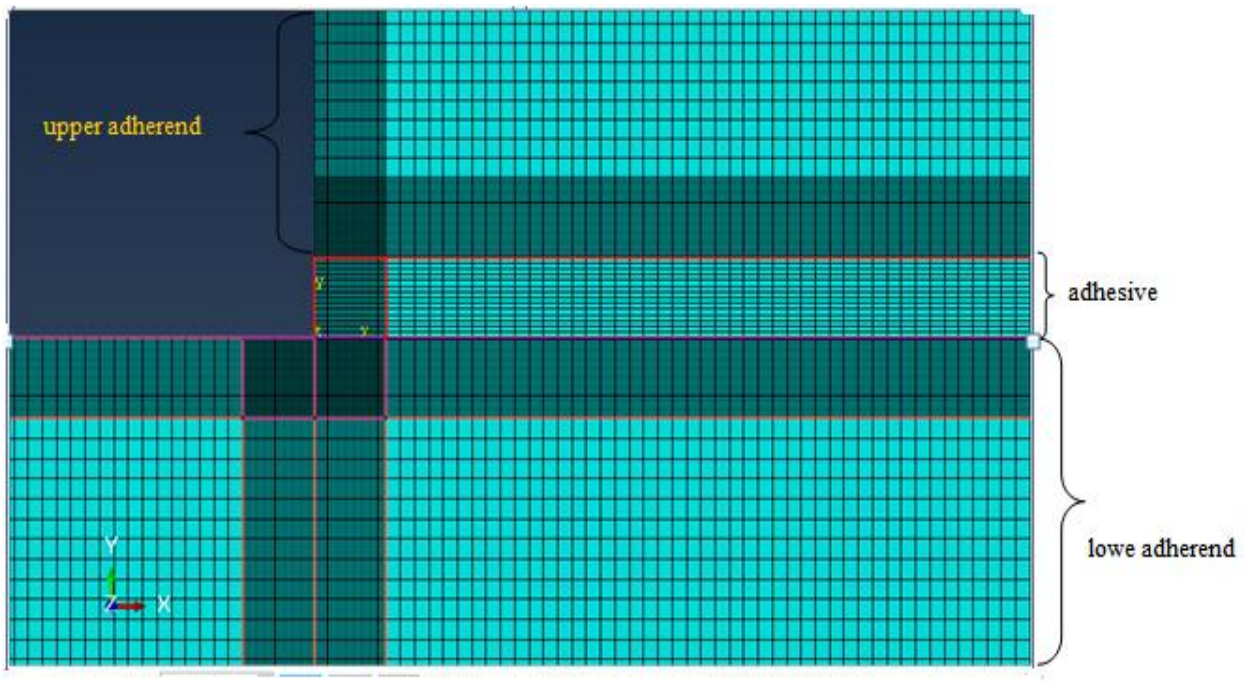

Figure 3-6.abaqus structured mesh near edges of the joint

Mesh convergence check

Mesh convergence check is done for Aluminum –Sikaflex – aluminum sandwich at the same load and other parameters like thickness, bond length, from maximum peel stress occurred at the end of the joint. During meshing finer size of element is choosed around the end of adhesive. 30 elements are fed for 0.5mm length from both end corners of adhesives for both type of meshing technique. The size of other areas rather than end area is set by global approximate size controlling tool on Abaqus. From the figure below the convergence occur after using approximate mesh size of 0.1

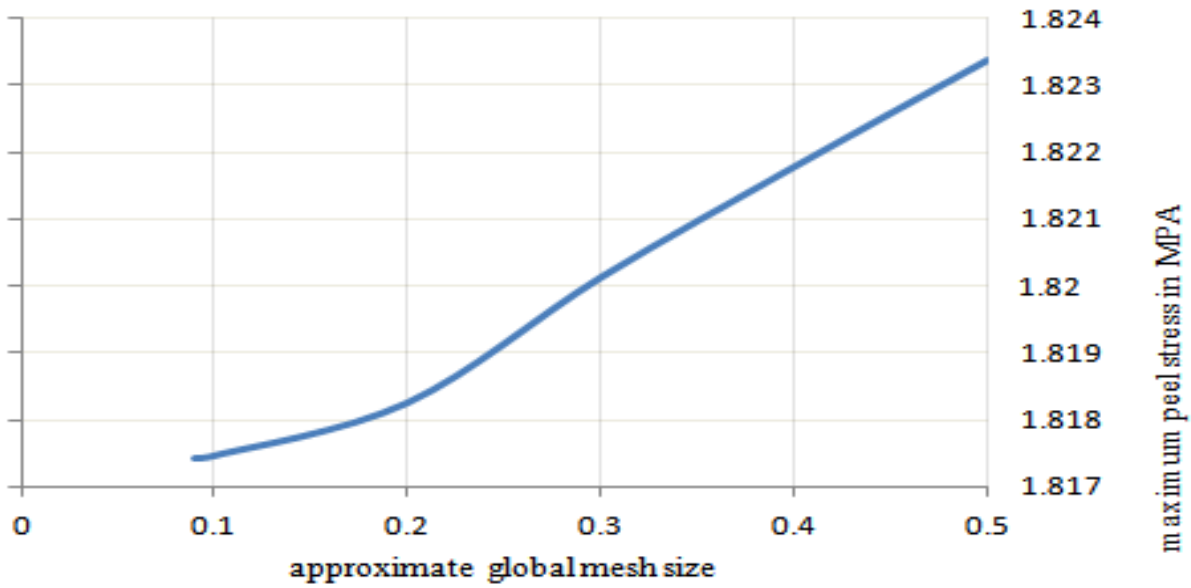

Figure 3-7 mesh convergence cheek for structured mesh

3.2.3. Element type selection

Continuum solid elements are most suited for linear analyses and also for complex non-linear problems involving plasticity and large deformations [40]. An adhesively bonded joint can be modeled in two dimensions (2D) or three dimensions (3D). The 2D continuous elements include plane stress, plane strain and generalized plane strain and also ABAQUS offer these three much related candidates of element type.

The plane stress elements are used when one of the dimensions of the body is very small in relation to the others. This situation occurs in plate where the stresses in the thickness direction are considered nil.

The plane strain elements are used when the width is much larger than the thickness. This is the case of a single lap joint where the strains in the width direction are considered nil.

In the case of the generalized plane strain elements, two parallel rigid planes exist that can only move away or closer to each other, which permits to account for the transversal strains. Continuous 3D elements suppress the approximation introduced by the plane stress or plane strain conditions. Despite a 3D analysis giving more accurate results than 2D analyses, the time and effort of a 3D analysis are often not justified. In adhesively bonded joints, a 2D analysis in plane strain conditions is often preferred. Despite 3D effects such as the lateral deformation (Adams and Peppiatt [41]) and the anticlastic bending (Adams and Davies [42]; Gonçalves [43]), various studies have shown that 2D analyses give accurate enough results (Adams [44]; Adams and Davies [39]).The elements are often Isoparametric quadratic elements of eight nodes. Isoparametric triangular elements of six nodes are also used, especially in areas that need mesh refinement. For this specific analysis plane strain element is selected for the 2D modeling for metallic adherends for the above mentioned reasons and 3D stress element type is selected for composite models

3.2.4. Load application

In this specific work the type of load selected to be applied to this joint are tensile load, moments and shear load in both analytical and numerical one. In numerical analysis we can easily apply tensile loads on nodes of elements. But we can't apply moments on nodes like we did for tensile load because of a node has no rotational degree of freedom. Therefore it is mandatory to apply some kinematical coupling on surfaces of interest as shown in fig 3.11 below. Shear load can be applied as tangential pressure on edges of adherend. At left end boundary conditions are Encastered or fixed with $U_1 = U_2 = UR_3 = 0$ and for left end only longitudinal displacement(U_1) is allowed while $U_2 = UR_3 = 0$

Also the tab placed on two ends of the modeling is to reduce the bending moment created due to eccentric loading conditions and also to simulate real phenomenon occur during gripping of testing machine in experimental case.

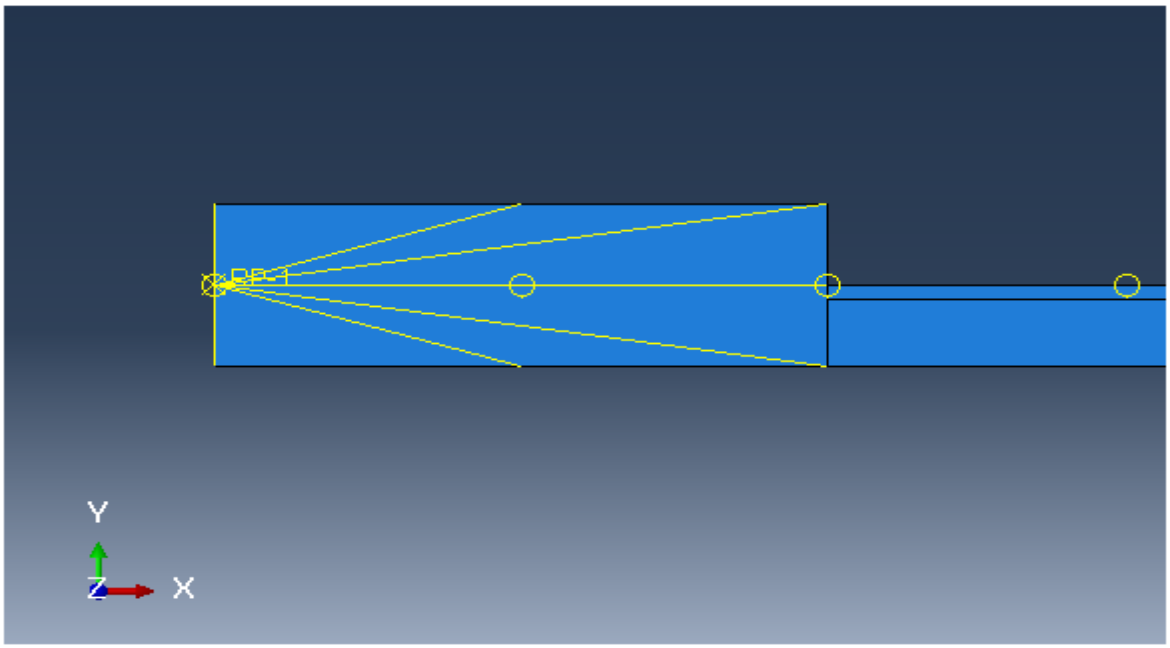

Figure 3-8. Kinematic coupling on left end of the single lap joint

3.2.5. Post processing.

The last step in this numerical is job submission and result interpretation. In single lap adhesive joint modeling the stress distribution through the layer is vary through thickness as well as along bond length. The stress designated S12 is shear stress and S22 is peel stress according to this specific analysis. One thing that should be noticed is abaqus has no units. So the stress values showed in the display is assumed to be consistent with the initial units assumed for geometry. In simple language if you assumed length you used for modeling is mm then the stress units in result must be expected as it is in MPa.

3.3. FAILURE CRITERIA

Alike analytical methods, literature for failure criteria is extensive. Generally, failure criteria can be grouped into the following categories: maximum stress or strain criteria, critical stress or strain at a distance or over a zone, limit state criteria, fracture mechanics criteria and damage mechanics criteria, Linear Drucker- Prager Yield Criterion [45]. From this linear drucker-prager yield criterion is preferable for below mentioned reasons.

3.3.1. Linear Drucker- Prager Yield Criterion

It is widely accepted that the yield behavior of polymers is dependent on both the deviatoric and hydrostatic stress components while the dependence of hydrostatic stress on yielding for metals, i.e. relying on the von Mises theory (distortional strain energy criterion which cannot predict hydrostatic stress state yielding) cannot truthfully describe realistically the post yielding behavior of the adhesives is significantly less pronounced [46]. Most adhesives under additional stress states, namely shear and compression, show that their yielding has certain sensitivity to the hydrostatic components of stress besides the shear components, especially for polymeric adhesives/toughened adhesives. Within the regions of strain concentration at the edges of the adhesive layer, those hydrostatic stress components reach a significant magnitude. Based on hydrostatic component of polymer behavior, there is a need of applying a modified failure criterion, which takes it into consideration without neglect the deviatoric stress, broached by von Mises on the failure criterion for metals, conditions which are considered by the Drucker-Prager

criterion [48]. This model was initially developed to describe geomaterials and soils behaviors, which are typically described using the theory of elastoplasticity. Since these materials exhibit pressure sensitive behavior, it is important to include this feature into the yield function employed in the constitutive equations [47]. Summarizing all these requirements, a failure mean stress criterion was developed (Drucker Prager or modified von Mises), which can be applied to polymeric materials, as follows.

Failure in polymer occurs when the following conditions are fulfilled.

$$\left(\frac{\lambda-1}{2\lambda}\right) \mathrm{I}_1 + \sqrt{\frac{3}{\lambda}J_2 + \left(\frac{\lambda-1}{2\lambda}\right)^2 {I_1}^2} \;=\; \sigma_F \;\ldots\ldots\ldots\ldots\ldots\ldots\ldots\ldots 36$$

Where I_1 is the first invariant of stress tensor and J_2 is the second invariant stress deviator given by

$$\mathrm{J}_2 = \frac{(\sigma_x-\sigma_y)^2+(\sigma_y-\sigma_z)^2+(\sigma_z-\sigma_x)^2+ 6(\tau^2{}_{xy}+\tau^2{}_{yz}+\tau^2{}_{zx})}{6} \ldots\ldots\ldots\ldots 37$$

$$\mathrm{I}_1 = \sigma_x + \sigma_y + \sigma_z \ldots\ldots\ldots\ldots\ldots\ldots\ldots\ldots\ldots\ldots\ldots\ldots\ldots 38$$

The parameter λ is related to material sensitivity to hydrostatic stress and can be defined by

$$\lambda = \left(\frac{1}{6}\right)\left(\beta^2 + \beta\sqrt{\beta^2+12} + 6\right) \ldots\ldots\ldots\ldots\ldots\ldots\ldots 39$$

$$\beta = 3\,\frac{1-\nu}{1+\nu}\;\frac{\tau_{msd}}{\sigma_{msd}} \;-\; \frac{(1-2\nu)^2}{(1-\nu)(1+\nu)}\,\frac{\sigma_{msd}}{\tau_{msd}} \ldots\ldots\ldots\ldots 40$$

Where (ν) is the Poisson coefficient for polymer or adhesive.

Using the presented criterion, the material yield stress under uniaxial tension σ_F can be calculated through two experimental data. Measured failure tensile stress σ_{msd} obtained from tensile experiment and measured failure shear stress τ_{msd} obtained from shear testing.

$$\sigma_F \;=\; \left[\frac{\lambda-1}{2\lambda} * \frac{1+\nu}{1-\nu} + \sqrt{\frac{1}{\lambda} * \left(\frac{1+\nu}{1-\nu}\right)^2 \left(\frac{1-2\nu}{1-\nu}\right)^2 + \left(\frac{\lambda-1}{2\lambda}\right)^2 *}\;\right] \quad * \sigma_{msd} \ldots\ldots 41$$

Mechanical property of Sikaflex 265 is obtained from manufactures material technical specification and listed in table below.

Table 3.1.input adhesive mechanical property[46]

Material name	Young's modulus	Yield strain	Yield shear stress	Tensile yield stress	Poisson ratio
Sikaflex 265	13.3Mpa	450%	4.5MPa	6Mpa	0.4

Using above material property magnitude and putting in equation (40)

$$\beta = 3\frac{1-\nu}{1+\nu}\frac{\tau_{msd}}{\sigma_{msd}} - \frac{(1-2\nu)^2}{(1-\nu)(1+\nu)}\frac{\sigma_{msd}}{\tau_{msd}} = 3\frac{1-0.4}{1+0.4}\frac{4.5}{6} - \frac{(1-2*0.4)^2}{(1-0.4)(1+.4)}\frac{6}{4.5}$$

$$\beta = 0.904$$

Substuting β value in equation (39) we can calculate material sensitivity to hydrostatic stress as

$$\lambda = \left(\frac{1}{6}\right)\left(\beta^2 + \beta\sqrt{\beta^2+12} + 6\right) = \left(\frac{1}{6}\right)\left(0.094^2 + 0.904\sqrt{0.904^2+12} + 6\right)$$

$$\lambda = 1.67$$

Again Substuting λ values in equation (41) we can easily found material yield stress as

$$\sigma_F = \left[\frac{\lambda-1}{2\lambda} * \frac{1+\nu}{1-\nu} + \sqrt{\frac{1}{\lambda} * \left(\frac{1-2\nu}{1-\nu}\right)^2 + \left(\frac{\lambda-1}{2\lambda}\right)^2 * \left(\frac{1+\nu}{1-\nu}\right)^2}\right] * \sigma_{msd}$$

$$\sigma_F = \left[\frac{1.67-1}{2*1.67} * \frac{1+0.4}{1-0.4} + \sqrt{\frac{1}{1.67} * \left(\frac{1-2*0.4}{1-0.4}\right)^2 + \left(\frac{1.67-1}{2*1.67}\right)^2 * \left(\frac{1+0.4}{1-0.4}\right)^2}\right] * 6\text{Mpa}$$

$$\sigma_F = 5.78\text{Mpa}$$

Now we the material first invariant of stress tensor $I_1$and second invariant stress deviator J_2 is the given by as follow.

Note: In this analysis longitudinal direct stress, σ_x= 0 and depth wise σ_z also not included since we are working on plane as mentioned in assumption made in general analysis derivation and the only two stress we are going to use in this analysis are adhesive peel (σ_y) and shear stress (τ_{yx}) respectively. Therefore first invariant of stress tensor $I_1 = \sigma_y$ and the second invariant stress deviator $J_2 = \frac{(\sigma_x-\sigma_y)^2+(\sigma_y-\sigma_z)^2+(\sigma_z-\sigma_x)^2+6(\tau^2_{xy}+\tau^2_{yz}+\tau^2_{zx})}{6}$……42

$$J_2 = \frac{(-\sigma_y)^2+(\sigma_y)^2+6(\tau^2_{xy})}{6} = \frac{2(\sigma_y)^2+6(\tau^2_{xy})}{6}$$……..……...43

$$J_2 = \frac{(\sigma_y)^2}{3} + \tau^2_{xy}$$…….……...……..44

Now we can write the failure criteria condition as

$$\left(\frac{\lambda-1}{2\lambda}\right) I_1 + \sqrt{\frac{3}{\lambda}J_2 + \left(\frac{\lambda-1}{2\lambda}\right)^2 {I_1}^2} = \sigma_F$$ ……...…45

$$\left(\frac{1.67-1}{2*1.67}\right)\sigma_y + \sqrt{\frac{3}{1.67}\left(\frac{(\sigma_y)^2}{3} + \tau^2_{xy}\right) + \left(\frac{1.67-1}{2*1.67}\right)^2 {\sigma_y}^2} = 5.78$$……..……46

$$0.2\sigma_y + \sqrt{1.8\left(\frac{(\sigma_y)^2}{3} + \tau^2_{xy}\right) + 0.04{\sigma_y}^2} = 5.78 \text{ MPa}$$……47

After some manipulation, the equation of failure envelope for this material will be

$$1.8\tau^2_{xy}+0.6\ {\sigma_y}^2+2.13\sigma_y = 33.4$$…….……48

Graphically it looks like that has been shown below

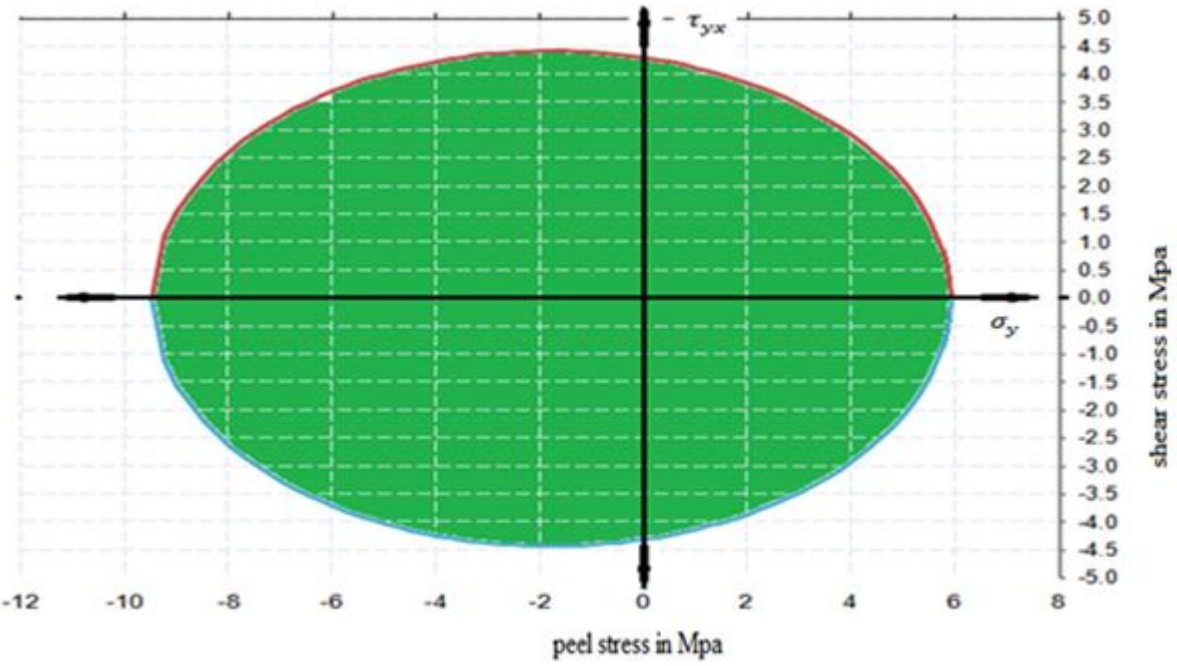

Figure 3-9. Failure envelop of Sikaflex 265, using Drucker-Prager criteria (the green area is safe region)

3.4. ANALYSIS INPUTS

Using above formulas and substituting corresponding values in equation will result in the required values of stresses. The adhesive type selected for this analysis is called Sikaflex 265 with Young's modulus of 13.3 MPa and poison ratio v=0.4 as indicated in table 3.1. This adhesive currently used by Anbessa bus body building garage to join front glass to frames of the body. Since the whole objective the research work is to apply some scientific analysis to joint and try to standardize this adhesive type is selected.

This adhesive strength is somewhat lower than other adhesive used for this application. Since the failure criteria is set that mean we can easily arrived at the values of loads that may cause the failure to the joint. The magnitude of the moment depends on the pattern it modeled in ABAQUS. In that software the moment is applied in kinematic coupling. And therefore direct multiplication tensile force with adhesive thickness is less sound and it is better to use reaction moments in post processing values of the analysis.

The geometries of joints are selected according to the standards which are mentioned in geometry subcategory in numerical modeling. Most of the time lengths of the joints are 20-25 mm and to reduce bending stress of adherend the thickness is set to 3mm. using above values and substituting in the equations simply the effect of the adhesive thickness can be shown by varying the adhesive thickness. Material specification of adherends are table below And their mechanical properties [48, 49] are also mentioned.

Table 3.2input adherend material specification

Adherend	Young's modulus In MPa	Poisson ratio
Steel	210000	0.3
Aluminum	73800	0.33
Glass(tempered)	70000	0.23
GFRP	E_1=26000,E_2=26000,E_3=8000, Nu_{12}= 0.1,Nu_{13}=0.25 Nu_{23}= 0.25 G_{12}=3800,G_{13}=2800,G_{23}=2800	

CHAPTER FOUR

4. RESULT AND DISCUSSION

4.1. Analytical vs. Numerical analysis results and interpretation

To validate both works two the result found of both analyses should be the equal or approximated. It is well know that the numerical results are somewhat approximate and may not exactly coincide with analytical one. After validification it is mandatory to stick to one of the either since the result is the same. Using the peel stress and shear stress equation derived in chapter two one can easily plot the stress profiles that is induced in the joint. The input material specifications and loading magnitudes are listed in table 4.1 and table 4.2

4.1.1. Peel stress results

From equation (21) the peel stress equation will be

$$\sigma_y = D_1 \cosh(m_1 x) + D_2 \sinh(m_1 x) + D_3 \cosh(n_1 x)\cosh(n_2 x) + D_4 \cosh(n_1 x)\sin(n_2 x)$$

$$+ D_5 \sinh(n_1 x)\cos(n_2 x) + D_6 \sinh(n_1 x)\sin(n_2 x)$$

Substuting the values of loads, adherend and adhesive in equation (31) up to equation (34) by using the below input parameters listed in table below

The adherend used for comparison of the two works are Aluminiu-sikaflex-Aluminium. The position of loads on analytical formula derivation should be consistent with the manner it has been putted in table 4.2

Table 4.1 detail input material specification

Adherend properties				Adhesive property	
E_1	73800 Mpa	E_2	73800 MPa	E_a	13.3Mpa
v_1	0.33	V_2	.33	v_a	0.4
G_1	27744MPa	G_2	27744MPa	G_a	4.8 MPa
L		L		L	20mm
h_1	3mm	h_2	3mm	T	0.5mm

Table 4.2 load values for analytical

T_{11}	10N	T_{12}	0
V_{11}		V_{12}	0
M_{11}	-39Nmm	M_{12}	0
T_{21}	0	T_{22}	10N
V_{21}	0	V_{22}	0
M_{21}	0	M_{22}	39Nmm

Up on substitution of the values input parameters the peeling stress equation will be

$\sigma_y = 3.8*10\hat{}\text{-}14\sinh(0.0176x) + 0.1314\cosh(0.0856x)\cosh(0.0856x) - 0.2335\cosh(0.0856x)\sin(0.0856x) - 0.2335\sinh(0.0856x)\cos(0.0856x) + 0.2856\sinh(0.0856x)\sin(0.0856x)$

Graphically

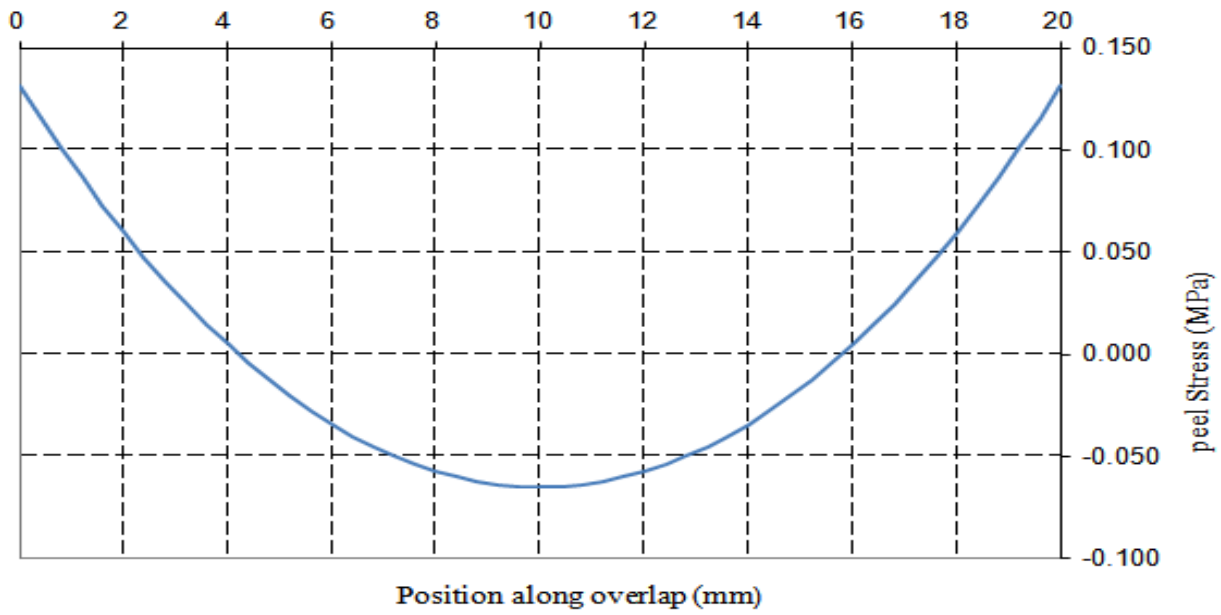

Figure 4-1 peel stress profile along adhesive length at middle of film

4.1.2. Shear stress results

Similarly the equation that represents the shear stress created in the joint (equation20) for this specific geometry and loading condition with substitution of the values will be as shown below

τ_{xy} = -9.18*10ˆ-1cosh(0.0176x) + 1.6*10ˆ-1 sinh(0.176x) -1.2*10ˆ-17cosh(0.0856x) $cosh$(0.0856x) -1.52*10ˆ-17 cosh(0.0856x) sin(0.0856x) 5.8*10ˆ-18sinh(0.0856x) cos(0.0856x) -3.2*10ˆ-19 sinh(0.0856x) sin(0.0856x) +4.08*10ˆ-1

Graphically

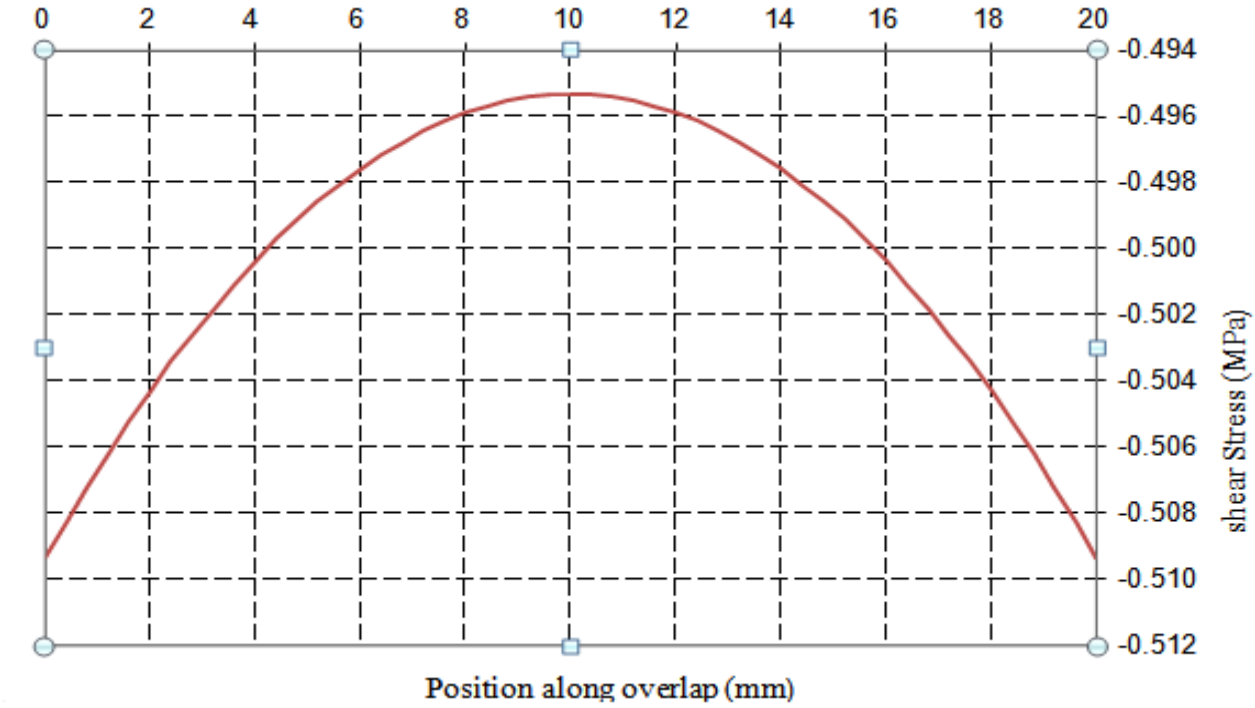

Figure 4-2. Analytical result for shear stress profile along bond length at middle of film

From this analytical graph the stress values at the end of bond length higher than the stress found at the middle of the bond length. But in numerical analysis the ends of bond length is almost lower and results stress free end. This is due to short come of analytical one. That means in the analytical analysis the issue at free end of bond length not included in work of Bigwood and Crocombe [19]. Since the ABAQUS includes this issue we can get accurate information form that. The stress used as a design stress for purpose of finding failure load is from Abaqus for the reason indicated above.

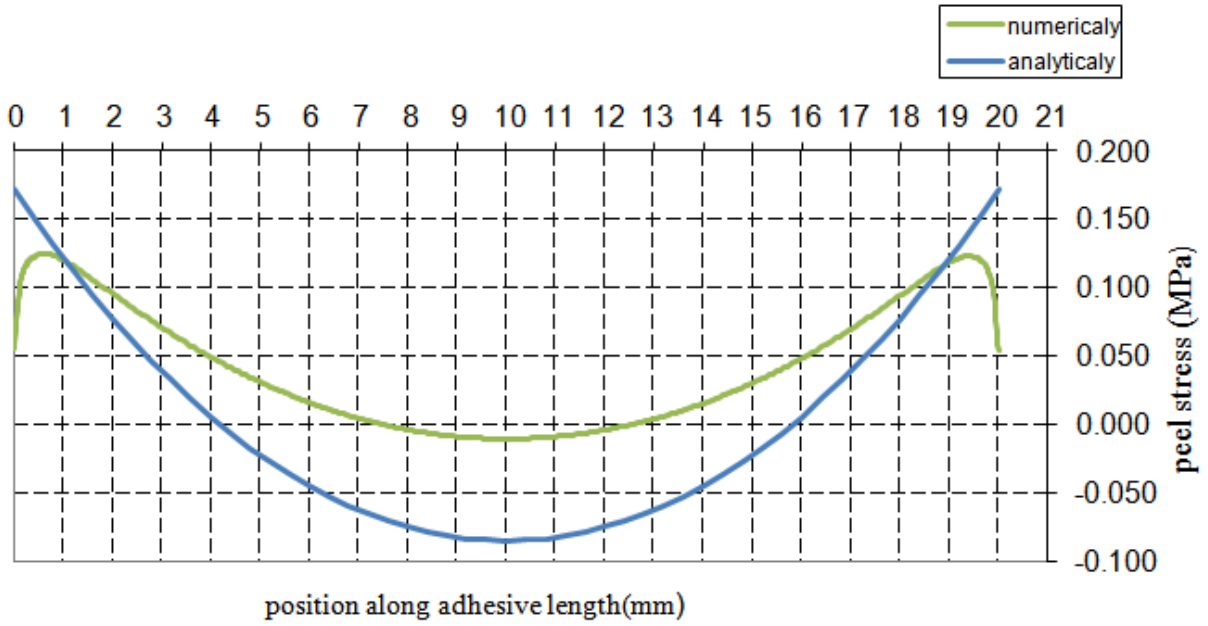

Figure 4-3.Numerical Vs Analytical peel stress result at middle of the film

From fig 4.3 the stress values at middle of somewhat deviate from each other. But at end of the bond length or a critical loaction that is mandatory to decide the design stress (at 1mm from left and 19mm at right) they coincide. Therefore their deviation from each other at middle of the film doesn't affect the entire work to decide the failure load or failure stresss since the mesh convergence is achieved for numerical analysis for structured type of meshing technique as shown in fig 3.7 and failure result is read from numerical one

Simmilarly the comparison of shear stress is also have the same issue that the analytical one donot include about the stress free end. But in shear stress profile at middle of the joint the two results coincide better than the peel stress as shown ing fig4.4 below

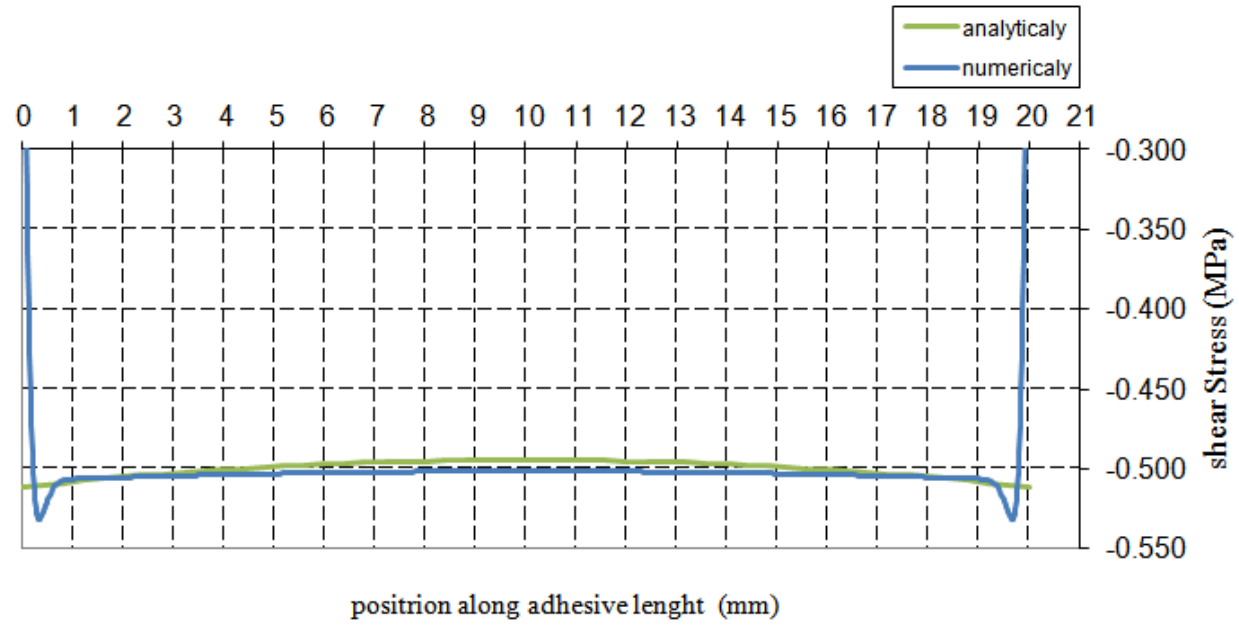

Figure 4-4.numerical vs. analytical shear stress result at middle if the film

After using this analysis for validification of both method work it is preferable to stick to one of the analysis as it requirements. The Numerical one give accurate results and indicate the position of high stress concentration. And this stress values can be used as design stress to decide the failure load.ABAQUS model that show issue of stress at end of bond length is shown in fig 4.5.below

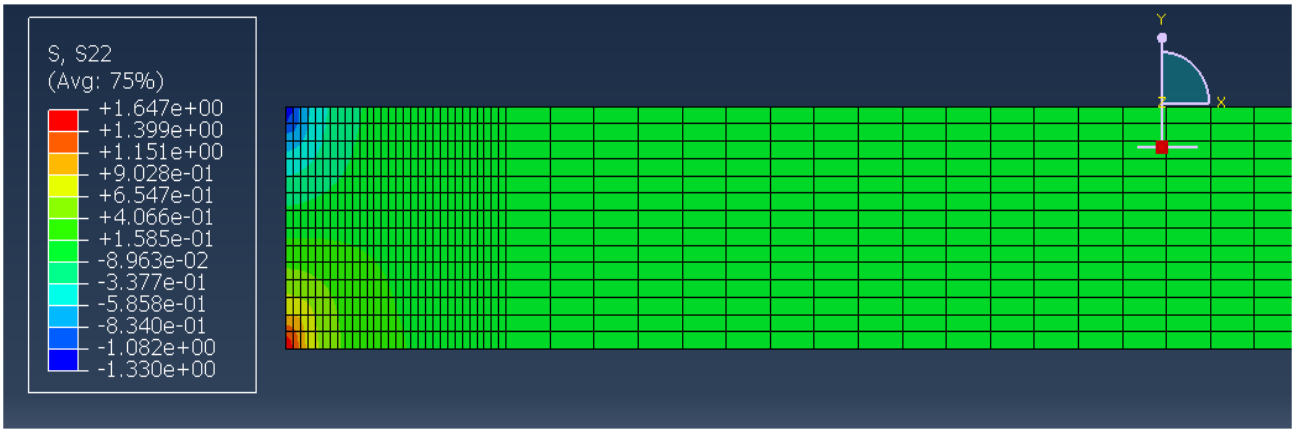

Figure 4-5.ABAQUS peel stress result at left free end

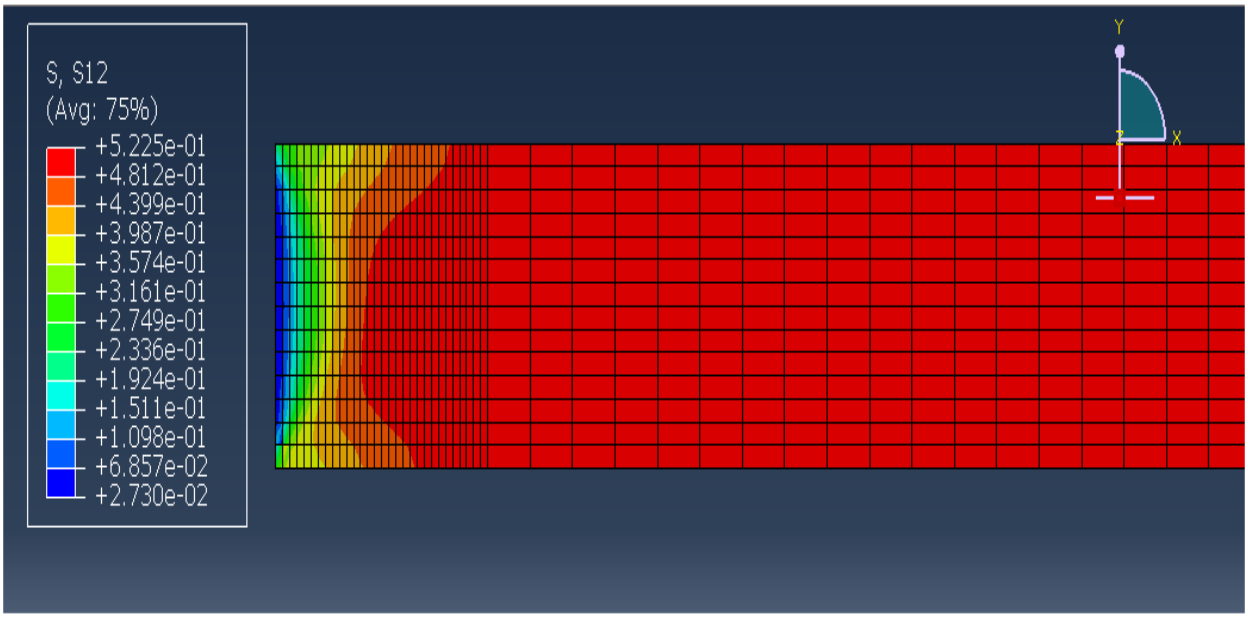

Figure 4-6.ABAQUS shear stress result at left free end

From fig.4.5 above the peel stress magnitude is high at the corners and those stress values can be used as a design stress. And again also from fig.4.6 one can easly see their coincidence with shear stress profile at fig. 13 that mean at left endof middle of the film the stress values are represented with blue color(lower relatively) whlie at some length (about 1.5mm from left end) the stress is represented in red meaning higher relative to the other bond length as usual representation in FE analysis.

Therefore to decide the magnitude the failure load appropriate selection of critical position is mandatory. In numerical analysis ABAQUS can tell directly the postion of maximum stress values. From fig 4.5 shows exact position of extreme stress values wich is at is corners. But for fig 4.6 it is not easy as fig 4.5 and then allowing the ABAQUS to tell the position will be the only solution.

4.2. Parametric analysis

In this analysis derivation, there are many variables that build up the peel stress and shear stress equation.Those variables are adhesieve bond length(L), adhesive thickness(t), adherend thickness (h_1,h_2), adherend matterial type that depend on youngs modulus(E_1,E_2), Load values(T,V,M) and adhesive type (E_a). By increasing and decreasing the values of those variables it is easy to show the effect of the variables on stress induced in the joint.

4.2.1. Effect of adhesive thickness

The tichkness of adhesive is one variable that build up the equation of the stress of single lap adhesive joint. Increasing the thickness increases the arm that is perpendicular to the tensile load wich will cause bending moment due to eccentricity of applied tensile load and reaction force at boundary[51]. At frist glance it seems that increasing the thickness of adhesive will increase strenght of the joint. For adhesive that has high ductlity like sikaflex, the probablity of affection by this created bending moment is high. But for adhesive with high strenght like epoxy the influence is very low. By varying this thickess value we can easly show its effect on strenght of joint.

Fig 4.5 and fig 4.6 shows peel and shear stress distribution in adhesive film respectively. Since peel stress magnitude is high at sharp corners of adhesive wich is at intererface, it is better to show the adhesive thickness effect by plotting it at interface rather than at middle of adhesive film.Fig.4.7 below show the effect of varous adhesive thickness for the adherend –adhesive sandwich made of steel and aluminium and sikaflex 265 as adhesive at same load of 32 N at adhesive adherend interface for peel stress. Fig 4.8 is for shear stress at mid of the film. From the values of maximum peel stress shown at top corner at left side of fig 4.7,The stress labelled 5.7 Mpa is for 0.5mm thickness and 4.29Mpa is for 0.1mm wich shows load carrying capacity of the joint decrease as thickness increase.

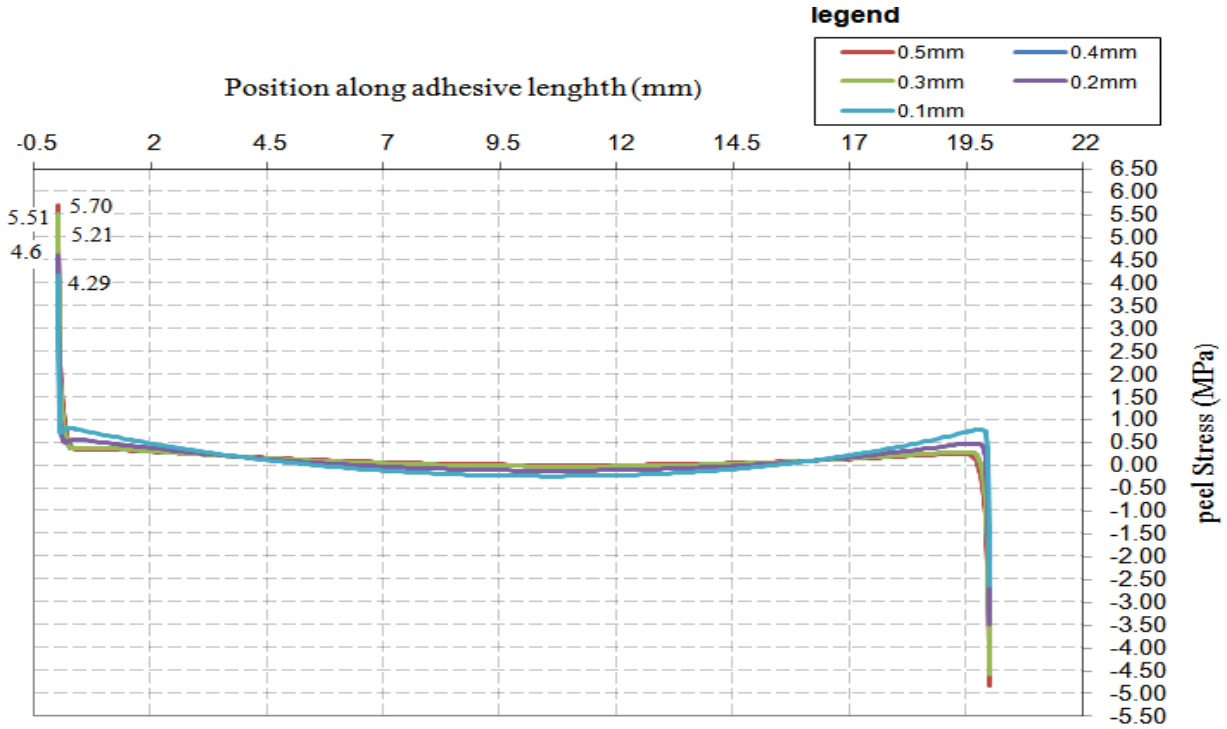

Figure 4-7.Peel stress of steel- Sikaflex- aluminum profile at bottom in interface for various thicknesses

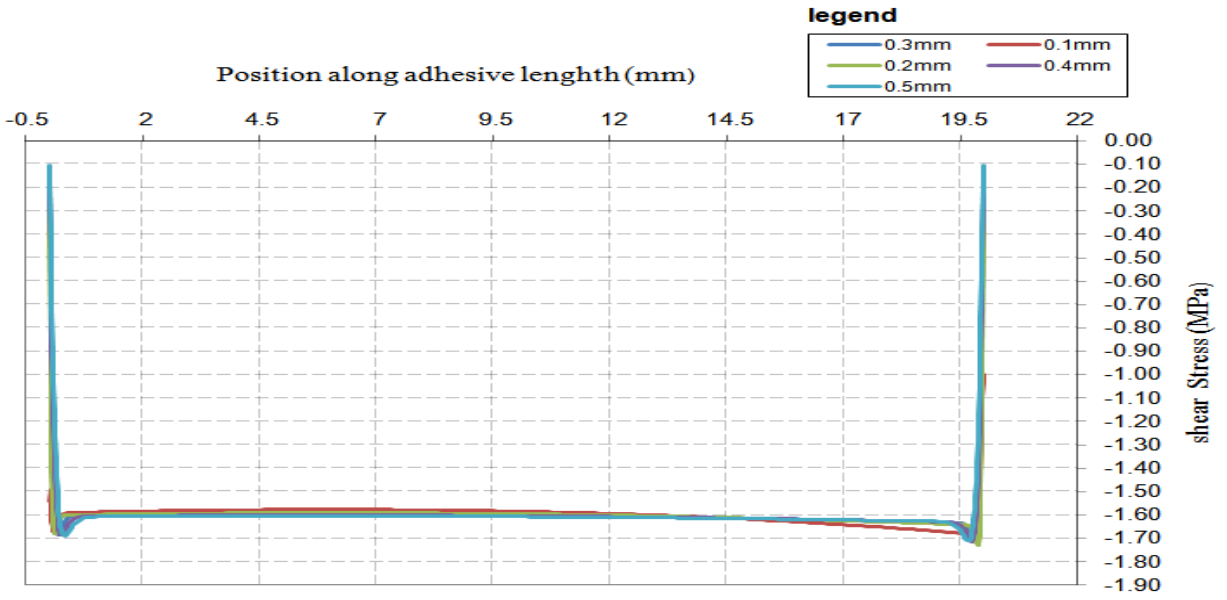

Figure 4-8.shear stress profile of aluminum-Sikaflex- steel for various thickness at mid of the film

The above two figures shows the variation of stress as the thickness of the film varies. This indicates that load carrying capacity of the joint depends the thickness as well other variables. Failure load for each thickness can be determined by using the failure envelope of this Sikaflex that is indicated in fig.3.8 and both stress magnitudes found at corners of the joint as shown in fig 4.5 and fig 4.6. The stress profile shown in fig 4.8 and fig 4.9 found at middle of the film and purpose of showing the effect of the variables. The failure stresses are those stresses at four corners of the films for peel stress and at about 1.5mm from left end for shear stresses. So the failure load for Aluminum- Sikaflex- steel sandwich is as shown below

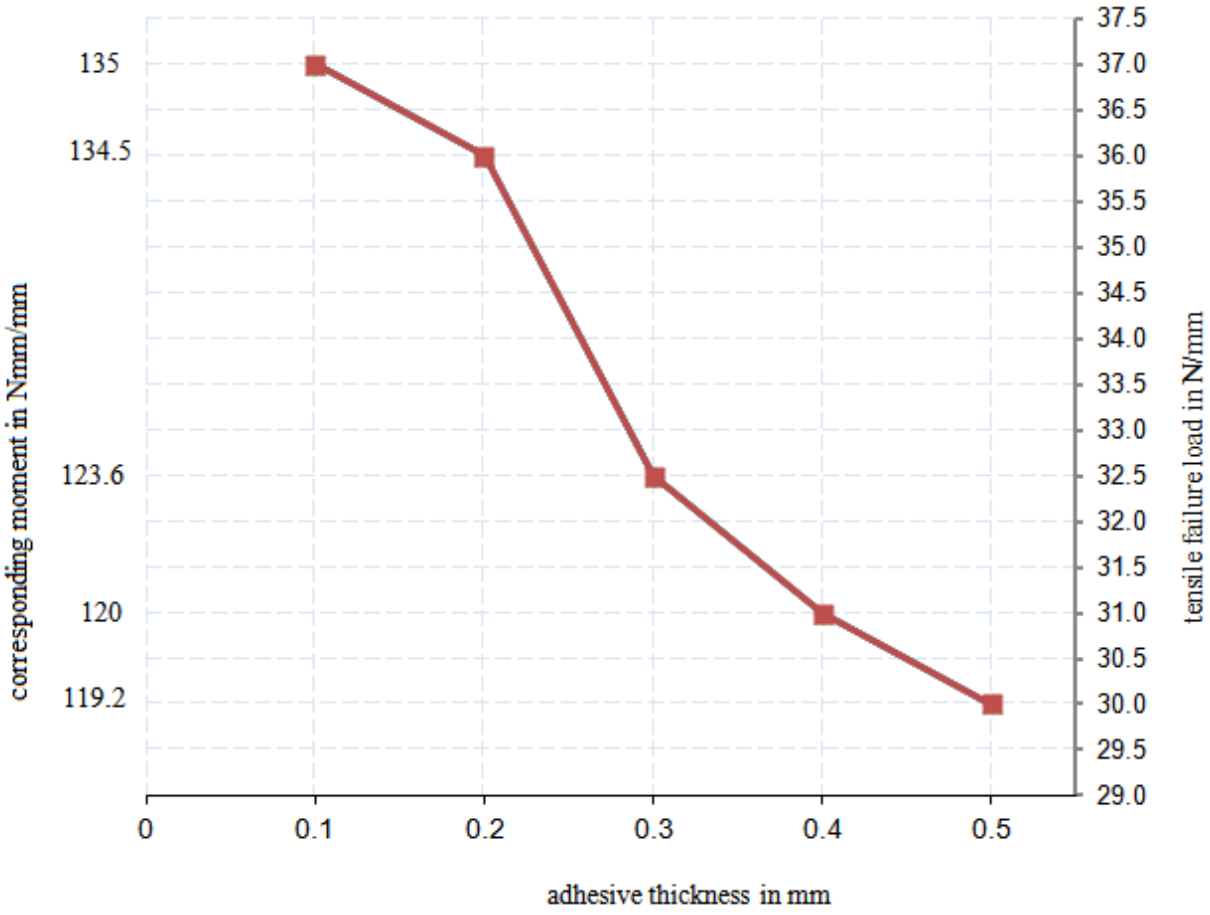

Figure 4-9. Failure load for various thickness for Aluminum- Sikaflex- steel sandwich

Therefore for above combination of material or variables the load values should not exceed these values to prevent failure in joint. One thing should be noted is those above figures can help to predict whether the failure occur or not and but how the failure occur (cohesive, adhesive, adherend failure) or simply failure type cannot predicted since it depends on experimental work.

By similar manner failure load and effect of thickness variation for steel-Sikaflex- Glass can be shown.fig 19 below is done for 35N tensile force for purpose of showing the effect.

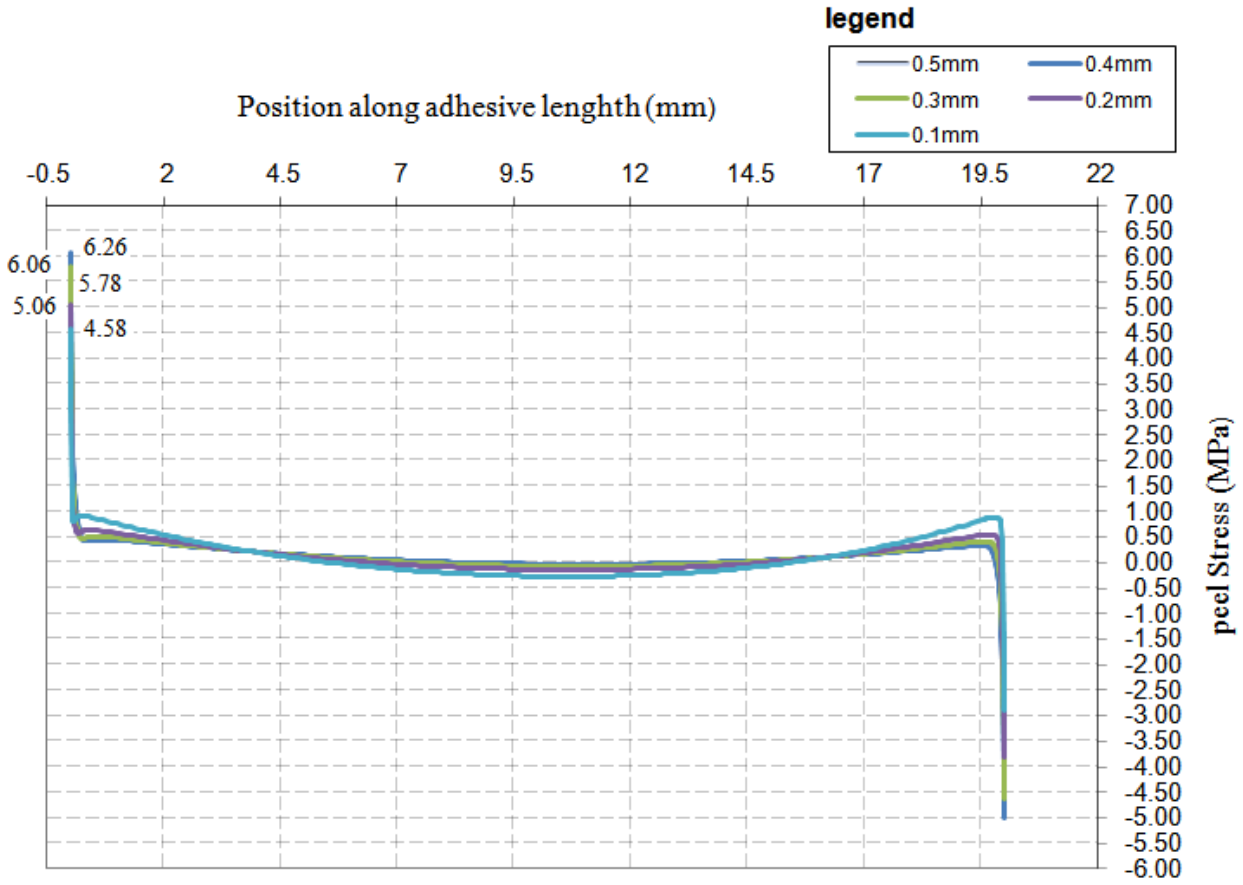

Figure 4-10.peel stress for various thickness for steel- Sikaflex-glass sandwich at bottom interface

As shown in fig 4.11. There are various stress magnitude and profile for various thickness of adhesive film. Therefore to prevent failure in joint exact values of loads for each thickness should be determined in the same manner done for steel aluminum sandwich. So the failure load for each thickness is shown in fig 4.12 below. Fig 4.13 is done for aluminum to aluminum at 40N load for purpose of showing adhesive thickness effect in similar way done for other metals.

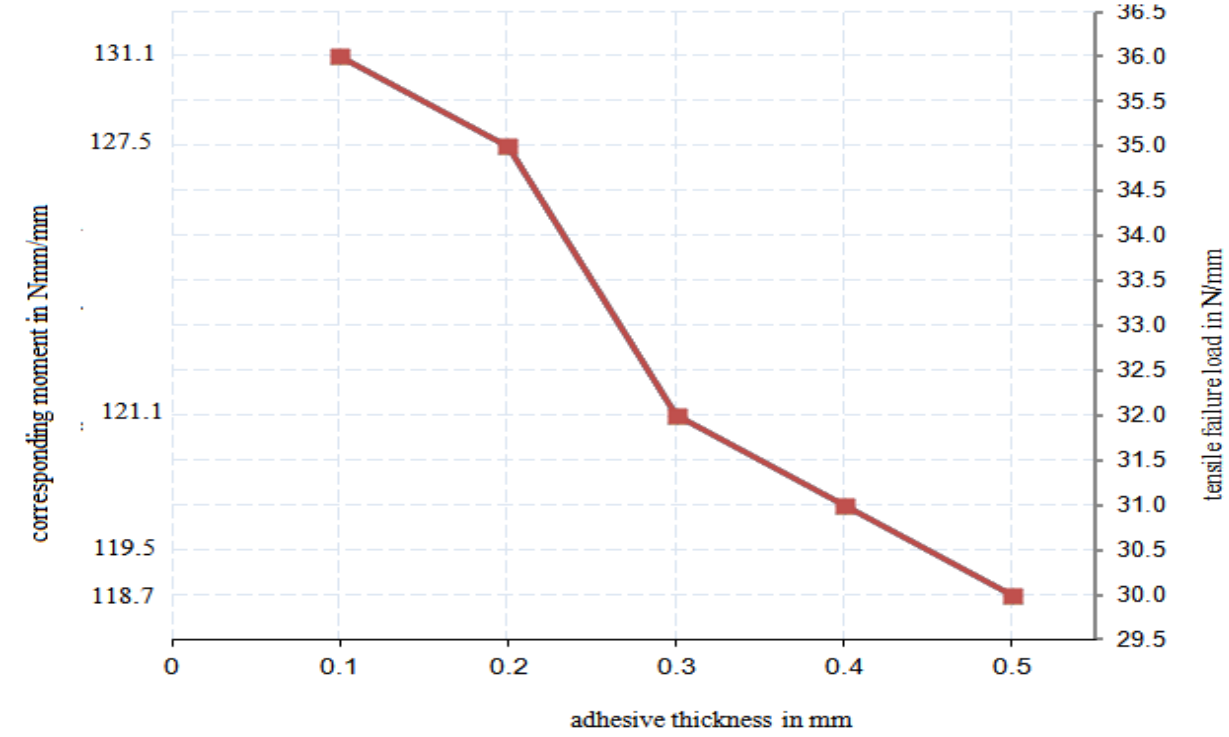

Figure 4-11. Failure loads for Steel-Sikaflex- Glass sandwich

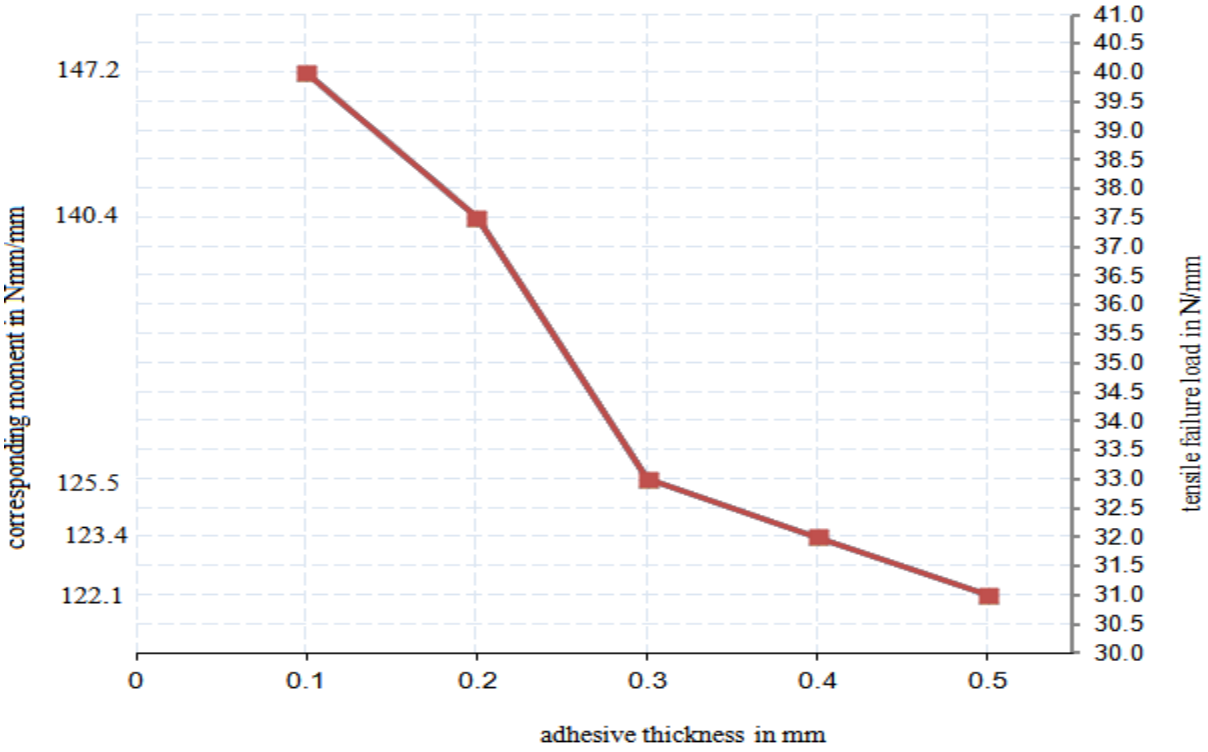

Figure 4-12. Failure loads for various thicknesses for steel-Sikaflex-steel

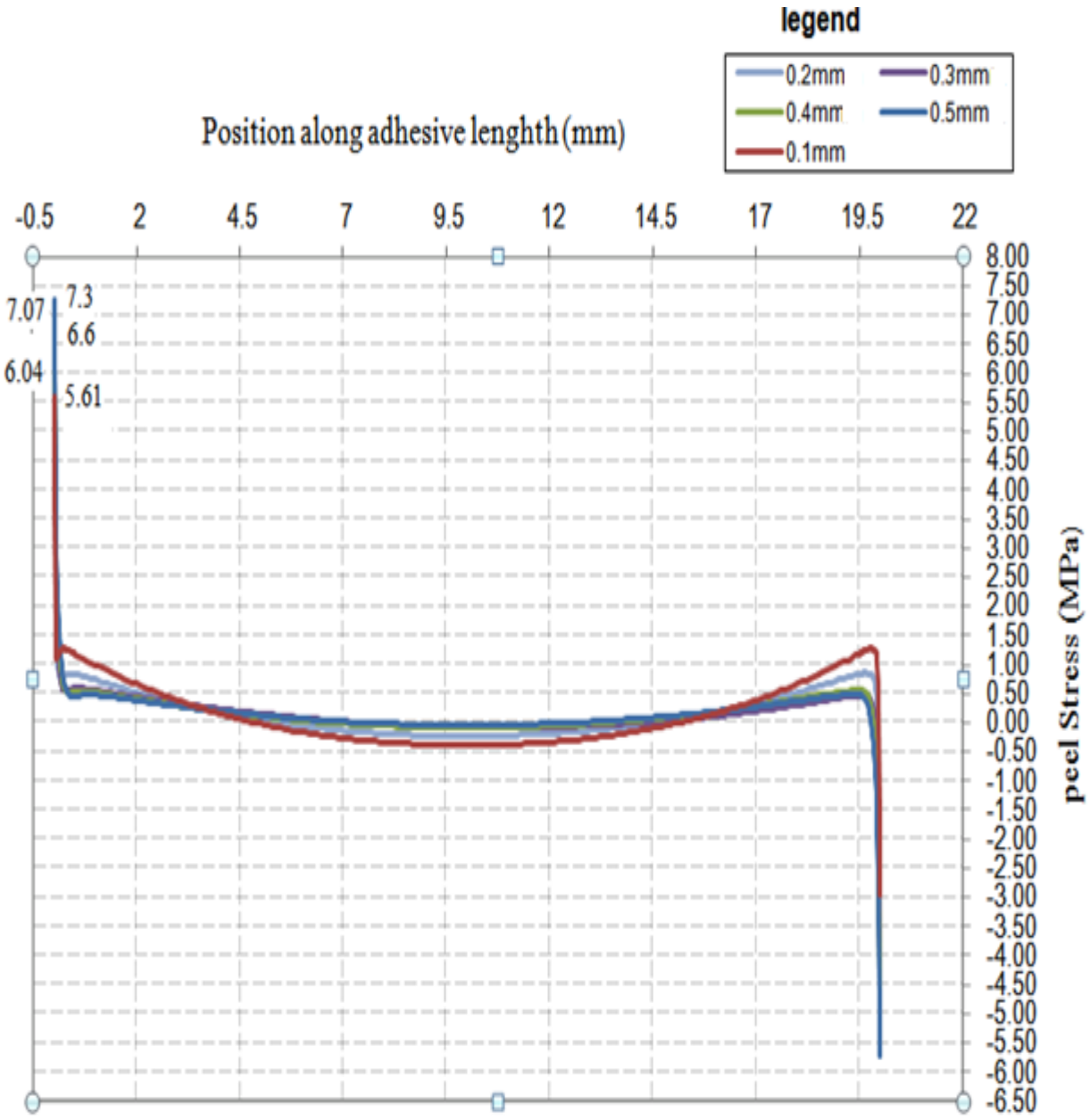

Figure 4-13.peel stress result for various thickness for AL-SIKA-AL at mid of film

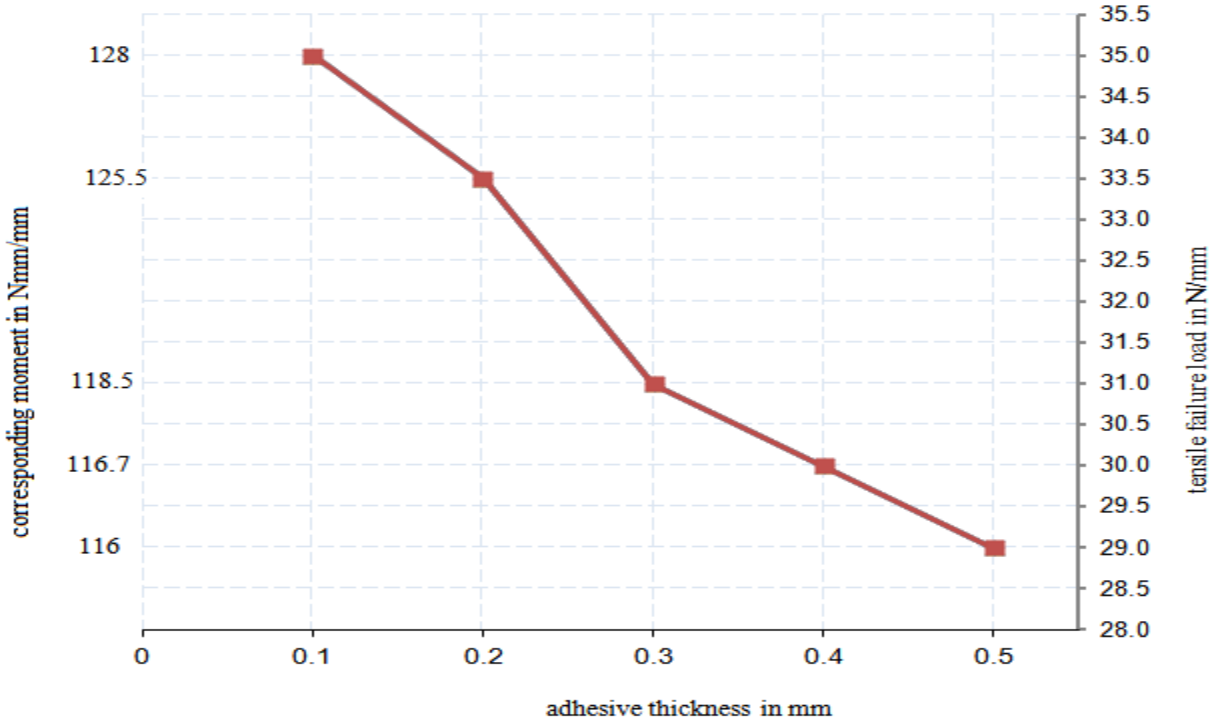

Figure 4-14. Failure load for aluminum-Sikaflex- aluminum sandwich for various thickness

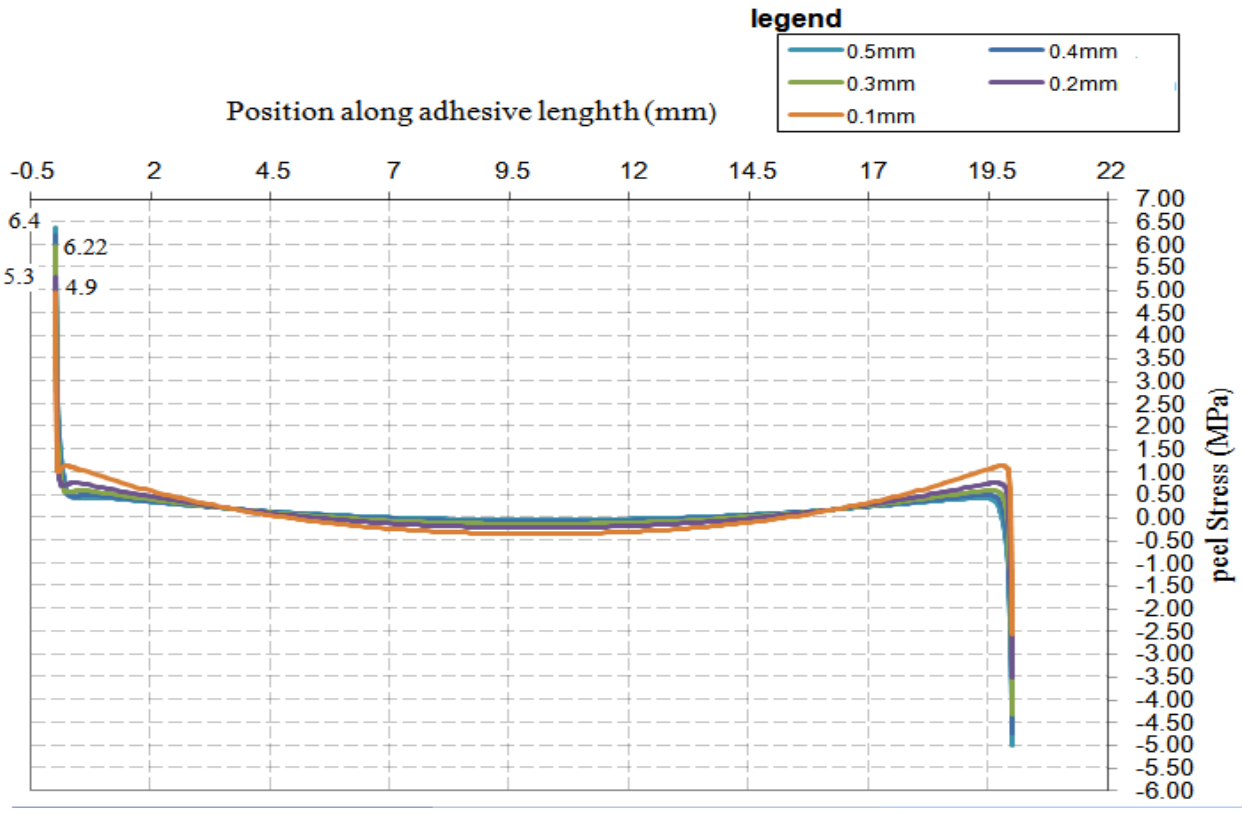

Figure 4-15. Aluminum-Sikaflex-glass stress profile for different thickness at mid of film

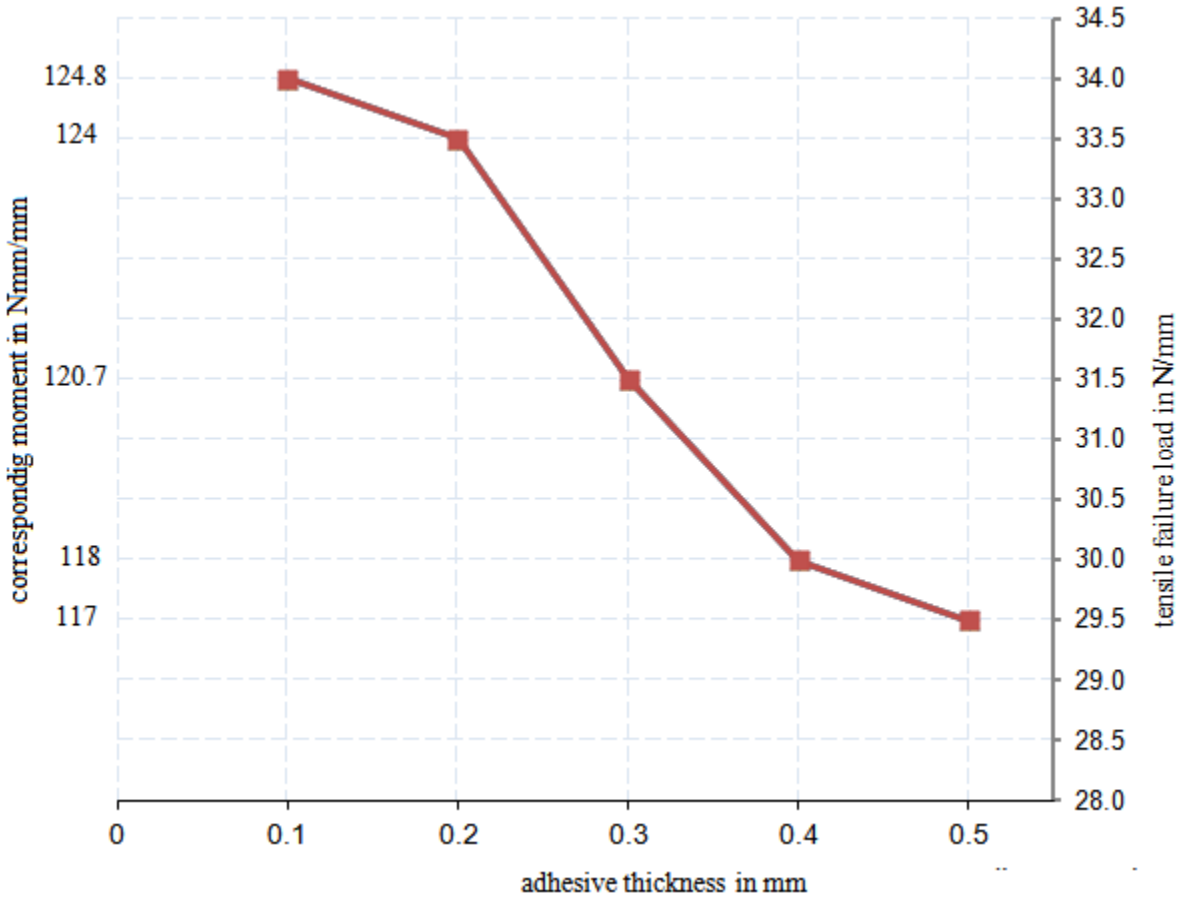

Figure 4-16.Failure loads for aluminum-Sikaflex-Glass

4.2.2. Effect bond length in joint

Total length of adhesive is called bond length. This variable is one the parameter that builds up the entire equation. The failure loads increased with Increasing overlap length because the overlap length provided a larger bonding area [51]. By varying this bond length the effect the parameter can be shown. Since the stress result depend on this variable, it is mandatory to know the magnitudes of the loads that each bond length can withstand. To do this the same procedure followed for effect of adhesive thickness can be used. By applying a tensile load then checking for readings of peel stress and shear stress if it fails in safe region of failure envelope of Sikaflex 265 of fig 3.13 or not. If it fails in safe region (the green one) that load cannot cause damage and the vice versa.

In similar way done for adhesive thickness, to determine failure load, selecting an area of high stress concentration mandatory. High stress magnitude is occurred corner end of interface of the adhesive and adherend. Fig 4.17 below shows stress profiles at upper interface of the joint and agrees with the idea that as bond length increase load carrying capacity of the joint increase. In similar manner Fig 4.18 below shows peel stress profile of the aluminum Sikaflex aluminum peel stress at bottom interface done for three different bond lengths under the same load, thickness, meshing technique, geometry except bond length. Bond length selected 15mm, 20mm and 25mm according to standard and the thickness is 0.2mm.

In similar manner failure load for steel, aluminum and glass is done depending of bond length effect as shown in fig 4.19 and fig 4.20

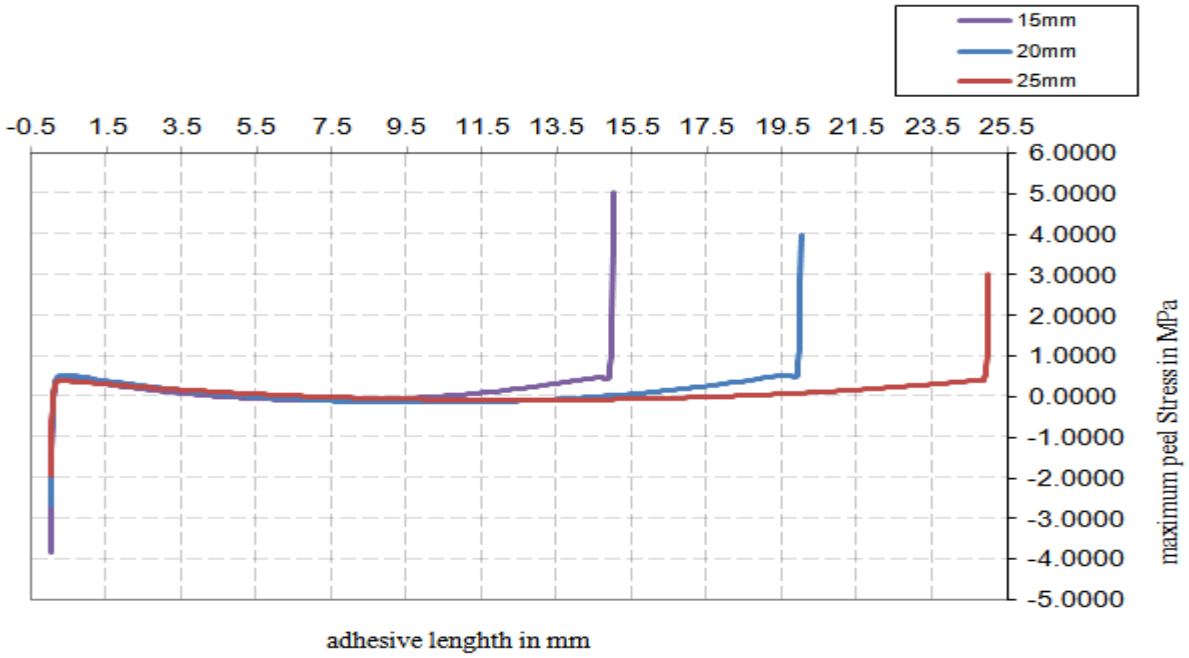

Figure 4-17.peel stress parametric study of effect of adhesive bond length for aluminum-Sikaflex- aluminum at upper interface (Numerically)

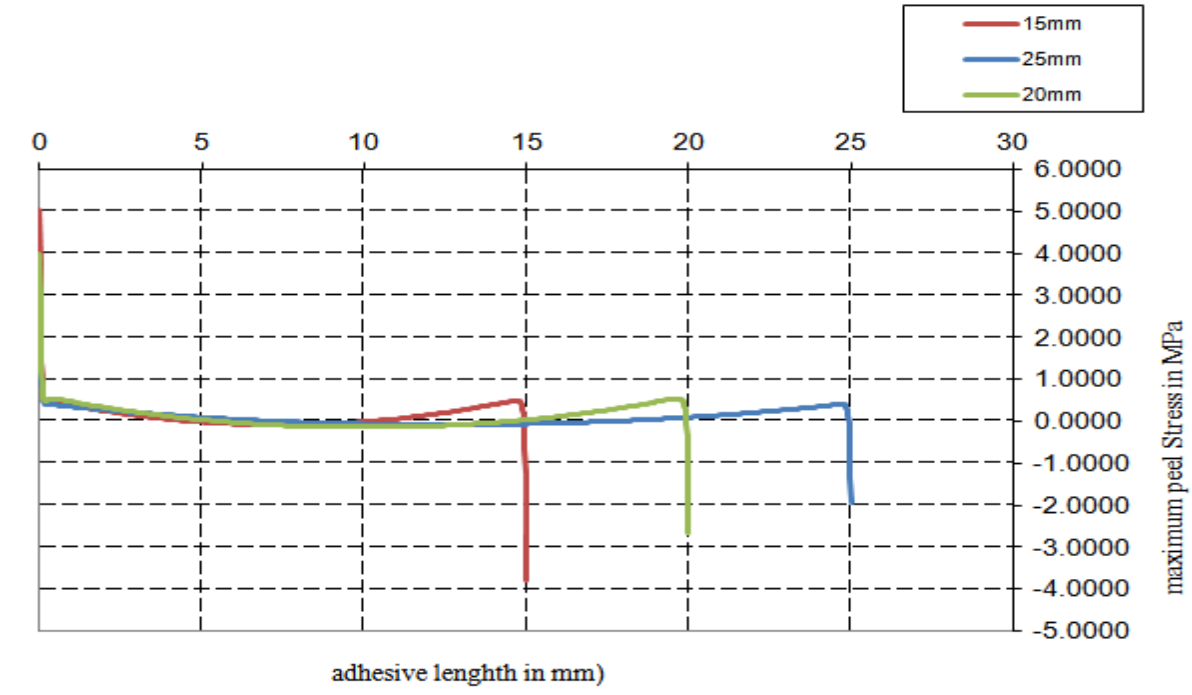

Figure 4-18.peel stress result for various bond length made Aluminiu-sikaflex-Aluminium at bottom interface (Numerically)

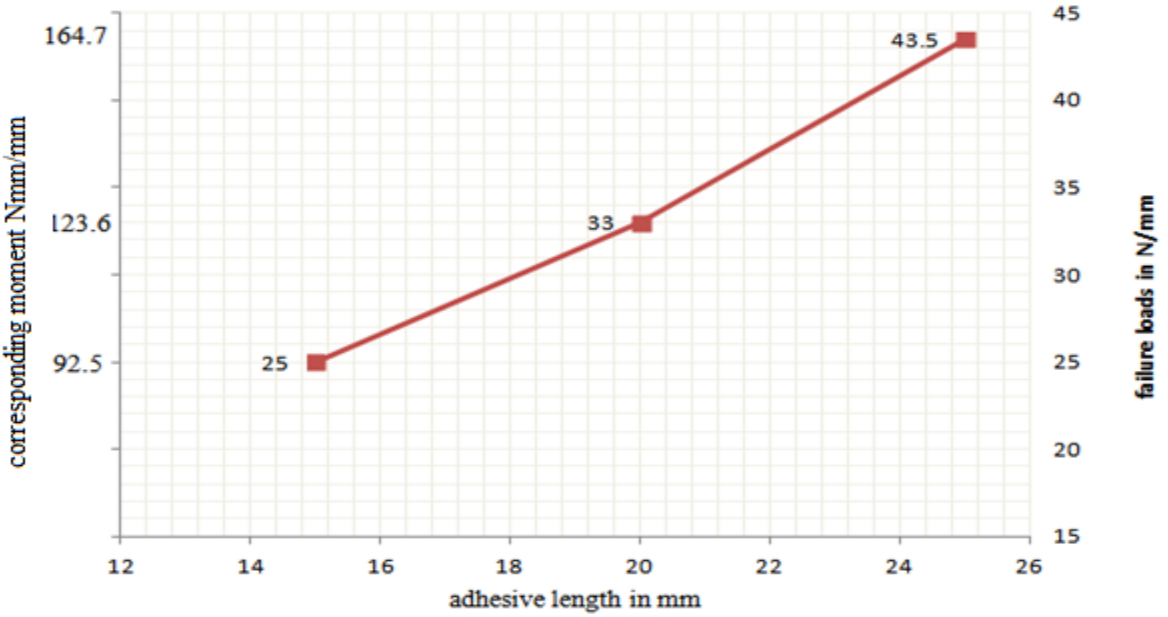

Figure 4-19. Failure loads for three bond length of Aluminum -Sikaflex - aluminum sandwich

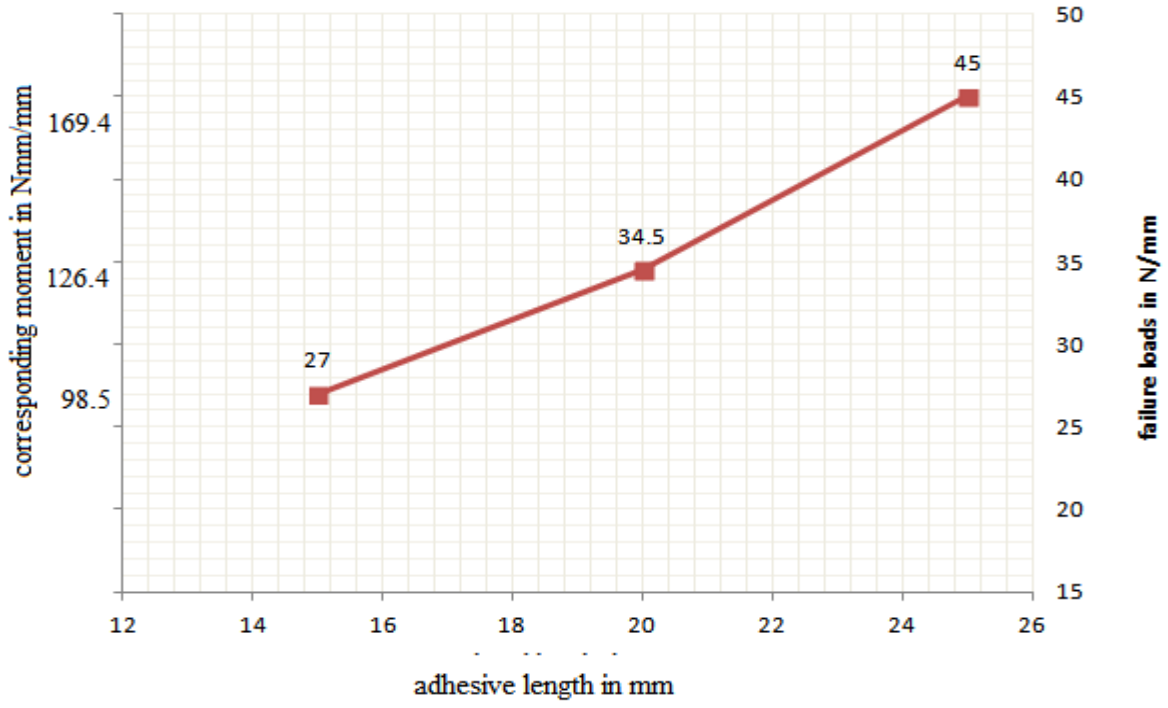

Figure 4-20.Failure loads for three bond length of steel -Sikaflex - glass sandwich

Composite materials

Composite material used in this analysis is GFRP (glass fiber reinforced plastic) and material property is defined in table 3.2 above. Unlike the previous analysis done, 3D solid extrusion modeling technique is selected to reduce the ambiguity to define fiber orientation of the composite adherend as shown in figure 4.22and 4.23 below. Geometries of adherends and adhesives are the same as done before for metals. Meshing technique used is the structured type of meshing so that it enables to eliminate element shape distortion that will have an influence on the result. Element type used is 3D stress which is compatible with this 3D modeling.

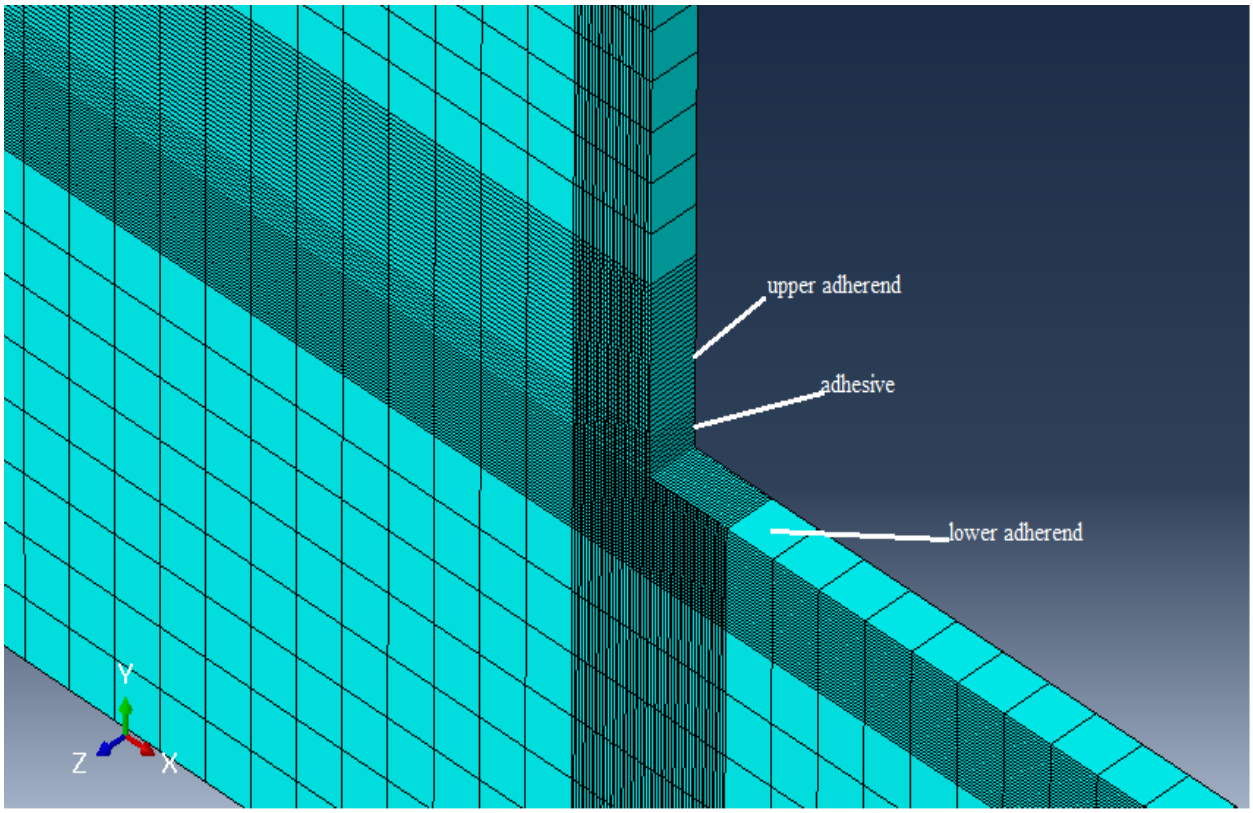

Figure 4-21 3D model of structured mes of composite single lap joint

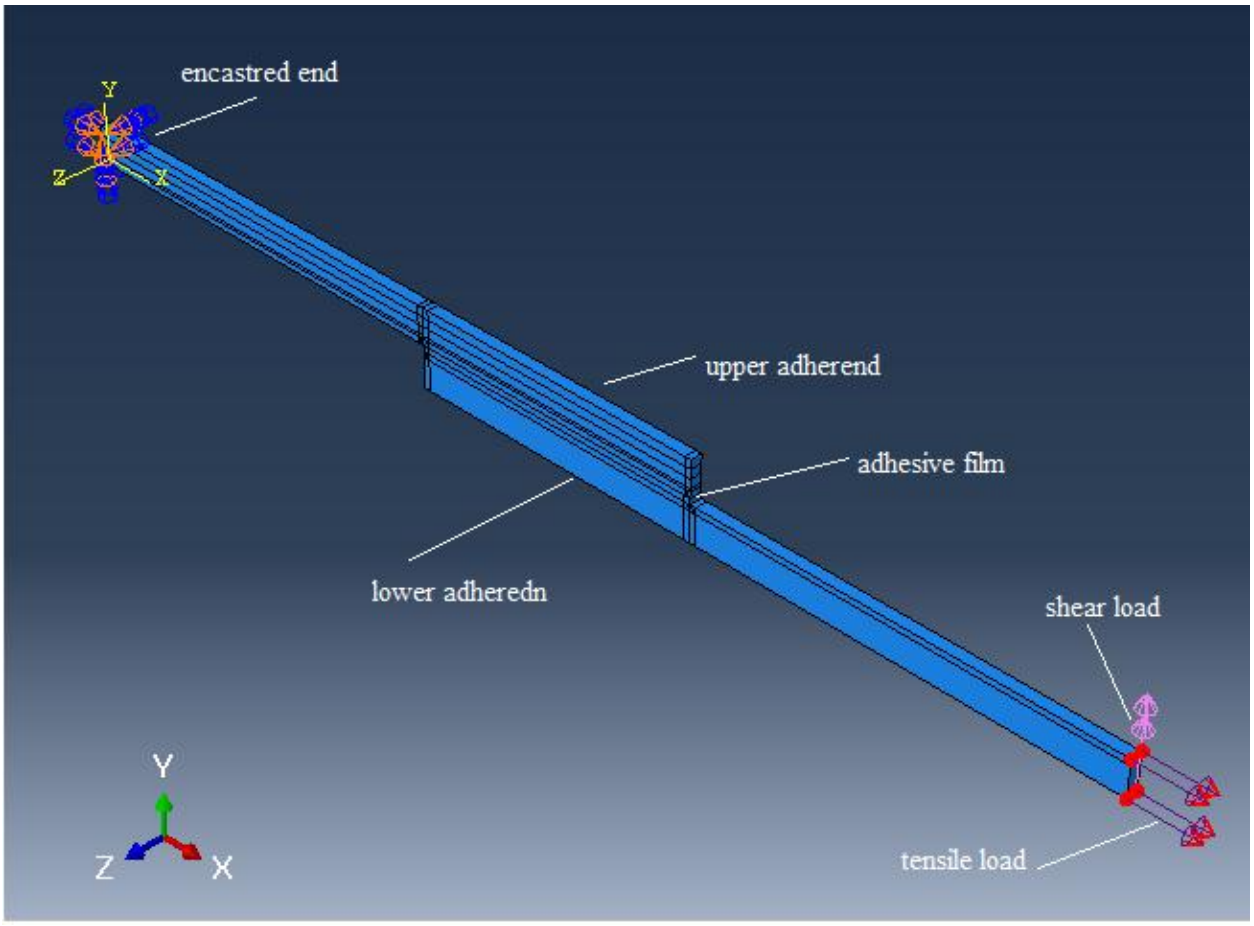

Figure 4-22 loading condition of the 3D composite single lap joint

Following the same procedures used in previous analysis effect of fiber orientation of composite on the joint strength is analyzed. The fiber orientation selected is 0/45/45/0, 0/45/0/45, 0/90/90/0, 0/90/0/90 and load for analysis is 25N tensile load and 2N shear load. The magnitudes of loads are lowered due to low load carrying capacity of the adhesive.

Fig 4.23 below shows the peel stress profile at bottom interface of the adhesive and adherend. From both interfaces the maximum stress is at the bottom that is why bottom is selected. Since the peel stress is high at sharp corners of adhesive which is found at end corners of interface it is recommended to plot the stress at this region to see the effects Rather than plotting at middle of film. The stress magnitude difference occurred at the two end is due to stiffness difference of the two adherends i.e. composite and metal. If the two adherend is the same material there is no difference in both two ends of adhesive end. Shear stress is not high at sharp corners therefore plotting at paths to corners will not show maximum stress.

Fig 4.25 below shows the design stress or the maximum peel stress occurred in the adhesive film for different fiber orientation of composite. It looks that the stresses are the same while it overlap as shown in fig 4.23 and 4.24 but at interface there is great difference as shown in fig 4.25 especially for symmetric and non symmetric composite used

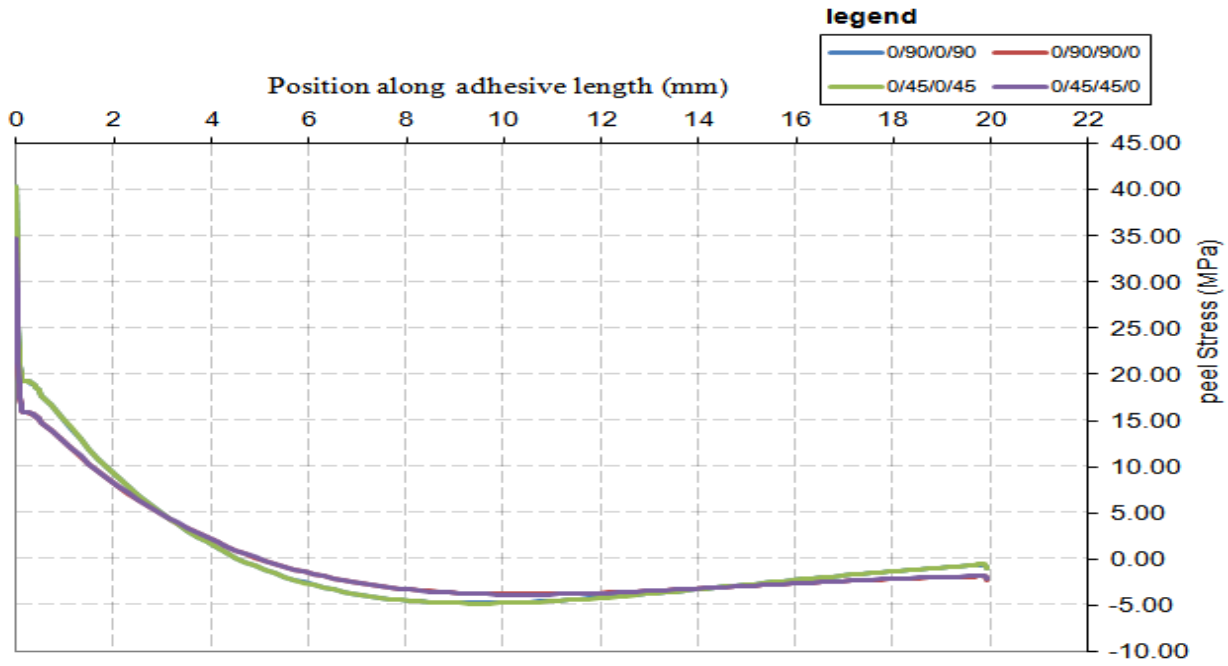

Figure 4-23 peel stress at bottom interface joint made of steel-Sikaflex-composite of different fiber orientation

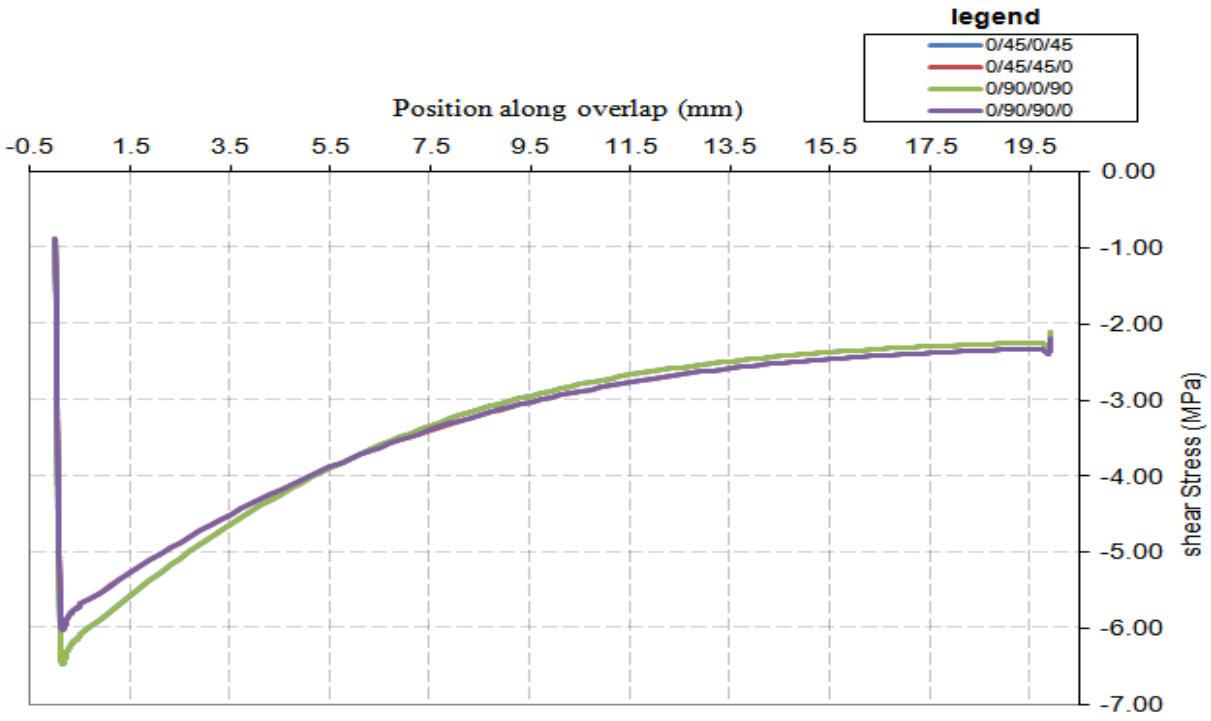

Figure 4-24 shear stress profile at middle of film of steel-Sikaflex-composite of different fiber orientation

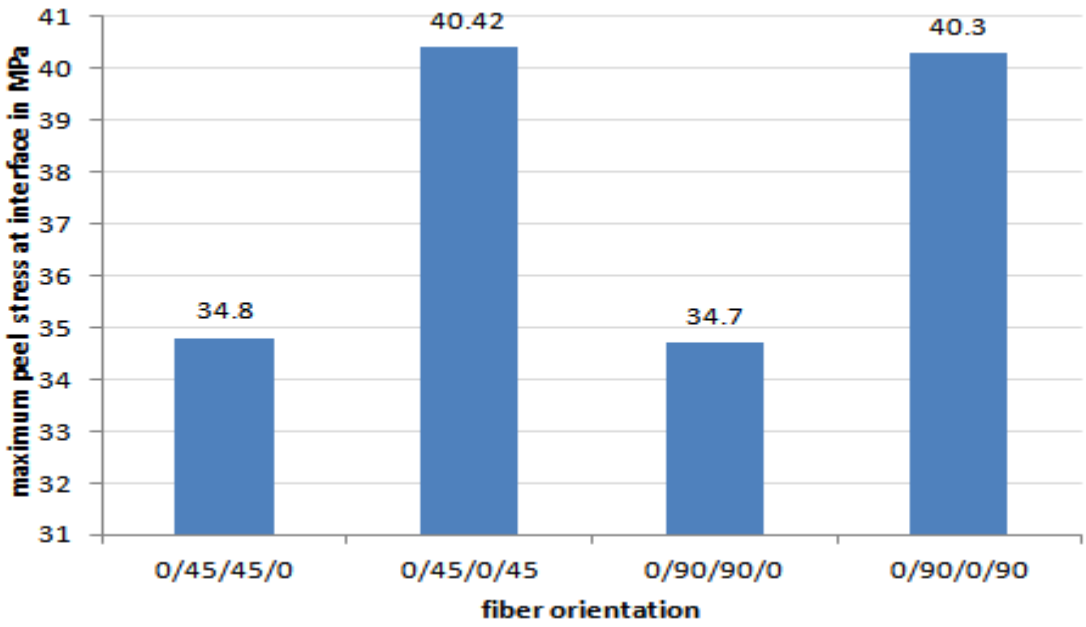

Figure 4-25 maximum peel stresses at joint bottom interface of steel-Sikaflex-composite of different fiber orientation

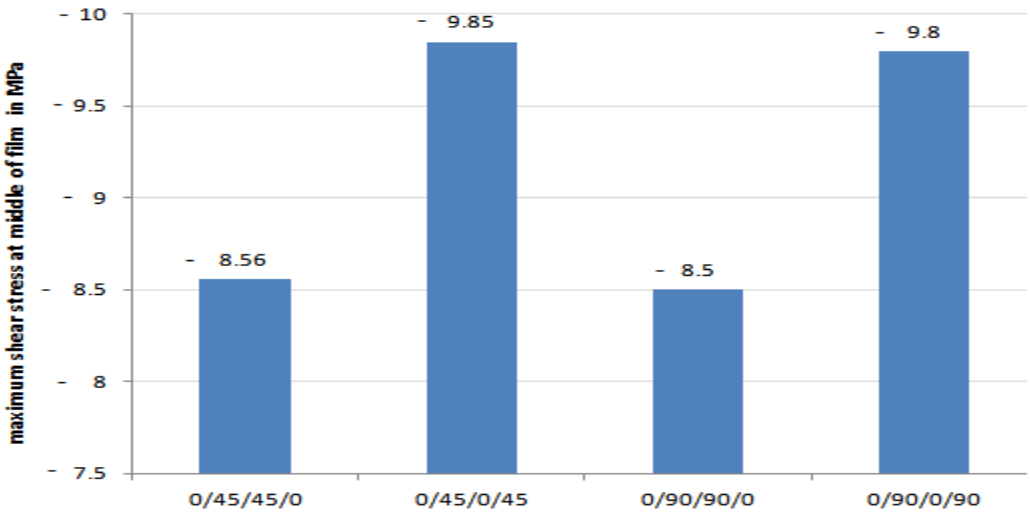

Figure 4-26.maximum shear stresses occurred in joint made of steel-Sikaflex-composite of different fiber orientation

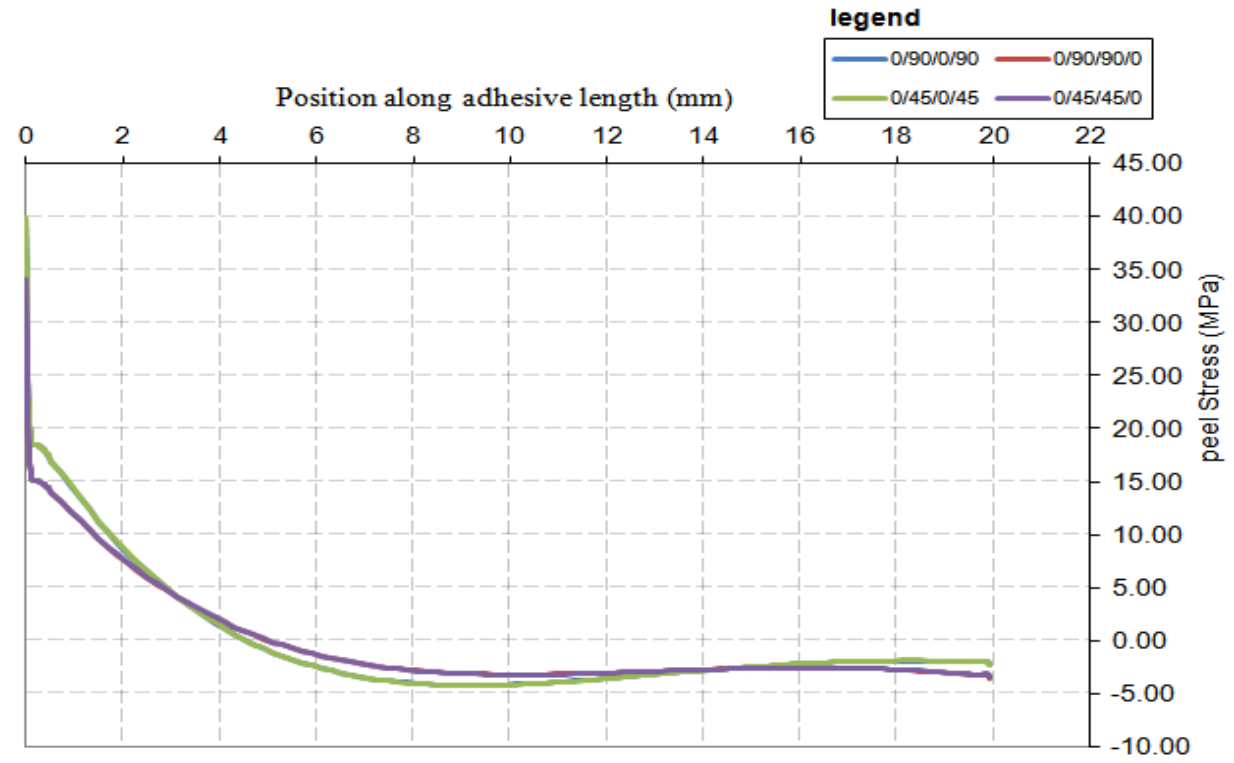

Figure 4-27 peel stress at bottom interface of joint made of aluminum-Sikaflex-composite of different fiber orientation

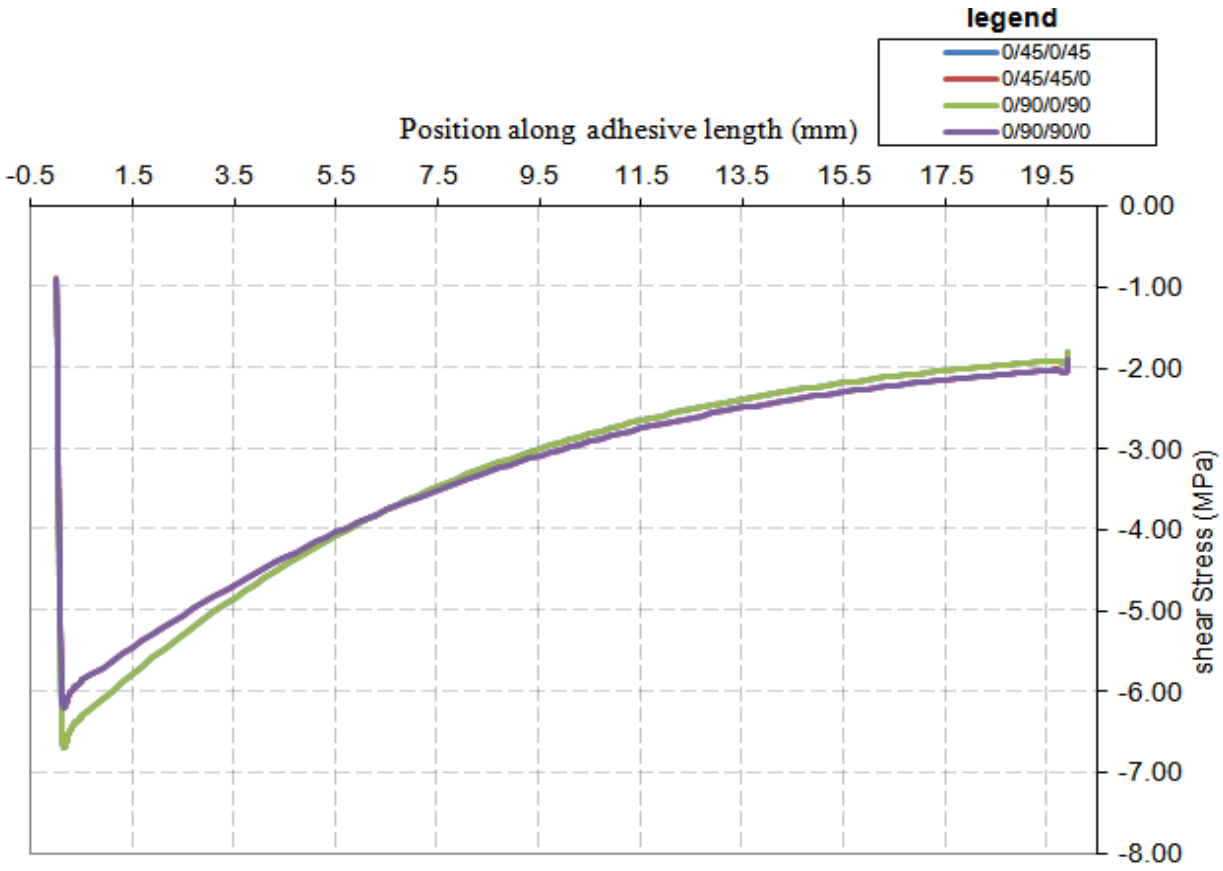

Figure 4-28.shear stress profile at middle of film of aluminum -Sikaflex-composite of different fiber orientation

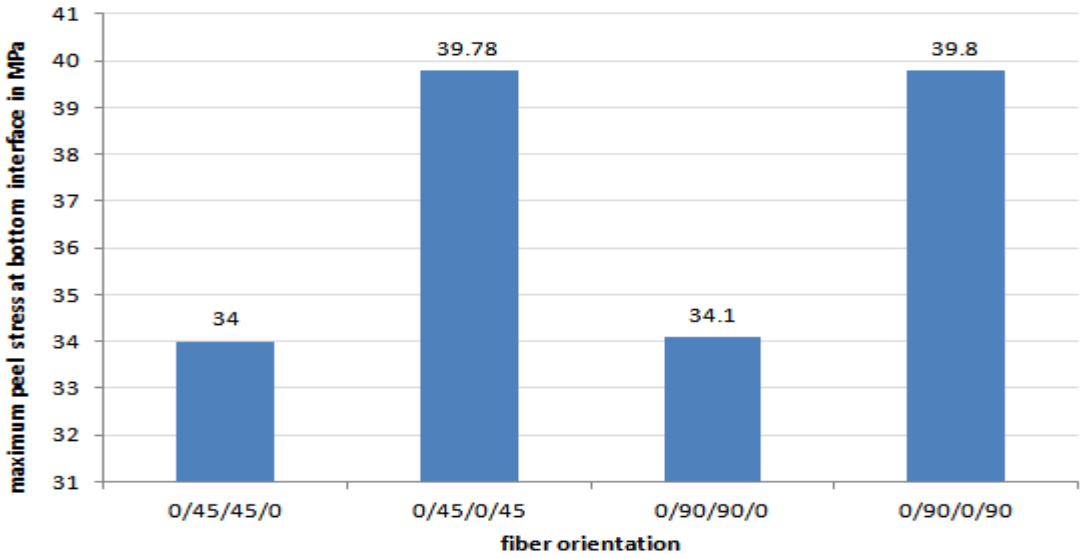

Figure 4-29.maximum peel stresses at bottom interface of joint made of aluminum-Sikaflex-composite of different fiber orientation

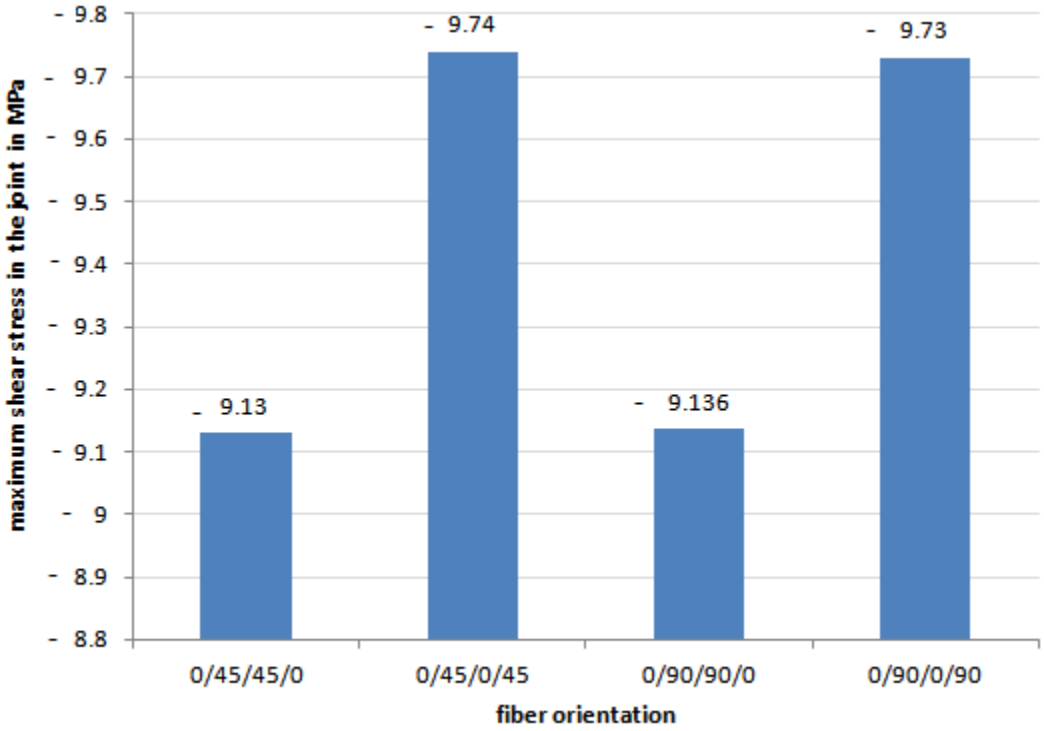

Figure 4-30.maximum shear stresses middle of the film made of aluminum-Sikaflex-composite of different fiber orientation

Analysis above is done to show load carrying capacity of symmetric composite and non symmetric one by using 0/45/45/0 vs. 0/45/45/0 and 0/90/90/0 vs. 0/90/0/90 as a candidate composite under the same loading values and condition. The result on bar shows the maximum stress (peel and shear) induced in the joint made of symmetric composite is less than that of non symmetric one. This true for the rest of other fiber orientation made symmetrically and used to join this specific adhesive.

CHAPTER FIVE

5. CONCLUSION AND RECOMMENDATION

5.1. Conclusion

As indicated in chapter four stress results, profile and magnitude of some selected adherend and adhesive sandwich of single lap joint has been shown. In real world such simple joint type i.e. single lap joint may not applied. But this joint is the basic and mandatory joint type for further analysis. The parametric analysis on both adhesive thickness and length shows stress magnitude variation as both parameters vary. Therefore for each combination of material type and geometries there are corresponding specific failure load. This failure load is the load magnitude that may cause stress values out of safe region of failure envelope. Therefore to prevent failure in joint the load that is going to applied to the joint should not exceed those magnitudes. For composite material the joint made of symmetric fiber orientation can withstand higher load than non symmetric one. It may lead to wrong to conclude all adhesive joint made of symmetric fiber orientation can withstand more load than other unless the analysis is done.

5.2. Recommendation and Future work

This research work enables one to predict the occurrence failures depending on values of stress induced in the joint. But to know the type of failure that may occur in joint another type of analysis called cohesive zone modeling is required. This method requires putting special element called cohesive element along the interface of adherend and adhesive. This special element requires many parameters that may found by extensive laboratory experiment. Therefore this category of modeling can be included as a future work

The other thing is most of the time the vehicles are exposed to cyclic load or fatigue load. The adhesive choosed for this analysis is local one (due to my interest to work on local problem) and is not known well and it is hard to find material specification that is sufficient for fatigue analysis. Shortly the future works can be summarized as follow

- ✓ Modeling adhesive joint by cohesive element method
- ✓ Fatigue analysis of adhesive joint

5.3. References

[1].Pike, Roscoe. *"adhesive*" . Encyclopædia Britannica Online . Encyclopædia Britannica Inc. Retrieved 9 April 2013.

[2].Kinloch,A.J.(1987).Adhesin and adhesive science and technology(reprinted.ed).London; Chapman and Hall .p.1

[3]Mazza, P; Martini, F; Sala, B; Magi, M; Colombini, M; Giachi, G; Landucci, F; Lemorini, C; Modugno, F; Ribechini, E (January 2006*). "A new Palaeolithic discovery: tar-hafted stone tools in a European Mid-Pleistocene bone- bearing bed"*. Journal of Archaeological Science . 33 (9): 1310. doi :10.1016/j.jas.2006.01.006 .

[4].Kozowyk, P. R. B.; Soressi, M.; Pomstra, D.; Langejans, G. H. J. (2017-08-31). "Experimental methods for the Palaeolithic dry distillation of birch bark: implications for the origin and development of Neandertal adhesive technology" . Scientific Reports . 7 (1). Bibcode: 2017NatSR...7.8033K . doi :10.1038/ s41598-017-08106-7 . ISSN 2045-2322 .

[5].Wadley, L; Hodgskiss, T; Grant, M (Jun 2009). *"Implications for complex cognition from the hafting of tools with compound adhesives in the Middle Stone Age, South Africa"* . Proceedings of the National Academy of Sciences of the United States of America . 106 (24): 9590–4. Bibcode: 2009PNAS..106.9590W . doi :10.1073/ pnas.0900957106 . ISSN 0027-8424 . PMC 2700998 . PMID 19433786 .

[6].Wadley, Lyn (1 June 2010). "*Compound-Adhesive Manufacture as a Behavioral Proxy for Complex Cognition in the Middle Stone Age"*. Current Anthropology . 51 (s1): S111–S119. doi : 10.1086/649836 .

[7].Ebnesajjad, Sina (2010). "History of Adhesives". Handbook of Adhesives and Surface Preparation : Technology, Applications and Manufacturing . Amsterdam: Elsevier. p. 137. ISBN 9781437744613 .

[8].Mittal, K.L.; A. Pizzi (2003). *"Historical Development of Adhesives and Adhesive Bonding"*. Handbook of Adhesive Technology (2nd ed., rev. and expanded. ed.). New York: Marcel Dekker, Inc. p. 1. ISBN 0824709861.

[9].Sauter F, Jordis U, Graf A, Werther, W(2000) *studies in organic archaeology identification of prehistoric adhesive used by the Tyrolean iceman to fix his weapons*.pp 735-747

[10] "History of Adhesives" (PDF). Bearing Briefs. Bearing Specialists Association. 2006.

[11].Ross, John; Charles Ross (10 October 1876). *"Improvement in Processes of Preparing Glue"* .United States Patent and Trademark Office. Retrieved 14 April 2013.

[12]. "Bonding- An Ancient Art" . Adhesives.org . Adhesives and Sealants Council. Retrieved 14 April 2013.

[13]. Adhesion Science and Engineering: Surfaces, Chemistry and Applications. Elsevier.

[14]. Market Study on Adhesives by Ceresana Research.(n.d.9) retrieved from https://www.ceresana.com/en/market-studies/industry/adhesives-world

[15]. Neha B. Thakare,A. B. Dhumne '*A Review on Design and Analysis of Adhesive Bonded Joint by Finite Element* Analysis'SSRG International Journal of Mechanical Engineering (SSRG-IJME) – volume 2 Issue 4–April 2015

[16] Adams, R.D. and Cawley, P.,"*A review of defect types and nondestructive testing techniques for composites and bonded joints*". NDT International,21(4): p. 208–222. 1988.

[17] Davis, M.J. and Bond, D.A."*The importance of failure mode identification in adhesive bonded aircraft structures and repairs*"in ICCM 12. Paris, France. 1999

[18] Marty, P.N., Desai, N., and Andersson, J.,NDT " *kissing bond in aeronautical structures*." 16th World Conference on NDT. Montreal, Canada. 2004

[19] "*Characterisation of Composite Materials. Materials Characterization Series",* C.R. Brundle and J.C.A. Evans: Momentum Press. 2010.

[20]. Yang, S., Gu, L., and Gibson, R.F."*Nondestructive detection of weak joints in adhesively bonded composite structures.Composite Structures*",51:p.63–71. 2001.

[21]. Jeenjitkaew, C., Luklinska, Z., and Guild, F.,"*Morphology and surface chemistry of kissing bonds in adhesive joints produced by surface contamination*." International Journal of Adhesion & Adhesives, 30: p. 643–653. 2010.

[22].adhesive bonding of composite. (n.d.). retrieved from *https://compositesuk.co.uk/system/files/documents/Adhesive%20bonding%20of%20composites_0.pdf*

[23].Volkersen."*Rivet strength distribution in tensile-stressed rivet joins with constant cross-section*" *Luftahrforschung* 15 No ½(1938) pp 41-47

[24].Goland and Reissner,E. '*the stress in cemented joints' J appl mech Trans ASME* 66 (1944) pp A17-A27

[25]. Volkersen ,O.*'Research on the theory of cemented joints*' *construction metallique* NO 4 (1965) pp 3-13

[26].Hart-Smith,L.J,' *adhesive bonded single lap joints- technical report*' *CR-112236* (NASA,Langley research centre,January 1973)

[27].Hart-Smith,L.J,' *adhesive bonded double lap joints- technical report*' *CR-112235* (NASA,Langley research centre,January 1973)

[28].Hart-Smith,L.J,' *adhesive bonded scarf-and stepped lap joints- technical report' CR-112236* (NASA,Langley research centre,January 1973)

[29]. Renton, W.J.and Vinson,J.R.*''the efficient design of adhesive bonded joints'* J Adhesion 7 (1975) pp 175-193

[30].Renton, W.J.and Vinson,J.R.' *analysis of adhesively bonded joints between panels of composite materials J appl mech Trans ASME* 44 (1977) pp 1001-106

[31]. Grant,P.and Taig, I.C,' *strength and stress analysis of bonded joints- technical report* ' British aircraft Corp.Ltd, Military aircraft division, report No SOR (P) 109,(March 1976)

[32]. Allman, D.J.' *A theory for elastic stresses in adhesive bonded lap joints' Quarterly J mech Appl Mathematics* 30 4,(November 1977) pp 415-436

[33]. Oljavo, I.U. and Eidinhoff, H.L.' *bond tichkness effect up on stress in single lap adhesive joint*' AIAAJ 16 No 3 (March 1978) pp 204- 211

[34].D.A. Bigwood and A.D. Crocombe, "*Elastic analysis and Engineering design formulae for bonded joint"s*, international J adhesion and adhesives, vol.9 N0.4(October 1989) pp 229 -242

[35] R.D. Adams, N.A. Peppiatt, *Stress analysis of adhesive-bonded lap joints*. J. Strain Anal.9, 185–196 (1974)

[36] A.D. Crocombe, R.D. Adams, *Influence of the spew fillet and other parameters on the stress distribution in the single lap joint.* J. Adhes.13, 141–155 (1981)

[37] R.D. Adams, J.A. Harris, *Strength prediction of bonded single lap joints by nonlinear finite element methods*. Int J Adhes Adhes4, 65–78 (1984)

[38] R.D. Adams, R. Davies, *Strength of lap shear joints, inThe Mechanics of Adhesion*, ed. by D.A. Dillard, A.V. Pocius (Elsevier, Amsterdam, 2002)

[39] R.S. Raghava, R. Cadell, G.S.Y. Yeh, *The macroscopic yield behavior of polymers*. J. Mater. Sci.8, 225–232 (1973)

[40]L. F. M. da Silva and R. D. S. G. Campilho,*Advances in Numerical Modelling of Adhesive Joints*, Springer Briefs in Computational Mechanics, DOI: 10.1007/978-3-642-23608-2_1,Lucas F. M. da Silva 2012For failure citeria

[41] R.D. Adams, N.A. Peppiatt*, Effects of Poisson's ratio strains in adherend on stresses of an idealized lap join*t. J. Strain Anal. 8, 134–139 (1973)

[42] R.D. Adams, R. Davies, *Strength of joints involving composites*. J. Adhesion59, 171–182 (1996)

[43] J.P.M. Gonçalves, M.F.S.F. de Moura, P.M.S.T. de Castro, *A three-dimensional finite element model for stress analysis of adhesive joints*. Int. J. Adhes. Adhes.22, 357–365 (2002)

[44] R.D. Adams, J. Comyn, W.C. Wake,*Structural Adhesive Joints* in Engineering,2nd edn.

(Chapman & Hall, London,1997

[45] Rene´ Quispe Rodrı´guez ,William Portilho de Paiva ,Paulo Sollero ,Marcelo Ricardo Bertoni Rodriguesa , E´der Lima de Albuquerque' *Failure criteria for adhesively bonded joints* International Journal of Adhesion & Adhesives, 37 (2012) 26–36

[46] Sika Corporation" product data sheet- Sikaflex-265"

[47]ASTM D1002-99' *Standard test method for apparent shear strength of single lap join adhesively bonded metal specimen by tension loading* ''

[48].Prof. Richard Lehman. "*mechanical properties of material*.pdf'.Internet: https://glassproperties.com/referance/mechprophandouts.pdf. June 4, 2018.

[49]. C. Menna, D. Asprone, G. Caprino, V. Lopresto și A. Prota, *Numerical Simulation Of Impact Tests On GFRP Composite Laminates*, International Journal of Impact Engineering, <10.1016/j.ijimpeng.2011.03.003>. <hal-00829115> Elsevier, 2011

[50].Waugh, R.C, *development of infrared techniques for practical defect identification in bonded joint*, 2016, XXVII, pp-149

[51]. Kadir Turan & Yeliz Pekbey (2015*) Progressive Failure Analysis of Reinforced-Adhesively Single-Lap Joint*, The Journal of Adhesion, 91:12, 962-977, DOI: 10.1080/00218464.2014.985379

5.4. Appendix

First derivation of shear stress equation

At x=0 we will have

$C_1\ [m_1*SINH(0*m_1)]+\ C_2\ [m_1*COSH(0*m_1)]\ +\ C_3\ [n_1*COS(n_2*0)*SINH(n_1*0)\ -\ n_2*SIN(n_2*0)*COSH(n_1*0)]\ +\ C_4\ [n_1*SIN(n_2*0)*SINH(n_1*0)\ +\ n_2*COS(n_2*0)*COSH(n_1*0)]\ +\ C_5\ [n_1*COS(n_2*0)*COSH(n_1*0)\ -\ n_2*SIN(n_2*0)*SINH(n_1*0)]\ +\ C_6\ [n_1*SIN(n_2*0)*COSH(n_1*0)\ +\ n2*COS(n_2*0)*SINH(n_1*0)]\ +\ C_7\ =\ G_a/t\ *\ (\ (1-v_1\text{^}2)/E_1\ *\ (T_{11}/h_1-6*M_{11}/h_1\text{^}2)\ -\ (1-v_2\text{^}2)/E_2\ *\ (T_{21}/h_2+6*M_{21}/h_2\text{^}2)\ )$ ……A1

Again at x=L

$C_1\ [m_1*SINH(L*m_1)]+\ C_2\ [m_1*COSH(L*m_1)]\ +\ C_3\ [n_1*COS(n_2*L)*SINH(n_1*L)\ -\ n_2*SIN(n_2*L)*COSH(n_1*L)]\ +\ C_4\ [n_1*SIN(n_2*L)*SINH(n_1*L)\ +\ n_2*COS(n_2*L)*COSH(n_1*L)]\ +\ C_5\ [n_1*COS(n_2*L)*COSH(n_1*L)\ -\ n_2*SIN(n_2*L)*SINH(n_1*L)]\ +\ C_6\ [n_1*SIN(n_2*L)*COSH(n_1*L)\ +\ n2*COS(n_2*L)*SINH(n_1*L)]\ +\ C_7\ =\ G_a/t\ *\ (\ (1-v_1\text{^}2)/E_1\ *\ (T_{12}/h_1-6*M_{12}/h_1\text{^}2)\ -\ (1-v_2\text{^}2)/E_2\ *\ (T_{22}/h_2+6*M_{22}/h_2\text{^}2)\ )$……A2

Twice differentiation of shear stress

At x= 0

$C_1\ \ [-K_1*m_1\text{^}3*SINH(m_1*0)\ +\ m_1\text{^}5*SINH(m_1*0)]\ +$

$C_2\ \ [-K_1*m_1\text{^}3*COSH(m_1*0)\ +\ m_1\text{^}5*COSH(m_1*0)]\ +$

$C_3\ \ [COS(0*n_2)*SINH(0*n_1)*n_1\text{^}5\ -\ 5*COSH(0*n_1)*SIN(0*n_2)*n_1\text{^}4*n_2\ -\ 10*COS(0*n_2)*SINH(0*n_1)*n_1\text{^}3*n_2\text{^}2\ +\ \ 10*COSH(0*n_1)*SIN(0*n_2)*n_1\text{^}2*n_2\text{^}3+\ 5*COS(0*n_2)*SINH(0*n_1)*n_1*n_2\text{^}4\ -\ COSH(0*n_1)*SIN(0*n_2)*n_2\text{^}5\ –\ K_1*(COS(0*n_2)*SINH(0*n_1)*n_1\text{^}3\ -\ 3*COSH(0*n_1)*SIN(0*n_2)*n_1\text{^}2*n_2\ -\ 3*COS(0*n_2)*SINH(0*n_1)*n_1*n_2\text{^}2\ +\ COSH(0*n_1)*SIN(0*n_2)*n_2\text{^}3)]\ +$

$C_4\ \ [SIN(0*n_2)*SINH(0*n_1)*n_1\text{^}5\ +\ 5*COS(0*n_2)*COSH(0*n_1)*n_1\text{^}4*n_2\ -\ 10*SIN(0*n_2)*SINH(0*n_1)*n_1\text{^}3*n_2\text{^}2\ -$

$10*COS(0*n_2)*COSH(0*n_1)*n_1\text{^}2*n_2\text{^}3\ +\ 5*SIN(0*n_2)*SINH(0*n_1)*n_1*n_2\text{^}4\ +\ COS(0*n_2)*COSH(0*n_1)*n_2\text{^}5\ -\ K1*(SIN(0*n_2)*SINH(0*n_1)*n_1\text{^}3\ +$

$3*COS(0*n_2)*COSH(0*n_1)*n_1\text{^}2*n_2 - 3*SIN(0*n_2)*SINH(0*n_1)*n_1*n_2\text{^}2 - COS(0*n_2)*COSH(0*n_1)*n_2\text{^}3)] +$

C_5 $[COS(0*n_2)*COSH(0*n_1)*n_1\text{^}5 - 5*SIN(0*n_2)*SINH(0*n_1)*n_1\text{^}4*n_2 - 10*COS(0*n_2)*COSH(0*n_1)*n_1\text{^}3*n_2\text{^}2 + 10*SIN(0*n_2)*SINH(0*n_1)*n_1\text{^}2*n_2\text{^}3 + 5*COS(0*n_2)*COSH(0*n_1)*n_1*n_2\text{^}4 - SIN(0*n_2)*SINH(0*n_1)*n_2\text{^}5 - K_1*(COS(0*n_2)*COSH(0*n_1)*n_1\text{^}3 - 3*SIN(0*n_2)*SINH(0*n_1)*n_1\text{^}2*n_2 - 3*COS(0*n_2)*COSH(0*n_1)*n_1*n_2\text{^}2 + SIN(0*n_2)*SINH(0*n_1)*n_2\text{^}3)] +$

C_6 $[COSH(0*n_1)*SIN(0*n_2)*n_1\text{^}5 + 5*COS(0*n_2)*SINH(0*n_1)*n_1\text{^}4*n_2 - 10*COSH(0*n_1)*SIN(0*n_2)*n_1\text{^}3*n_2\text{^}2 - 10*COS(0*n_2)*SINH(0*n_1)*n_1\text{^}2*n_2\text{^}3 + 5*COSH(0*n_1)*SIN(0*n_2)*n_1*n_2\text{^}4 + COS(0*n_2)*SINH(0*n_1)*n_1\text{^}5 - K_1*(COSH(0*n_1)*SIN(0*n_2)*n_1\text{^}3 + 3*COS(0*n_2)*SINH(0*n_1)*n_1\text{^}2*n_2 - 3*COSH(0*n_1)*SIN(0*n_2)*n_1*n_2\text{^}2 - COS(0*n_2)*SINH(0*n_1)*n_2\text{^}3)] +$ C_7

$=-(E_a*K_2/t)*(-M_{11}/D_1+M_{21}/D_2)$ …….A3

At x= L

C_1 $[-K_1*m_1\text{^}3*SINH(m_1*L) + m_1\text{^}5*SINH(m_1*L)] +$

C_2 $[-K_1*m_1\text{^}3*COSH(m_1*L) + m_1\text{^}5*COSH(m_1*L)] +$

C_3 $[COS(L*n_2)*SINH(L*n_1)*n_1\text{^}5 - 5*COSH(L*n_1)*SIN(L*n_2)*n_1\text{^}4*n_2 - 10*COS(L*n_2)*SINH(L*n_1)*n_1\text{^}3*n_2\text{^}2 + 10*COSH(L*n_1)*SIN(L*n_2)*n_1\text{^}2*n_2\text{^}3 + 5*COS(L*n_2)*SINH(L*n_1)*n_1*n_2\text{^}4 - COSH(L*n_1)*SIN(L*n_2)*n_2\text{^}5 – K_1*(COS(L*n_2)*SINH(L*n_1)*n_1\text{^}3 - 3*COSH(L*n_1)*SIN(L*n_2)*n_1\text{^}2*n_2 - 3*COS(L*n_2)*SINH(L*n_1)*n_1*n_2\text{^}2 + COSH(L*n_1)*SIN(L*n_2)*n_2\text{^}3)] +$

C_4 $[SIN(L*n_2)*SINH(L*n_1)*n_1\text{^}5 + 5*COS(L*n_2)*COSH(L*n_1)*n_1\text{^}4*n_2 - 10*SIN(L*n_2)*SINH(L*n_1)*n_1\text{^}3*n_2\text{^}2 -$

$10*COS(L*n_2)*COSH(L*n_1)*n_1\text{^}2*n_2\text{^}3 + 5*SIN(L*n_2)*SINH(L*n_1)*n_1*n_2\text{^}4 + COS(L*n_2)*COSH(L*n_1)*n_2\text{^}5 -$

$K1*(SIN(L*n_2)*SINH(L*n_1)*n_1\text{^}3 + 3*COS(L*n_2)*COSH(L*n_1)*n_1\text{^}2*n_2 - 3*SIN(L*n_2)*SINH(L*n_1)*n_1*n_2\text{^}2 - COS(L*n_2)*COSH(L*n_1)*n_2\text{^}3)] +$

$C_5 \quad [COS(L*n_2)*COSH(L*n_1)*n_1\text{^}5 - 5*SIN(L*n_2)*SINH(L*n_1)*n_1\text{^}4*n_2 - 10*COS(L*n_2)*COSH(L*n_1)*n_1\text{^}3*n_2\text{^}2 + 10*SIN(L*n_2)*SINH(L*n_1)*n_1\text{^}2*n_2\text{^}3 + 5*COS(L*n_2)*COSH(L*n_1)*n_1*n_2\text{^}4 - SIN(L*n_2)*SINH(L*n_1)*n_2\text{^}5 - K_1*(COS(L*n_2)*COSH(L*n_1)*n_1\text{^}3 - 3*SIN(L*n_2)*SINH(L*n_1)*n_1\text{^}2*n_2 - 3*COS(L*n_2)*COSH(L*n_1)*n_1*n_2\text{^}2 + SIN(L*n_2)*SINH(L*n_1)*n_2\text{^}3)] +$

$C_6 \quad [COSH(L*n_1)*SIN(L*n_2)*n_1\text{^}5 + 5*COS(L*n_2)*SINH(L*n_1)*n_1\text{^}4*n_2 - 10*COSH(L*n_1)*SIN(L*n_2)*n_1\text{^}3*n_2\text{^}2 - 10*COS(L*n_2)*SINH(L*n_1)*n_1\text{^}2*n_2\text{^}3 + 5*COSH(L*n_1)*SIN(L*n_2)*n_1*n_2\text{^}4 + COS(L*n_2)*SINH(L*n_1)*n_1\text{^}5 - K_1*(COSH(L*n_1)*SIN(L*n_2)*n_1\text{^}3 + 3*COS(L*n_2)*SINH(L*n_1)*n_1\text{^}2*n_2 - 3*COSH(L*n_1)*SIN(L*n_2)*n_1*n_2\text{^}2 - COS(L*n_2)*SINH(L*n_1)*n_2\text{^}3)] + \quad C_7$

$= -(E_a*K_2/t)*(-M_{12}/D_1 + M_{22}/D_2)$ ……A4

Three times derivation of shear stress equation

At = 0

$C_1 [-COSH(0*m_1)*(E_a*K_2)/(2*t)*(-(h_1+t)/D_1 + (h_2+t)/D_2) - COSH(0*m_1)*k_1*m_1\text{^}4 + COSH(0*m_1)*m_1\text{^}6] +$

$C_2 [-SINH(0*m_1)*(Ea*K_2)/(2*t)*(-(h_1+t)/D_1 + (h_2+t)/D_2) - SINH(0*m_1)*K_1*m_1\text{^}4 + SINH(0*m_1)*m1\text{^}6] + C_3 [SIN(0*n_2)*SINH(0*n_1) * (4*K_1*n_1\text{^}3*n_2 - 6*n_1\text{^}5*n_2 - 4*K_1*n_1*n_2\text{^}3 + 20*n_1\text{^}3*n_2\text{^}3 - 6*n_1*n_2\text{^}5) + COS(0*n_2)*COSH(0*n_1) * (-(Ea*K_2)/(2*t)*(-(h_1+t)/D_1 + (h_2+t)/D_2) – K_1*n_1\text{^}4 + n_1\text{^}6 + 6*K_1*n_1\text{^}2*n_2\text{^}2 - 15*n_1\text{^}4*n_2\text{^}2 – K_1*n_2\text{^}4 + 15*n_1\text{^}2*n_2\text{^}4 – n_2\text{^}6)] +$

$C_4 [COS(0*n_2)*SINH(0*n_1) * (-4*K_1*n_1\text{^}3*n_2 + 6*n_1\text{^}5*n_2 + 4*K_2*n_1*n_2\text{^}3 - 20*n_1\text{^}3*n_2\text{^}3 + 6*n_1*n_2\text{^}5) + SIN(0*n_2)*COSH(0*n_1) * (-(Ea*K_2)/(2*t)*(-(h_1+t)/D_1 + (h_2+t)/D_2) – K_1*n_1\text{^}4 + n_1\text{^}6 + 6*K_1*n_2\text{^}2*n_2\text{^}2 - 15*n_1\text{^}4*n_2\text{^}2 – K_1*n_2\text{^}4 + 15*n_1\text{^}2*n_2\text{^}4 – n_2\text{^}6)] +$

C_5 [SIN(0*n_2)*COSH(0*n_1) * (4*K_1*$n_1^{3*}n_2$ - 6*$n_1^{5*}n_2$ -4*K_1*n_1*n_2^3 + 20*$n_1^{3*}n_2$^3 - 6*n_1*n_2^5) + COS(0*n_2)*SINH(0*n_1) * (-(Ea*K_2)/(2*t)*(-(h_1+t)/D_1 + (H_2+t)/D_2) –K_1*n_1^4 + n_1^6 + 6*K_1*$n_1^{2*}n_2$^2 -15*$n_1^{4*}n_2$^2 –K_1*n_2^4 +15*$n_1^{2*}n_2$^4 –n_2^6)] +

C_6 [COS(0*n_2)*COSH(0*n_1) * (-4*K_1*$n_1^{3*}n_2$ + 6*$n_1^{5*}n_2$ +4*K_1*n_1*n_2^3 - 20*$n_1^{3*}n_2$^3 + 6*n_1*n_2^5) + SIN(0*n_2)*SINH(0*n_1) * (-(Ea*K_2)/(2*t)*(-(h+1+t)/D1 + (h+2+t)/D_2) – K_1*n_1^4 + n_1^6 + 6*K_1*$n_1^{2*}n_2$^2 -15*$n_1^{4*}n_2$^2 –K_1*n_2^4 +15*$n_1^{2*}n_2$^4 –n_2^6)] +

C_7 [-(Ea*K_2)/(2*t) * (-(h_1+t)/D_1 + (h_2+t)/D_2)]

= -(Ea*k_2)/t * (-V_{11}/D_1+V_{21}/D_2)……A5

At x=L

C_1 [-COSH(L*m_1)*(E_a*K_2)/(2*t)*(-(h_1+t)/D_1 + (h_2+t)/D_2) - COSH(L*m_1)*k_1*m_1^4 + COSH(L*m_1)*m_1^6] +

C_2 [-SINH(L*m_1)*(Ea*K_2)/(2*t)*(-(h_1+t)/D_1 + (h_2+t)/D_2) - SINH(L*m_1)*K_1*m_1^4 + SINH(L*m_1)*m1^6] +

C_3 [SIN(L*n_2)*SINH(L*n_1) * (4*K_1*$n_1^{3*}n_2$ - 6*$n_1^{5*}n_2$ -4*K_1*n_1*n_2^3 + 20*$n_1^{3*}n_2$^3 - 6*n_1*n_2^5) + COS(L*n_2)*COSH(L*n_1) * (-(Ea*K_2)/(2*t)*(-(h_1+t)/D_1 + (h_2+t)/D_2) –K_1*n_1^4 + n_1^6 + 6*K_1*$n_1^{2*}n_2$^2 -15*$n_1^{4*}n_2$^2 –K_1*n_2^4 +15*$n_1^{2*}n_2$^4 –n_2^6)] +

C_4 [COS(L*n_2)*SINH(L*n_1) * (-4*K_1*$n_1^{3*}n_2$ + 6*$n_1^{5*}n_2$ +4*K_2*n_1*n_2^3 - 20*$n_1^{3*}n_2$^3 + 6*n_1*n_2^5) + SIN(L*n_2)*COSH(L*n_1) * (-(Ea*K_2)/(2*t)*(-(h_1+t)/D_1 + (h_2+t)/D_2) –K_1*n_1^4 + n_1^6 + 6*K_1*$n_2^{2*}n_2$^2 -15*$n_1^{4*}n_2$^2 –K_1*n_2^4 +15*$n_1^{2*}n_2$^4 –n_2^6)] +

C_5 [SIN(L*n_2)*COSH(L*n_1) * (4*K_1*$n_1^{3*}n_2$ - 6*$n_1^{5*}n_2$ -4*K_1*n_1*n_2^3 + 20*$n_1^{3*}n_2$^3 - 6*n_1*n_2^5) + COS(L*n_2)*SINH(L*n_1) * (-(Ea*K_2)/(2*t)*(-(h_1+t)/D_1 + (H_2+t)/D_2) –K_1*n_1^4 + n_1^6 + 6*K_1*$n_1^{2*}n_2$^2 -15*$n_1^{4*}n_2$^2 –K_1*n_2^4 +15*$n_1^{2*}n_2$^4 –n_2^6)] +

C_6 [COS(L*n_2)*COSH(L*n_1) * (-4*K_1*$n_1^{3*}n_2$ + 6*$n_1^{5*}n_2$ +4*K_1*n_1*n_2^3 - 20*$n_1^{3*}n_2$^3 + 6*n_1*n_2^5) + SIN(L*n_2)*SINH(L*n_1) * (-(Ea*K_2)/(2*t)*(-(h+1+t)/D1 + (h+2+t)/D_2) – K_1*n_1^4 + n_1^6 + 6*K_1*$n_1^{2*}n_2$^2 -15*$n_1^{4*}n_2$^2 –K_1*n_2^4 +15*$n_1^{2*}n_2$^4 –n_2^6)] +

C_7 [-(Ea*K_2)/(2*t) * (-(h_1+t)/D_1 + (h_2+t)/D_2)]

$= -(Ea*K_2)/t * (-V_{12}/D_1+V_{22}/D_2)$…….A6

Integration of shear stress along bond length

$C_1 [SINH(L*m_1)/m_1] + C_2 [(COSH(L*m_1)-1)/m_1] +$

$C_3 [(COS(L*n_2)*SINH(L*n_1)*n_1 + SIN(L*n_2)*COSH(L*n_1)*n_2) / (n_1\text{^}2+n_2\text{^}2)] +$

$C_4 [(SIN(L*n_2)*SINH(L*n_1)*n_1 + (1-COS(L*n_2)*COSH(L*n_1))*n_2) / (n_1\text{^}2+n_2\text{^}2)] +$

$C_5 [((-1+COS(L*n_2)*COSH(L*n_1))*n_1 + SIN(L*n_2)*SINH(L*n_1)*n_2) / (n_1\text{^}2+n_2\text{^}2)] +$

$C_6 [(COSH(L*n_1)*SIN(L*n_2)*n_1 - COS(L*n_2)*SINH(L*n_1)*n_2) / (n_1\text{^}2+n_2\text{^}2)] + C_7 [L] =$

$-T_{11}+T_{12}$ ……..A7

Twice derivation of peel stress

At x= 0

$D_1 [COSH(0*m_1)*m_1\text{^}2] + D_2 [SINH(0*m_1)*m_1\text{^}2] + D_3 [COS(0*n_2)*COSH(0*n_1)*(n_1\text{^}2-N_2\text{^}2)$
$- 2*SIN(0*n_2)*SINH(0*n_1)*n_1*n_2] + D_4 [COSH(0*n_1)*SIN(0*n_2)*(n_1\text{^}2-n_2\text{^}2) +$
$2*COS(0*N_2)*SINH(0*n_1)*n_1*n_2] + D_5 [COS(0*n_2)*SINH(0*n_1)*(n_1\text{^}2-n_2\text{^}2) -$
$2*COSH(0*n_1)*SIN(0*n_2)*n_1*n_2] +$

$D_6 [SIN(0*n_2)*SINH(0*n_1)*(n_1\text{^}2-n_2\text{^}2) + 2*COS(0*n_2)*COSH(0*n_1)*n_1*n_2]$

$= (E_a/t)*(-M_{11}/D_1+M_{21}/D_2)$……A8

At x= L

$D_1 [COSH(L*m_1)*m_1\text{^}2] + D_2 [SINH(L*m_1)*m_1\text{^}2] + D_3 [COS(L*n_2)*COSH(L*n_1)*(n_1\text{^}2-N_2\text{^}2)$
$- 2*SIN(L*n_2)*SINH(L*n_1)*n_1*n_2] + D_4 [COSH(L*n_1)*SIN(L*n_2)*(n_1\text{^}2-n_2\text{^}2) +$
$2*COS(L*N_2)*SINH(L*n_1)*n_1*n_2] + D_5 [COS(L*n_2)*SINH(L*n_1)*(n_1\text{^}2-n_2\text{^}2) -$
$2*COSH(L*n_1)*SIN(L*n_2)*n_1*n_2] +$

$D_6\ [SIN(L*n_2)*SINH(L*n_1)*(n_1\text{^}2-n_2\text{^}2) + 2*COS(L*n_2)*COSH(L*n_1)*n_1*n_2]$

$= (E_a/t)*(-M_{12}/D_1+M_{22}/D_2)$……A9

Four time derivation of peel stress

At x = 0

$D_1\ [COSH(0*m_1)*(K_3+m_1\text{^}4)]\ +\ D_2\ [SINH(0*m_1)*(K_3+m_1\text{^}4)]+$

$D_3\ [SIN(0*n_2)*SINH(0*n_1)*4*(n_1*n_2\text{^}3-n_1\text{^}3*n_2) + COS(0*n_2)*COSH(0*n_1)*(K_3+n_1\text{^}4-6*n_1\text{^}2*n_2\text{^}2+n_2\text{^}4)]+ D_4\ [COS(0*n_2)*SINH(0*n_1)*4*(n_1\text{^}3*n_2-n_1*n_2\text{^}3) + COSH(0*n_1)*SIN(0*n_2)*(K_3+n_1\text{^}4-6*n_1\text{^}2*n_2\text{^}2+n_2\text{^}4)]+$

$D_5\ [SIN(0*n_2)*COSH(0*n_1)*4*(n_1*n_2\text{^}3-n_1\text{^}3*n_2) + COS(0*n_2)*SINH(0*n_1)*(K_3+n_1\text{^}4-6*N_1\text{^}2*n_2\text{^}2+n_2\text{^}4)]+\ D_6\ [COS(0*n_2)*COSH(0*n_1)*4*(n_1\text{^}3*n_2-n_1*n_2\text{^}3) + SIN(0*n_2)*SINH(0*n_1)*(K_3+n_1\text{^}4-6*n_1\text{^}2*n_2\text{^}2+n_2\text{^}4)]$

$= (G_a*K_4/t) * ((1-V_1\text{^}2)/E_1 * (T_{11}/h_1-6*M_{11}/h_1\text{^}2) - (1-V_2\text{^}2)/E_2 * (T_{21}/h_2+6*M_{21}/h_2\text{^}2))$…A10

At x= L

$D_1\ [COSH(L*m_1)*(K_3+m_1\text{^}4)]\ +\ D_2\ [SINH(L*m_1)*(K_3+m_1\text{^}4)]+\ D_3\ [SIN(L*n_2)*SINH(L*n_1)*4*(n_1*n_2\text{^}3-n_1\text{^}3*n_2) + COS(L*n_2)*COSH(L*n_1)*(K_3+n_1\text{^}4-6*n_1\text{^}2*n_2\text{^}2+n_2\text{^}4)]+\ D_4\ [COS(L*n_2)*SINH(L*n_1)*4*(n_1\text{^}3*n_2-n_1*n_2\text{^}3) + COSH(L*n_1)*SIN(L*n_2)*(K_3+n_1\text{^}4-6*n_1\text{^}2*n_2\text{^}2+n_2\text{^}4)]+ D_5\ [SIN(L*n_2)*COSH(L*n_1)*4*(n_1*n_2\text{^}3-n_1\text{^}3*n_2) + COS(L*n_2)*SINH(L*n_1)*(K_3+n_1\text{^}4-6*N_1\text{^}2*n_2\text{^}2+n_2\text{^}4)]+ D_6\ [COS(L*n_2)*COSH(L*n_1)*4*(n_1\text{^}3*n_2-n_1*n_2\text{^}3) + SIN(L*n_2)*SINH(L*n_1)*(K_3+n_1\text{^}4-6*n_1\text{^}2*n_2\text{^}2+n_2\text{^}4)]$

$= (G_a*K_4/t) * ((1-V_1\text{^}2)/E_1 * (T_{12}/h_1-6*M_{12}/h_1\text{^}2) - (1-V_2\text{^}2)/E_2 * (T_{22}/h_2+6*M_{22}/h_2\text{^}2))$…….A11

Three times peel stress derivation

At x=0

$D_1\ [SINH(0*m_1)*m_1\text{^}3] + \quad D_2\ [COSH(0*m_1)*m_1\text{^}3] \quad +$

$D_3\ [COS(0*n_2)*SINH(0*n_1)*(n_1\text{^}3-3*n_1*n_2\text{^}2) + COSH(0*n_1)*SIN(0*n_2)*(-3*n_1\text{^}2*n_2+n_2\text{^}3)] +$
$D_4\ [SIN(0*n_2)*SINH(0*n_1)*(n_1\text{^}3-3*n_1*n_2\text{^}2) + COS(0*n_2)*COSH(0*n_1)*(3*n_1\text{^}2*n_2-n_2\text{^}3)] +$
$D_5\ [COS(0*n_2)*COSH(0*n_1)*(n_1\text{^}3-3*n_1*n_2\text{^}2) + SIN(0*n_2)*SINH(0*n_1)*(-3*n_1\text{^}2*n_2+n_2\text{^}3)] +$
$D_6\ [COSH(0*n_1)*SIN(0*n_2)*(n_1\text{^}3-3*n_1*n_2\text{^}2) + COS(0*n_2)*SINH(0*n_1)*(3*n_1\text{^}2*n_2-n_2\text{^}3)]$

$= (E_a/t)\ *(-V_{11}/D_1 + V_{21}/D_2 - (-(t+h_1)/D_1+(T+h_2)/D_2)*\ (C_1\ COSH(m_1 * 0) + C_2\ SINH(m_1 * 0)$
$+ C_3\ COSH(n_1 * 0)\ COSH(n_2 * 0) \quad + C_4\ COSH(n_1 * 0)\ \ SIN(n_2 * 0)$

$+ C_5\ SINH(n_1 * 0)\ COS(n_2 * 0) + C_6\ SINH(n_1 L)\ SIN(n_2 * 0) + C_7\ )/2)$……..A12

At x=L

$D_1\ [SINH(L*m_1)*m_1\text{^}3] + D_2\ [COSH(L*m_1)*m_1\text{^}3] + D_3\ [COS(L*n_2)*SINH(L*n_1)*(n_1\text{^}3-$
$3*n_1*n_2\text{^}2) + COSH(L*n_1)*SIN(L*n_2)*(-3*n_1\text{^}2*n_2+n_2\text{^}3)] + D_4\ [SIN(L*n_2)*SINH(L*n_1)*(n_1\text{^}3-$
$3*n_1*n_2\text{^}2) + COS(L*n_2)*COSH(L*n_1)*(3*n_1\text{^}2*n_2-n_2\text{^}3)] + D_5$
$[COS(L*n_2)*COSH(L*n_1)*(n_1\text{^}3-3*n_1*n_2\text{^}2) + SIN(L*n_2)*SINH(L*n_1)*(-3*n_1\text{^}2*n_2+n_2\text{^}3)] +$

$D_6\ [COSH(L*n_1)*SIN(L*n_2)*(n_1\text{^}3-3*n_1*n_2\text{^}2) + COS(L*n_2)*SINH(L*n_1)*(3*n_1\text{^}2*n_2-n_2\text{^}3)]$

$= (E_a/t)\ *(-V_{12}/D_1 + V_{22}/D_2 - (-(t+h_1)/D_1+(T+h_2)/D_2)*\ (C_1\ COSH(m_1 L) + C_2\ SINH(m_1 L) + C_3$
$COSH(n_1 L)\ COSH(n_2 L) \quad + C_4\ COSH(n_1 L)\ \ SIN(n_2 L)$

$+ C_5\ SINH(n_1 L)\ COS(n_2 L) + C_6\ SINH(n_1 L)\ SIN(n_2 L) + C_7\ )/2)$……A13